



HHS Public Access

Author manuscript

J Med Chem. Author manuscript; available in PMC 2021 April 23.

Published in final edited form as:

J Med Chem. 2020 April 23; 63(8): 4256–4292. doi:10.1021/acs.jmedchem.0c00193.

Design, Synthesis, and Biological Evaluation of Quinazolin-4-one-Based Hydroxamic Acids as Dual PI3K/HDAC Inhibitors

Ashish Thakur,

National Center for Advancing Translational Sciences, National Institutes of Health, Rockville, Maryland 20850, United States;

Gregory J. Tawa,

National Center for Advancing Translational Sciences, National Institutes of Health, Rockville, Maryland 20850, United States

Mark J. Henderson,

National Center for Advancing Translational Sciences, National Institutes of Health, Rockville, Maryland 20850, United States;

Carina Danchik,

National Center for Advancing Translational Sciences, National Institutes of Health, Rockville, Maryland 20850, United States

Suiyang Liu,

Dana-Farber Cancer Institute, Boston, Massachusetts 02215, United States

Pranav Shah,

National Center for Advancing Translational Sciences, National Institutes of Health, Rockville, Maryland 20850, United States

Amy Q. Wang,

National Center for Advancing Translational Sciences, National Institutes of Health, Rockville, Maryland 20850, United States

Garrett Dunn,

Corresponding Authors: **Ashish Thakur** – *National Center for Advancing Translational Sciences, National Institutes of Health, Rockville, Maryland 20850, United States*; Phone: +1-301-827-7179; ashish.thakur@nih.gov, **Gurmit Grewal** – *National Center for Advancing Translational Sciences, National Institutes of Health, Rockville, Maryland 20850, United States*; Phone: +1-508-740-7465; gurmit.grewal@gmail.com.

Author Contributions

The manuscript was written through contributions of all authors. All authors have given approval to the final version of the manuscript.

Supporting Information

The Supporting Information is available free of charge at <https://pubs.acs.org/doi/10.1021/acs.jmedchem.0c00193>.

PI3K/HDAC enzyme inhibitory activities of selected 5-substituted quinazolinones; HPLC-MS chromatogram of compounds **19b**, **46b**, **48b**, **48c**, **48n**, and **48o**, respectively; figures showing compound **19b** bound to HDAC1, 2 (Glu567, Asp568), HDAC3 (Asp567, Asp568), HDAC8 (Tyr567, Asp568), HDAC4, 5, 7, 9 (Asp567, Thr568), HDAC10 (Asp567, Ala568), and HDAC11 (Pro567, Asn568), respectively; kinome scan of compound **48c**, and immunoblot analysis for PI3K δ and HDAC6 expression ([PDF](#))

Molecular strings for all final compounds ([CSV](#))

The content of this publication does not necessarily reflect the views or policies of the Department of Health and Human Services, nor does mention of trade names, commercial products, or organizations imply endorsement by the U.S. Government.

The authors declare the following competing financial interest(s): Ashish Thakur, Gurmit Grewal, Gregory J. Tawa and Anton Simeonov are inventors of a patent application associated with this work.

National Center for Advancing Translational Sciences, National Institutes of Health, Rockville, Maryland 20850, United States

Md Kabir,

National Center for Advancing Translational Sciences, National Institutes of Health, Rockville, Maryland 20850, United States

Elias C. Padilha,

National Center for Advancing Translational Sciences, National Institutes of Health, Rockville, Maryland 20850, United States

Xin Xu,

National Center for Advancing Translational Sciences, National Institutes of Health, Rockville, Maryland 20850, United States

Anton Simeonov,

National Center for Advancing Translational Sciences, National Institutes of Health, Rockville, Maryland 20850, United States

Surender Kharbanda,

Dana-Farber Cancer Institute, Boston, Massachusetts 02215, United States

Richard Stone,

Dana-Farber Cancer Institute, Boston, Massachusetts 02215, United States

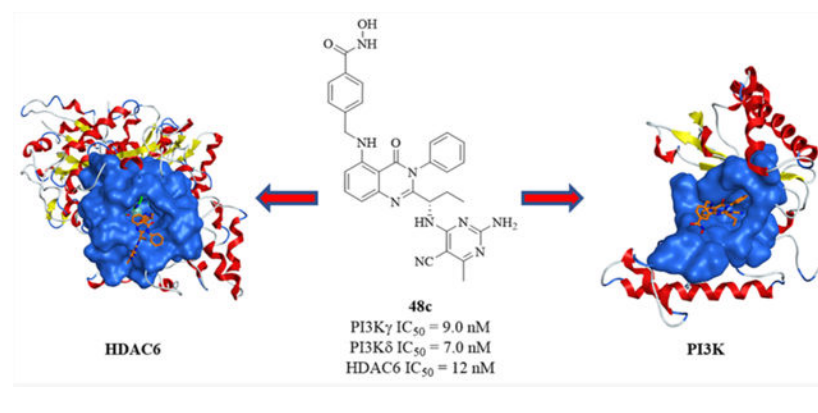
Gurmit Grewal

National Center for Advancing Translational Sciences, National Institutes of Health, Rockville, Maryland 20850, United States;

Abstract

A series of quinazolin-4-one based hydroxamic acids was rationally designed and synthesized as novel dual PI3K/HDAC inhibitors by incorporating an HDAC pharmacophore into a PI3K inhibitor (Idelalisib) via an optimized linker. Several of these dual inhibitors were highly potent ($IC_{50} < 10$ nM) and selective against PI3K γ , δ and HDAC6 enzymes and exhibited good antiproliferative activity against multiple cancer cell lines. The lead compound **48c**, induced necrosis in several mutant and FLT3-resistant AML cell lines and primary blasts from AML patients, while showing no cytotoxicity against normal PBMCs, NIH3T3, and HEK293 cells. Target engagement of PI3K δ and HDAC6 by **48c** was demonstrated in MV411 cells using the cellular thermal shift assay (CETSA). Compound **48c** showed good pharmacokinetics properties in mice via intraperitoneal (ip) administration and provides a means to examine the biological effects of inhibiting these two important enzymes with a single molecule, either in vitro or in vivo.

Graphical Abstract



INTRODUCTION

Most of the currently approved drugs based on the “single-target single drug” model are becoming less effective in the treatment of complex, heterogeneous, multigenic diseases, like cancer.^{1,2} While drug combination therapies are employed as an alternative approach to achieve efficacy, their benefits are often negated by adverse drug–drug interactions, unpredictable pharmacokinetic (PK) and safety profiles, and poor patient compliance.^{3,4} In recent years, there has been an increasing inclination toward discovering “multitarget drugs” to address the limited efficacy and resistance or toxicity associated with many single-target or combination-based therapies.^{5–12}

Class I phosphoinositide 3-kinases (PI3Ks) are lipid kinase enzymes that transduce signals from cell surface receptors (RTK, GPCR, etc.) to downstream effectors (Akt, mTOR, etc.), leading to a variety of cellular processes, including cell proliferation, survival, differentiation, metabolism, and angiogenesis.^{13,14} Specifically, class I PI3Ks phosphorylate phosphatidylinositol (4,5)-bisphosphate (PI(4,5)P₂ or PIP₂) in vivo to form the secondary messenger phosphatidylinositol (3,4,5)-trisphosphate (PI(3,4,5)P₃ or PIP₃), which activates the pleckstrin homology (PH)-domain of protein kinases (Akt, BTK, etc.), leading to downstream signaling.^{15,16} The four isoforms of Class I PI3Ks (PI3K α , PI3K β , PI3K γ , and PI3K δ) exist as heterodimers, consisting of a catalytic p110 (α , β , δ , γ) subunit and a regulatory p85 (α , β , δ) or p101/p84 (γ) subunit.¹⁴ The PI3K α and PI3K β isoforms are ubiquitously expressed, whereas PI3K γ and PI3K δ expression is limited to leukocytes.¹⁶ Aberrant regulation of class I PI3Ks has been implicated in several cancer types, and their inhibition continues to be an active cancer therapeutic area with four recently approved PI3K inhibitor drugs (Idelalisib, Copanlisib, Duvelisib, and Alpelisib) (Figure 1) and several others in ongoing clinical trials.^{17–20} Despite tremendous progress in the discovery of PI3K inhibitors (PI3Ki) over the past decade, clinical trials with PI3Ki as a monotherapy have shown poor efficacy,²¹ prompting their evaluation in combination therapies and/or developing PI3K-based multitarget drugs.¹⁹

Histone deacetylases (HDACs) are an important class of epigenetic enzymes that regulate gene expression by removing acetyl groups from ϵ -amino lysine residues on histones.²² HDACs play an important role in regulating expression of various proteins, including tumor suppressors (p53, p21, etc.) and transcription factors (e.g., TFIIIE, TCF, SF1, etc.).²³

Dysregulation of HDACs is involved in cancer initiation and proliferation.²⁴ HDAC inhibition has emerged as a therapeutic approach for cancer and several inhibitors, including Vorinostat (SAHA), Romidepsin, Belinostat, Panobinostat, and Chidamide, have been approved in recent years (Figure 2A).²⁵ Pan-HDAC inhibitors, such as Panobinostat and Vorinostat (SAHA), modulate the acetylation status of a wide range of protein targets leading to a therapeutic response; however, these molecules also have undesirable effects, including hematological, gastrointestinal, and cardiac toxicity.^{25–27} SAHA monotherapy was approved by the U.S. Food and Drug Administration (FDA) in 2006 for the treatment of cutaneous T-cell lymphoma (CTCL), however, it has been demonstrated to have little efficacy.²⁸

Although both PI3K and HDAC inhibitor drugs are limited by insufficient efficacy and resistance mutations, there is strong evidence that simultaneous inhibition of both PI3K and HDAC can synergistically inhibit tumor growth and address these limitations by improving efficacy, limiting resistance, and providing a better therapeutic window than single inhibitors.^{28–30} Selective inhibitors of specific isoforms of HDAC and PI3K potentially would have a better toxicity profile and therefore bigger therapeutic window.³¹ In this context, several dual PI3K/HDAC inhibitors have been recently reported in literature,^{32–34} with Curis Inc.'s Fimepinostat (CUDC-907) currently being evaluated in phase 2 clinical trials for treatment of diffuse large B-cell lymphoma (DLBCL) [Figure 2B].^{19,35,36} Dual inhibitors, such as CUDC-907, may thus offer improved therapeutic benefit through synergistic effects in inhibiting cancer cell proliferation and their compensatory pathways for survival.^{19,35} However, CUDC-907 exhibits pan-HDAC and pan-PI3K inhibition, which might lead to toxicity and low tolerability.^{37,38} Thus, there remains an unmet need for new dual inhibitors having high potency and selectivity.

Herein we report the design, synthesis, and biological evaluation of potent and selective dual PI3K/HDAC inhibitors.

RESULTS AND DISCUSSION

Design of Dual Inhibitors.

The rational design of our PI3K/HDAC dual inhibitors commenced by analyzing the crystal structures of Idelalisib (**1**) bound to PI3K δ [PDB 4XE0]³⁹ (Figure 3A) and Vorinostat (**2**) bound to HDAC2 [PDB 4LXZ]⁴⁰ (Figure 3B), respectively. As shown in Figure 3A, the purine moiety in Idelalisib binds to the hinge (Glu826, Val828) and the quinazolinone core extends up into a pocket formed by the G loop residues, Trp760 and Met752. The carbonyl and fluoro group in the quinazolinone core at fourth and fifth positions, respectively, extend into the solvent exposed area, and therefore, serve as desired locations to attach the HDAC pharmacophore. The phenyl ring on the nitrogen in the quinazolinone core is largely solvent exposed (on top) but makes hydrophobic contacts underneath to methyl groups on Thr833 and Met900. In the Vorinostat-HDAC2 structure (Figure 3B), Zn²⁺ is penta-coordinated (Asp181, Asp260, His183, and both oxygens on hydroxamic acid) and the hydroxamic acid group forms hydrogen bonds to two charge relay histidines (His145 and His146) and a nearby Tyr308. The Vorinostat aliphatic chain traverses a hydrophobic portion of the pocket

(Leu144, Phe155). The phenyl group forms a hydrogen bond to the rim of the pocket at Asp104 via the amino nitrogen.

In general, most of the HDAC inhibitors, including Vorinostat, share these three common structural components: a zinc binding group (e.g., hydroxamic acid), a linker occupying the hydrophobic tunnel in the active site, and a cap group that sits outside the hydrophobic tunnel and interacts with the HDAC surface residues (Figure 4).⁴¹ More importantly, the HDAC inhibitors can accommodate a wide variety of cap groups, which allows for replacement of the cap with a second target pharmacophore to design HDAC inhibitor based multitarget drugs.^{32,33,42–50} Thus, by assessing the binding features of Idelalisib and Vorinostat in PI3K δ and HDAC2 enzymes, respectively, we designed quinazoline- and quinazolinone-based dual PI3K/HDAC inhibitors (**3** and **4**, Figure 4) by incorporating the PI3K δ inhibitor as the cap group of an HDAC pharmacophore and optimizing for the appropriate linker-hydroxamic acid combination at quinazolinone's C-4 position (**3**) or quinazolinone's C-5 position (**4**) to achieve potencies against both the targets.

Chemistry.

The C-4 substituted quinazoline compounds (**10a,b** and **14a,b**) were synthesized from *tert*-butyl (*S*)-(1-(4-chloroquinazolin-2-yl)propyl)carbamate **5**⁵¹ in 6–7 steps as outlined in Scheme 1. The compound **5** was subjected to Sonogashira cross-coupling reactions with alkynes **6a** and **6b**, using a copper-free Pd/P^tBu₃-catalytic system to afford **7a,b**. Reduction of alkyne group to alkane in **7a,b** using Pd/C hydrogenation, followed by boc-deprotection and nucleophilic aromatic substitution of 6-chloro-9-(tetrahydro-2*H*-pyran-2-yl)-9*H*-purine **8** with the resulting free amine, yielded compounds **9a,b**. Hydrolysis of the alkyl ester in **9a,b** to the respective carboxylic acid, followed by coupling with NH₂OTHP (THP = tetrahydropyran) and THP-deprotection using trifluoroacetic acid formed the target compounds **10a,b**.

The synthesis of C-4 amino-alkyl substituted compounds (**14a,b**) began by subjecting compound **5** to nucleophilic aromatic substitution with amines **11a,b** to yield compounds **12a,b**. Boc-deprotection in **12a,b**, followed by the installation of a purine kinase hinge binding moiety using nucleophilic aromatic substitution (S_NAr) on **8**, afforded compounds **13a,b**. Target compounds **14ab,b** were synthesized from **13a,b** by converting alkyl ester to hydroxamic acid, in a fashion similar to that described above for compounds **10a,b**.

The procedure for syntheses of C-5 alkyl/aryl substituted quinazolinone-based compounds is depicted in Scheme 2. The quinazolinone compound **15a**⁵² was subjected to Sonogashira cross-coupling reactions with alkynes **16a–c** to yield compounds **17a–c**. Hydrogenation of alkyne in **17a–c** followed by Boc-deprotection and nucleophilic aromatic substitution on purine **8** afforded compounds **18a–c**. Target compounds **19a–c** were derived from **18a–c** by either: (a) hydrolyzing the alkyl ester to carboxylic acid, coupling with NH₂OTHP followed by deprotection of THP-protecting groups using TFA, or (b) converting the alkyl ester directly to hydroxamic acid using aq NH₂OH/LiOH and subsequent removal of the THP-protecting group using TFA. The latter method also formed carboxylic acid as the minor side product due to ester hydrolysis (see Supporting Information).

For C-5 aryl substituted quinazolinone-based compounds, 5-bromo or 5-chloro-quinazolinone (**15a** or **15a'**) was either subjected to a Suzuki–Miyaura cross-coupling reaction with boronic acids **20a,b** or first converted to boronate ester **21** using Pd(dppf)Cl₂/Bpin₂, followed by Suzuki–Miyaura coupling with aryl bromide **20c**, to form compounds **22a–c**. These C-5 arylated molecules **22a–c** were converted to target compounds **24a–c** in a sequence of steps similar to that previously described for compounds **19a–c**.

The synthesis of C-5 amino-alkyl/aryl substituted quinazolinones involved the Pd/XantPhos-catalyzed amination of 5-bromo-quinazolinone **15a,b** with amines **25a–h**, yielding compounds **26a–i** (Scheme 3). Subsequent attachment of purine 8 and conversion of alkyl esters to hydroxamic acids afforded the target compounds **28a–h**. For compound **28i**, the methyl ester in **27d** was converted to *N*-methyl hydroxamic acid via hydrolysis to carboxylic acid, followed by its coupling with *N*-methyl hydroxylamine using HATU/DIPEA.

The procedure for synthesizing C-5 alkyl-amino substituted quinazolinones commenced from the Pd-catalyzed cyanation of C-5 bromide in **15a,b** and subsequent hydrogenation of the nitrile group to form compounds **30a,b** (Scheme 4). The free amine in **30a** was reacted with ethyl 2-bromothiazole-4-carboxylate, **31** to yield **32a**, which was converted to final compound **33** using a similar sequence of steps as described in previous schemes. For target compounds **37**, **40a,b**, and **43**, compound **29a** was subjected to Boc-deprotection and nucleophilic aromatic substitution on purine **8** to afford **34** (Scheme 4). Hydrogenation of the nitrile group in **34** to free amine was utilized in synthesizing a variety of linkers using (a) amide-coupling with **35**, (b) reductive amination with **38a,b**, and (c) substitution with **41**, to form compounds **36**, **39a,b**, and **42**. Subsequent conversion of alkyl esters to hydroxamic acids and removal of the THP protecting groups afforded the target compounds, **37**, **40a,b**, and **43**.

C-5 alkyl-substituted quinazolinones with pyrimidine kinase hinge binding groups (**46a–d**) were readily synthesized from **17b,c** in four steps as shown in Scheme 5. The alkyne group in **17b,c** was hydrogenated using Raney-Ni followed by Bocdeprotection and S_NAr on chloropyrimidines **44a–c** to form compounds **45a–d**. Subsequent conversion of methyl esters in **45a–d** to hydroxamic acids using hydroxylamine afforded the target compounds **46a–d**.

C-5 amino-alkyl substituted quinazolinones (**48a–o**) were synthesized in a similar fashion from compounds **26b,d,g,i** by attaching the pyrimidine kinase binding moieties using S_NAr reactions on **44a,b,d–l** and converting methyl esters in **47a–o** to hydroxamic acids.

For synthesis of quinazolinones **51** and **54**, the nitrile group in compound **29b** was hydrogenated using Raney Ni/H₂ to generate free amine, which was either coupled to 4-(methoxycarbonyl)benzoic acid **35** using HATU/DIPEA or subjected to S_NAr reaction with ethyl 2-chloropyrimidine-5-carboxylate **41** to form compounds **49** and **52**, respectively (Scheme 6). Subsequent attachment of the pyrimidine kinase hinge binding group and transformation of alkyl esters to hydroxamic acids yielded the target compounds **51** and **54**.

PI3K and HDAC: Enzyme Inhibition Activity and SAR.

The dual inhibitors were screened against PI3K and HDAC enzymes at Reaction Biology Corporation, Malvern, PA, USA. Initially, we compared the enzyme inhibitory activities of 4-substituted quinazolines vs 5-substituted quinazolinones by screening against PI3K δ and HDAC1–11 enzymes (Table 1). In general, 5-substituted quinazolinones were consistently found to be more potent than the 4-substituted quinazolines for PI3K and HDAC enzyme inhibition. As shown for a few examples in Table 1, 5-substituted quinazolinones having 4- and 5-carbon alkylene linkers (**19a**, **19b**) and amino-propylene linker (**28a**), showed more potent PI3K/HDAC activities than their 4-substituted quinazolinone counterparts (**10a**, **10b**, **14a**). Additionally, the 5-substituted compounds showed high potency and selectivity for HDAC6 inhibition, leading us to focus only on 5-substituted quinazolinones.

Next, we explored the linker region on 5-substituted quinazolinones by incorporating a variety of aryl, heteroaryl, and amino-aryl groups on the PI3K core. Initially we screened against PI3K isoforms (α , β , γ , δ) and HDAC isoforms (1, 2, 3, 6, 8, and 10) at a single dose (1 μ M for PI3Ks and 10 μ M for HDAC enzymes). As shown in Table 2, dual inhibitors with a variety of linkers were synthesized and tested to establish SAR. Dual inhibitors with aryl (**24a**) and heteroaryl linkers such as benzothiazole (**24c**) showed high potency for PI3K δ and HDAC6, 8, whereas benzyl linker (**24b**) only showed high PI3K δ activity. The use of amino-alkyl heterocycle linkers such as 3-(methylamino) pyridine (**28f**) and 2-(methylamino) thiazole (**33**) showed good inhibition for PI3K and HDAC6, but the corresponding alkyl-amino furan (**28h**) lost its potency against both enzymes. Linkers containing basic amines (**40a,b**) exhibited modest to high HDAC6 activity (80% for **40a**, 99% for **40b**) but were inactive against PI3Ks. Select dual inhibitors that showed high single-point potency (% inhibition) in both PI3K δ and HDAC6 were subsequently tested in 10-dose IC₅₀ titration against PI3Ks (α , β , γ , δ) and HDAC 1–11 isozymes.

Table 3 shows the PI3K and HDAC enzyme potencies of the 5-substituted quinazolinone with purine hinge binding group. The dual inhibitor containing the pentyl group as linker (**19b**) exhibited high activity and selectivity for both PI3K δ (IC₅₀ = 0.2 nM, >210-fold selectivity over PI3K α,β,γ) and HDAC6 (IC₅₀ = 13 nM, >65 fold-selectivity over HDAC1–5,7–11). Substitution with a homobenzyl (**19c**) or phenyl linker (**24a**) showed high PI3K δ inhibition but poor activity against HDAC6. Swapping the homobenzylic linker with 1-(methylamino) benzyl group (**28d**) restored HDAC6 activity and selectivity along with good PI3K δ activity. Interestingly, substituting the 1-(methylamino) benzyl linker in **28d** with a 1-(methylamino)-3-methylbenzyl group in **28e** maintained the PI3K δ activity but completely abolished the HDAC activity. A similar trend in PI3K δ /HDAC6 potency was observed with (3-methylamino)pyridyl linker in **28f**, where HDAC6 activity was lost, presumably due to hydrogen-bonding interaction of the pyridyl N atom with O–H group on hydroxamic acid, thereby impacting the chelation of hydroxamic acid with Zn in the HDAC6 enzyme (Figure 5). To further support this hydrogen bonding rationale, we designed and synthesized compound **28g** with a (2-methylamino)pyridyl linker, where the possibility of H-bonding interaction with the pyridyl N atom and –OH group of hydroxamic acid was eliminated. Gratifyingly, the HDAC6 potency was restored in **28g** (IC₅₀ = 9 nM) when compared with **28f** (IC₅₀ = 169 nM) (Figure 5).

Substituting the hydroxamic acid in **28d** to *N*-methyl hydroxamic acid as zinc-binding group in **28i** led to a 2-fold drop in PI3K δ potency and complete loss in activity against all HDACs tested. The dual inhibitor containing *N*-methylbenzamide (**37**) as the linker resulted in high activity and selectivity in both PI3K δ and HDAC6. Compound **43** with a 2-(aminomethyl)-pyrimidine linker also showed good potency and selectivity against PI3K δ and HDAC6 inhibition.

Despite high activity and selectivity observed with several 5-substituted quinazolinones against PI3K δ /HDAC6, most did not show expected antiproliferative/cell kill activities when tested against the NCI-60 panel (see section titled, “NCI-60 Human Tumor Cell Lines Screen”). We hypothesized that their poor cellular potency might be due to low permeability (predicted by PAMPA permeability)⁵³ generally observed with these dual inhibitors. Table 4 shows the PAMPA permeability values of selected 5-substituted quinazolinones with a purine hinge binding group.

To improve upon the cellular potencies of 5-substituted quinazolinones, we investigated a new series of dual inhibitors by substituting the purine kinase hinge binding moiety with amino-pyrimidine groups.^{52,54–56} Table 5 shows the PI3K and HDAC enzyme inhibition data for selected 5-substituted quinazolinones with amino-pyrimidine hinge binding groups. Compounds **46a,b** with 2,4-diamino-6-pyrimidine-5-carbonitrile and 2-amino-6-methylpyrimidine-5-carbonitrile hinge binding groups, respectively, showed excellent PI3K δ activity (IC₅₀ = 0.2–0.7 nM), but a weaker HDAC6 potency (IC₅₀ = 28–69 nM), when compared with compound **19b** from the purine series (PI3K δ IC₅₀ = 0.2 nM, HDAC6 IC₅₀ = 13 nM). Compound **46d** with a homobenzyl linker and 2,4-diamino-6-pyrimidine-5-carbonitrile hinge binding group was highly active against PI3K δ (IC₅₀ = 0.2 nM) but showed a modest potency for HDAC6 (IC₅₀ = 77 nM). Dual inhibitors with amino-benzyl/ amino-methylpyridyl linkers were explored with a variety of amino-pyrimidine kinase hinge binders to establish SAR. Replacement of the pentyl linker in **46b** with aminobutyl linker in **48a** with the same hinge binding group showed high potencies for PI3K γ,δ but no activity against HDACs. Compound **48b** with 2,4-diamino-6-pyrimidine-5-carbonitrile hinge binder showed moderate potency for PI3K γ,δ but high potency and selectivity for HDAC6. The PI3K potency was restored in **48c** using a 2-amino-6-methylpyrimidine-5-carbonitrile hinge binding group while maintaining good potency for HDAC6. Removing the nitrile group in **48c** gave compound **48d**, which was inactive against PI3K. Dual inhibitors with amino-pyrimidines lacking the 2-amino group in the hinge region (**48e,f,g**) showed high HDAC6 activity (IC₅₀ = 3–4 nM) but poor PI3K δ potency (PI3K δ IC₅₀ = 60 nM for **48e**, 133 nM for **48f**, 189 nM for **48g**). Similar detrimental effects on PI3K potencies were observed when the C-5 nitrile group on the aminopyrimidine was changed to Cl (**48h**, **48j**) and the C-2 amino group was changed to Me (**48i**). Replacement of the C-6 methyl/amino group in the kinase hinge to CF₃, cyclopropyl, and CF₂H, respectively, were also not good for PI3K activity (**48k**, **48l**, **48m**). Overall, only 2-amino-6-methylpyrimidine-5-carbonitrile and 2,4-diamino-6-pyrimidine-5-carbonitrile hinge binding groups were revealed as optimal hinge binders for achieving high potencies for both PI3K and HDAC enzymes. While HDAC6 activity and selectivity obtained by using these amino-pyrimidine hinge binders were similar to their purine hinge binder counterparts, less PI3K selectivity was observed with

aminopyrimidine series, with almost equipotent activities against PI3K γ and PI3K δ in many examples. Swapping the ethyl group at R¹ with a methyl group was tolerated well to obtain compounds (**48n**, **48o**) with single-digit nM activities against PI3K γ, δ and HDAC6. Compounds having 2,4-diamino-6-pyrimidine-5-carbonitrile as hinge binder with *N*-methylbenzamide and 2-(amino-methyl)-pyrimidine linkers (**51** and **54**) also showed high PI3K/HDAC6 activity. In general, dual inhibitors with aminopyrimidine hinge binders showed comparatively better PAMPA permeability (Table 6) than their purine hinge binding counterparts. Additionally, 5-substituted quinazolinones with amino-pyrimidine hinge binders showed potent cell activities when tested in the NCI-60 panel (see section NCI-60 assays and Supporting Information).

Molecular Modeling: HDAC6 Binding and Selectivity.

The dual inhibitor **19b** was docked into the solved crystal structure of hHDAC6 (PDB 5EDU.pdb) (Figure 6A).⁵⁷ The geometry of the protein around the **19b** hydroxamic acid headgroup mirrors that of Vorinostat (see Figure 3). The aliphatic linker chain, in similar fashion, traverses a hydro-phobic region of the pocket. The capping group, which is composed of a quinazolinone ring system, on the other hand, forms a hydrogen bond to Ser568 via the quinazolinone carbonyl. This hydrogen bonding interaction on the rim of the pocket is distinctly different than that made by Vorinostat.

HDAC6 Selectivity.—Using the procedure described in Methods, we identified Ser568 as the only residue on HDAC6 that could be responsible for the HDAC selectivity profile of **19b**. As shown in Figure 6A, Ser568 in HDAC6 forms a hydrogen bond with the quinazolinone carbonyl on **19b**. In the case of HDACs-1, 2, 3, and 8, Ser568 becomes Asp568 (Figure 6B). The negatively charged carboxyl group on Asp568 is a hydrogen bond acceptor and does not form a hydrogen bond with the quinazolinone carbonyl on **19b** (Figure S1–S3, Supporting Information). Rather, the Asp568 carboxyl repulses the quinazolinone carbonyl and swings away from the ligand. The nearby presence of Glu567 (HDAC1,2, Figure S1, Supporting Information) and Asp567 (HDAC3, Figure S2, Supporting Information) contributes to this process as these residues have negatively charged carboxyl side chains.

In the case of HDAC8, the residue adjacent to Asp568 is tyrosine, which contains a neutral phenyl side chain (Figure S3, Supporting Information). As a result, the conformational shift in the carboxyl group on position 568 is less significant than for HDACs-1,2,3. Nevertheless, the H bond to the quinazolinone carbonyl is still broken. In the case of HDACs-4,5,7, and 9, threonine occupies position 568. Thr568 contains a hydrogen bond donor (hydroxyl), but the hydroxyl group does not interact with the quinazolinone carbonyl on the ligand. That is because the extra methyl group on the Thr568 side chain clashes with nearby Gly619 and prevents the OH group from obtaining a favorable hydrogen bonding position with respect to the quinazolinone carbonyl. In fact, it is easier for the Thr568 OH group to hydrogen bond with the carboxyl side chain of nearby Asp567 (Figure S4, Supporting Information). In the case of HDAC10, Ser568 becomes Ala568 resulting in an obvious loss of hydrogen bonding to the quinazolinone carbonyl on the ligand (Figure S5, Supporting Information). In HDAC11, Ser568 becomes Asn568. Although asparagine has a hydrogen bond donating

nitrogen group, its side chain is one carbon too long to adopt a reasonable orientation for hydrogen bonding to the quinazolinone carbonyl on the ligand (Figure S6, Supporting Information). The **19b**-HDAC interaction energies relative to **19b**-HDAC6 were computed for each of the scenarios described above. These interaction energies are completely consistent with the idea that there is one less hydrogen bond between **19b** and HDACs-1, 2, 3, 4, 5, 7, 8, 9, 10,11 than there is between **19b** and HDAC6 hence, explaining the selectivity of **19b** to HDAC6.

Kinase Selectivity.

The kinase selectivity of **48c** was investigated at 1 μM concentration against a panel of 412 kinases, including 24 atypical kinases and 17 lipid kinases at Reaction Biology Corporation, PA. As shown in Figure 7A, the dual inhibitor **48c** showed very high selectivity across the diverse kinase families, including atypical kinases, with less than 50% inhibition among all the kinases tested (Table S2, Supporting Information). In the case of the highly homologated lipid kinases (Figure 7B), compound **48c** showed between 74 and 83% inhibition for PI3K α , β , and other PI3K mutants while maintaining the high selectivity for PI3K γ and PI3K δ (99% inhibition), as previously observed.

NCI-60 Human Tumor Cell Lines Screen.

The dual inhibitors were tested against 60 human cancer cell lines at the National Cancer Institute (NCI-60 panel).⁵⁸ The NCI-60 employs an initial single-dose (10 μM compound concentration) growth inhibition screen against 60 cancer cell lines and selects only the most potent compounds for subsequent 5-point dose–response studies. As previously mentioned, most of the dual inhibitors (except **28d**) with the purine hinge binding group showed a poor growth inhibition profile (average growth inhibition (%) = 0–33%) across all the 60 cell lines tested and therefore were not evaluated in dose–response IC₅₀. Compound **28d** with the amino-benzyl linker and purine hinge binder was the only dual inhibitor (from the purine series) selected for NCI-60–cell line dose–response and showed potent antiproliferative activities against multiple human cancer cell line types (Table 7). In contrast to the purine series, several dual inhibitors bearing amino-pyrimidine kinase hinge binding groups were evaluated for dose–response, with a few of them even showing better GI₅₀ than Idelalisib and SAHA.

Dual Inhibitors Decrease Survival and Induce Cell Death in Diverse Types of AML Cells.

Dual inhibitor **48c** was evaluated in cell viability assays against several myeloma and leukemia cell lines as shown in Figure 8A,B. Cell-viability was determined using the CellTiter-Glo (Promega) assay⁵⁹ or by the trypan blue exclusion assay.⁶⁰ Compound **48c** showed good inhibitory activity against FLT3-ITD mutant AML cell lines, MOLM-14 and MV411. Further studies were performed with **48c** in other types of AML cell lines. THP-1 is a spontaneously immortalized monocyte-like cell line derived from the peripheral blood of a childhood case of acute monocytic leukemia (M5 subtype).⁶¹ HL-60 is a human promyelocytic leukemia cell line with p53-null mutation.⁶² Compound **48c** demonstrated antiproliferative activity against these cell lines with IC₅₀ values in the 2–5 μM range (Figure 8A). Like MOLM-14 cells, MOLM-13 AML cells have one wild-type FLT3 and one

FLT3-ITD allele.⁶³ Treatment of MOLM-13 cells with **48c** resulted in inhibition of growth that was concentration-dependent [Figure 8B(2)]. As shown previously, loss of MOLM-13 cell survival was observed in response to treatment with the type II ATP competitive inhibitor HG-7-85-01 (HG) (data not shown).⁶⁰ Interestingly, MOLM-13 cells selected for resistance to HG were also sensitive to compound **48c** treatment [Figure 8B(3)], indicating that targeting PI3K δ /HDAC6 is effective against MOLM-13 cells resistant to FLT3 inhibitors. Dual inhibitors **48c**, **48n**, and **48o**, when screened alongside Idelalisib,⁶⁴ SAHA⁶⁵ and CUDC-907⁶⁶ (at their IC₅₀ range) against MV411 cell line displayed better potency than Idelalisib and SAHA but were less potent than the pan PI3K/HDAC inhibitor, CUDC-907, as expected (Figure 8C). Importantly, dual inhibitor **48c** showed no cytotoxicity against normal human peripheral blood mononuclear cells (PBMCs) [Figure 8D], demonstrating its high selectivity in targeting leukemia cells over PBMCs. Additionally, dual inhibitors **48c**, **48n**, and **48o**, were nontoxic against NIH3T3 normal fibroblasts, whereas significant toxicity was observed with the pan-inhibitor CUDC-907, even at a low concentration of 50 nM (Figure 8E). These studies clearly indicate that our isoform-selective dual inhibitors display potent antitumor activity with no toxicity in normal cells.

To further define the activity of these dual inhibitors on AML cell lines, we determined potential induction of cell death as measured by propidium iodide (PI) alone or PI/Annexin V staining followed by flow cytometry.⁶⁷ Dual inhibitors **48c**, **48n**, and **48o** induced cell death via necrosis in multiple AML cell lines as shown in Figure 9A–C. Both compounds **48n** and **48o** were able to induce >50% necrosis at 5 μ M concentration in MOLM-14, MV4-11, and HL-60 tumor cells (Figure 9A,B). Similarly, dual inhibitor **48c** was highly active for inducing necrosis across several AML cell lines, including >60% necrosis in MOLM-13 FLT3 inhibitor-resistant cell line (MOLM-13 HG Res) (Figure 9C). To determine whether primary AML cells also respond to compound **48c**, blasts from a patient with AML were grown in short-term culture. The AML primary cells were then treated with 5 μ M compound **48c** for 72 h. The results demonstrate induction of substantial necrosis in these primary cells (Figure 9D). Notably, dual inhibitors **48c**, **48n**, and **48o** displayed no significant necrotic activity against normal human HEK293 cells, whereas pan-inhibitors SAHA and CUDC-907, induced necrosis in these cells, again demonstrating the selective targeting of tumor cells over normal cells by our compounds.

Clonogenic Survival Assay.

Encouraged by their growth inhibitory activities against multiple AML cell lines, dual inhibitors **48c** and **48o** were tested in an in vitro clonogenic assay for inhibition against MOLM-14 colony formation (Figure 10). MOLM-14 cells were seeded in 6-well plates for 24 h and then left untreated or treated with either 2.5 or 5 μ M of **48c** and **48o**, respectively. After 48 h, the cells were washed and seeded in soft agar for the generation of colonies. After 10 days, colonies of >50 cells were counted. Plating efficiency of untreated MOLM-14 cells as colony formation is very high as multiple colonies (>50 cells) were seen. Gratifyingly, treatment of MOLM-14 cells with our dual inhibitors **48c** and **48o** resulted in significant decrease in clonogenic survival as shown below in Figure 10.

PI3K δ Inhibition Decreases Activation of Downstream Effectors.

PI3K activates the AKT pathway. MOLM-14 cells were treated for 1, 6, and 24 h, with dual inhibitor **48c** (5.0 μ M) and analyzed for p-Akt and total Akt levels by immunoblotting. In concert with the demonstration that dual inhibitors downregulate PI3K activation, treatment of MOLM-14 cells with compound **48c** was associated with complete inhibition of p-AKT with no change in the total AKT protein levels as shown in Figure 11.

CETSA.

Next, we examined target engagement using the cellular thermal shift assay (CETSA).⁶⁸ Three lymphocytic cell lines were profiled by immunoblot for HDAC6 and PI3K δ expression, and MV411 was selected for subsequent experiments based on detection of both targets (Figure S7, Supporting Information). The CETSA melt profile (T_{agg}) of each protein was then measured (Figure 12A,B), and 58 1/2C (HDAC6) and 52 1/2C (PI3K δ) were selected for isothermal dose–response experiments. The control compounds showed the anticipated responses, with CAY10603 (HDAC6 inhibitor) stabilizing HDAC6 and Idelalisib (PI3K δ inhibitor) stabilizing PI3K δ . For the dual inhibitors, robust HDAC6 stabilization was observed for **48c**, with less stabilization observed for **46b** and HDAC6 only inhibitor **48d** (Figure 12C). For PI3K δ , PI3K inhibitor **45b**, and dual inhibitor, **48c** stabilized the protein, whereas **46b** and **48d** did not (Figure 12D). These results indicate compound **48c** can engage both HDAC6 and PI3K δ in the complex cellular environment.

In Vitro ADME Assays.

Selected dual inhibitors were evaluated in multispecies (human, mouse, and rat) liver microsome/cytosol stability and Caco-2 permeability and efflux assays (Table 8). Compound **19b** showed good stability in human liver microsomes (HLM) but was poor in mouse (MLM) and rat liver microsomes (RLM). **19b** displayed low ($t_{1/2} < 30$ min) to moderate ($30 < t_{1/2} < 60$ min) metabolic stability in liver cytosol from the three species. Additionally, it was found to have low permeability in Caco-2 cell monolayer assay and an efflux ratio of 11, indicating the involvement of efflux transporters. Dual inhibitor **46b**, the pyrimidine hinge binding analogue of **19b**, showed similar stability in HLM and MLM assays as **19b** but was significantly better in RLM and cytosol assays. In contrast to compounds **19b** and **46b**, the dual inhibitors bearing amino-benzyl linker (**48b**, **48c**, **48n**, **48o**) displayed moderate to high stability in MLM and RLM assays but the HLM stability varied from low to high with compound **48n**, showing high stability across the three species tested. Additionally, these compounds show high cytosolic stability in human, mouse, and rat assays. The lead compound **48c** had low cell permeability (1.9×10^{-6} cm/s), however, its efflux ratio of 3.5 was found to be on the lower side.

Pharmacokinetics.

Because of its potent PI3K/HDAC inhibitory and antitumor activity, compound **48c** was progressed to an in vivo pharmacokinetic (PK) study in female Balb/c mice (Table 9 and Figure 13). The plasma PK of **48c** via intravenous (iv) route at 3 mg/kg dose revealed its high clearance at 57 mL/min/kg with terminal half-life ($t_{1/2}$) of 1 h (Figure 13A). Unfortunately, po administration of **48c** at 10 mg/kg dose exhibited very low exposure with

an oral bioavailability (F) of only 0.7% (Figure 13A). When administered intraperitoneally (ip) at 50 and 150 mg/kg dose, respectively, compound **48c** displayed better PK properties with significantly improved in vivo exposure in terms of C_{\max} and AUC when compared to po administration (Figure 13B). This preliminary PK assessment suggested that ip administration would be the preferred dosing route for the proof of concept (POC) purpose in the in vivo antitumor efficacy study in mouse model.

CONCLUSIONS

In summary, we have rationally designed and synthesized a series of quinazolin-4-one-based hydroxamic acids for the dual inhibition of PI3K and HDAC enzymes. Structure–activity relationship (SAR) exploration revealed several compounds as potent and selective PI3K γ , δ /HDAC6 inhibitors with good cellular potencies against a panel of 60 different cancer cell lines at National Cancer Institute (NCI-60). Particularly, compound **48c** was identified as potent dual inhibitor with high kinome selectivity and potent antiproliferative activity against various cancer cell lines, including leukemia, melanoma, renal, nonsmall cell lung cancer, central nervous system (CNS) cancer, and breast cancer. Dual inhibitor **48c** also showed good potency in inducing cell death via necrosis in multiple AML cell lines, including the FLT3-ITD mutant and FLT3-inhibitor resistant cell lines, and AML patient's primary cells. The dual PI3K δ /HDAC6 activity of **48c** was further supported by the target engagement studies in MV411 cell line using the cellular thermal shift assay (CETSA). Compound **48c** showed decent microsomal stability and in vivo PK profile and warrants further exploration in antitumor efficacy study in mice. Further lead optimization efforts to achieve new potent dual inhibitors with favorable in vivo PK profiles are currently underway in our laboratory.

EXPERIMENTAL SECTION

Chemistry.

All air or moisture sensitive reactions were performed under positive pressure of nitrogen with oven-dried glassware. Chemical reagents and anhydrous solvents were obtained from commercial sources and used as is. Preparative purification was performed on a Waters semipreparative HPLC instrument. The column used was a Phenomenex Luna C18 (5 μm , 30 mm \times 75 mm) at a flow rate of 45 mL/min. The mobile phase consisted of acetonitrile and water (each containing 0.1% trifluoroacetic acid). A gradient from 10% to 50% acetonitrile over 8 min was used during the purification. Fraction collection was triggered by UV detection (220 nm). Alternately, flash chromatography on silica gel was performed using forced flow (liquid) of the indicated solvent system on Biotage KP-Sil prepacked cartridges and using the Biotage SP-1 automated chromatography system. Analytical analysis for purity was determined by two different methods denoted as final QC methods 1 and 2. Method 1: Analysis was performed on an Agilent 1290 Infinity series HPLC instrument. UHPLC long gradient equivalent from 4% to 100% acetonitrile (0.05% trifluoroacetic acid) in water over 3 min run time of 4.5 min with a flow rate of 0.8 mL/min. A Phenomenex Luna C18 column (3 μm , 3 mm \times 75 mm) was used at a temperature of 50 $^{\circ}\text{C}$. Method 2: Analysis was performed on an Agilent 1260 with a 7 min gradient from 4% to 100%

acetonitrile (containing 0.025% trifluoroacetic acid) in water (containing 0.05% trifluoroacetic acid) over 8 min run time at a flow rate of 1 mL/min. A Phenomenex Luna C18 column (3 μ m, 3 mm \times 75 mm) was used at a temperature of 50 $^{\circ}$ C. Purity determination was performed using an Agilent diode array detector for both method 1 and method 2. Mass determination was performed using an Agilent 6130 mass spectrometer with electrospray ionization in the positive mode. All assay compounds had >95% purity based on both analytical methods. 1 H NMR spectra were recorded on Varian 400 MHz spectrometers. All proton spectra are referenced relative to the deuterated solvent peak: 7.27 ppm for CDCl_3 , 2.50 ppm (center line signal) for $\text{DMSO-}d_6$. High resolution mass spectrometry results were recorded on Agilent 6210 time-of-flight LC/MS system.

General Procedure for Sonogashira Cross-Coupling Reaction (GP1).—Aryl bromide (1.0 equiv), allylpalladium(II) chloride dimer (0.05 equiv), tri-*tert*-butylphosphonium tetrafluoroborate (0.20 equiv), and alkyne (1.2 equiv) (if solid at room temperature) were weighed and added to a MW vial equipped with a stir bar. The vial was covered with a rubber septum and placed under nitrogen atmosphere. In a separate scintillation vial, DABCO was weighed and dissolved in dry 1,4-dioxane (5 mL/mmol of aryl bromide). This DABCO solution and alkyne (if liquid at room temperature) were added to the MW vial via syringe, and the resulting mixture was bubbled with nitrogen for 5 min followed by stirring for 16 h at room temperature under nitrogen atmosphere. After 16 h, the crude reaction mixture was filtered through a short pad of Celite and concentrated in vacuo. The remaining residue was purified by flash chromatography on silica using forced flow of ethyl acetate/hexanes system on Biotage KP-Sil prepacked cartridges and using the Biotage SP-1 automated chromatography system to afford the cross-coupled product.

General Procedure for Pd/C-Catalyzed Hydrogenation (GP2).—The substituted alkyne (1.0 equiv) and 10 wt % Pd/C were added to a 20 mL scintillation vial fitted with a rubber septum. The reaction vial was evacuated followed by the addition of dry EtOAc (0.1M). The vacuum was removed, and the reaction vial was stirred for 20 h under an atmosphere of hydrogen using a balloon. After completion of reaction (determined by LC-MS), the crude reaction mixture was filtered using Celite, concentrated in vacuo, and carried over to the next step without purification.

General Procedure for Attachment of Purine Hinge Binding Group (GP3).—The Boc-protected amine (1.0 equiv) was dissolved in DCM (0.1 M) in a vial, and trifluoroacetic acid (20 equiv) was added dropwise to it. The resulting mixture was stirred at room temperature for 3 h. After completion of reaction (by LC-MS), the reaction mixture was worked-up by either of the following two methods. Method A: The crude reaction was quenched with aqueous saturated NaHCO_3 solution and extracted three times with DCM. The combined organic layers were dried over anhydrous MgSO_4 , filtered, and concentrated in vacuo to afford the free amine. Method B: The crude reaction mixture was concentrated in vacuo, redissolved in 1–2 mL of DCM, and passed through preconditioned PL- HCO_3 MP SPE device (bicarbonate resin solid phase extraction) and washed with 2 mL of DCM. The filtrate was concentrated in vacuo to afford the free amine. The resulting free amine was dissolved in ethanol (0.4 M) in a microwave vial equipped with a stir bar followed by the

addition of 6-chloro-9-(tetrahydro-2*H*-pyran-2-yl)-9*H*-purine (1.5–2.0 equiv) and triethylamine (3.0–4.0 equiv) to it. The vial was sealed and heated for 4 h at 100 1/2C in a microwave. After completion of reaction (by LCMS), the reaction mixture was concentrated in vacuo and the remaining residue was purified by flash chromatography on silica gel using forced flow of indicated solvent system on Biotage KP-Sil prepacked cartridges and using the Biotage SP-1 automated chromatography system to afford the product.

General Procedure for Conversion of Alkyl Ester to Hydroxamic Acid (GP4).—

The alkyl ester was converted to hydroxamic acid in the final product by either of the following two methods. Method A: The alkyl ester was dissolved in THF/water (0.1 M, 1:1 by vol) in a vial equipped with a stir bar, and LiOH·H₂O (2.0 equiv) was added to it. The resulting mixture was stirred at room temperature for 10 h and concentrated in vacuo to afford the carboxylic acid. The crude carboxylic acid was dissolved in DMF (0.1 M) in a vial, and *O*-(tetrahydro-2*H*-pyran-2-yl)hydroxylamine [NH₂OTHP] (3.1 equiv), *N*-methyl morpholine (3.0 equiv), 3-(((ethylimino)methylene)-amino)-*N,N*-dimethylpropan-1-amine hydrochloride [EDC·HCl] (1.4 equiv), and 1*H*-[1,2,3]triazolo[4,5-*b*]pyridin-1-ol [HOAT] (1.2 equiv) were added to it. The resulting mixture was stirred at room temperature for 16 h, concentrated in vacuo, and purified by flash chromatography on silica using forced flow of 0–10% MeOH/DCM system on Biotage KP-Sil prepacked cartridges and using the Biotage SP-1 automated chromatography system. The purified compound was dissolved in DCM (0.1 M), and TFA (20.0 equiv) was added to it. The resulting mixture was stirred for 20 h. After completion of reaction (by LC-MS), the reaction mixture was concentrated in vacuo and purified on preparative HPLC to afford the final compound. Method B: The alkyl ester was dissolved in MeOH (0.1M) or THF/MeOH (0.1 M, 1:1 by vol) in a MW vial equipped with a stir bar and LiOH·H₂O (1.1 equiv), and 50% hydroxylamine in water solution (30.0 equiv) were added at to it 0 1/2C. The MW vial was sealed, and the resulting solution was stirred at 0 1/2C for 2 h, then allowed to warmup to room temperature overnight. After completion of reaction by LC-MS, the reaction mixture was concentrated in vacuo, dissolved in DCM/MeOH (0.1M, 1:1 by vol), and TFA (20.0 equiv) was added to it. The resulting mixture was stirred at room temperature for 20 h. After completion of reaction (by LC-MS), the reaction mixture was concentrated in vacuo and purified on preparative HPLC to afford the final compound.

Procedure for Synthesis of C4-Substituted Quinazolines (10a,b and 14a,b, Scheme 1).—Sonogashira Cross-Coupling of Compound 5 with Alkynes **6a,b**. (S)-tert-Butyl 5-(2-(1-((tert-Butoxycarbonyl)-amino)propyl)quinazolin-4-yl)pent-4-ynoate (**7a**). The general procedure GP1 was used with (S)-tert-butyl (1-(4-chloroquinazolin-2-yl)propyl)carbamate **5** (180.0 mg, 0.56 mmol), allylpalladium(II) chloride dimer (10.1 mg, 0.028 mmol), tri-tert-butylphosphonium tetrafluoroborate (16.0 mg, 0.06 mmol), DABCO (125.0 mg, 1.12 mmol), and tert-butyl pent-4-ynoate **6a** (104.0 mg, 0.67 mmol) in dry 1,4-dioxane (2.8 mL). The remaining residue was purified by flash chromatography on silica using 0–25% ethyl acetate/hexanes system to afford (S)-tert-butyl 5-(2-(1-((tert-butoxycarbonyl)amino)propyl)-quinazolin-4-yl)pent-4-ynoate **7a** (150.0 mg, 0.34 mmol) as a yellow oil in 61% yield. LC-MS (method 1): t_R = 3.85 min, m/z (M + H)⁺ = 440.3. ¹H NMR (400 MHz, CDCl₃) δ 8.29–8.24 (m, 1H), 7.99 (d, J = 8.5 Hz, 1H), 7.88 (ddd, J = 8.5,

6.9, 1.4 Hz, 1H), 7.62 (ddd, $J = 8.3, 6.9, 1.2$ Hz, 1H), 5.90 (d, $J = 8.2$ Hz, 1H), 5.02 (d, $J = 7.3$ Hz, 1H), 2.91 (t, $J = 7.4$ Hz, 2H), 2.69 (t, $J = 7.1$ Hz, 2H), 2.15–2.02 (m, 1H), 1.89 (dt, $J = 14.0, 7.3$ Hz, 1H), 1.49 (s, 9H), 1.47 (s, 9H) 0.90 (t, $J = 7.4$ Hz, 3H).

Methyl (S)-6-(2-(1-((tert-Butoxycarbonyl)amino)propyl)-quinazolin-4-yl)hex-5-ynoate (7b). The general procedure GP1 was used with (*S*)-*tert*-butyl (1-(4-chloroquinazolin-2-yl)propyl)-carbamate **5** (225.0 mg, 0.70 mmol), allylpalladium(II) chloride dimer (13.0 mg, 0.04 mmol), tri-*tert*-butylphosphonium tetrafluoroborate (20.0 mg, 0.07 mmol), DABCO (157.0 mg, 1.4 mmol), and methyl hex-5-ynoate **6b** (115.0 mg, 0.91 mmol) in dry 1,4-dioxane (3.5 mL). The remaining residue was purified by flash chromatography on silica using 0–30% ethyl acetate/hexanes system to afford the product, methyl (*S*)-6-(2-(1-((*tert*-butoxycarbonyl)amino)-propyl)quinazolin-4-yl)hex-5-ynoate **7b** (163.6 mg, 0.398 mmol) as a yellow oil in 57% yield. LC–MS (method 1): $t_R = 3.51$ min, m/z ($M + H$)⁺ = 412.3. ¹H NMR (400 MHz, CDCl₃) δ 8.26 (ddd, $J = 8.3, 1.5, 0.7$ Hz, 1H), 8.03–7.97 (m, 1H), 7.90 (ddd, $J = 8.4, 6.9, 1.4$ Hz, 1H), 7.65 (ddd, $J = 8.2, 6.8, 1.2$ Hz, 1H), 5.91 (d, $J = 8.2$ Hz, 1H), 5.03 (d, $J = 6.9$ Hz, 1H), 3.72 (s, 3H), 2.74 (t, $J = 7.1$ Hz, 2H), 2.60 (t, $J = 7.3$ Hz, 2H), 2.10 (p, $J = 7.2$ Hz, 2H), 1.90 (dt, $J = 13.6, 7.2$ Hz, 2H), 1.46 (s, 9H), 0.91 (dd, $J = 8.2, 7.0$ Hz, 3H).

(S)-5-(2-(1-((9H-Purin-6-yl)amino)propyl)quinazolin-4-yl)-N-hydroxypentanamide (10a). Step 1. (i) *Alkyne hydrogenation*. The general procedure GP2 was used with compound **7a** (45.0 mg, 0.102 mmol) and 10 wt % Pd/C (4.5 mg). After completion of reaction (determined by LC-MS), the crude reaction mixture was filtered using Celite, concentrated in vacuo, and carried over to the next step without purification. (ii) *Attachment of purine hinge binding group*. The general procedure GP3 was used on the hydrogenated product (formed above) with trifluoroacetic acid (233.0 mg, 2.04 mmol, 0.16 mL) in DCM (1.0 mL). The crude reaction was worked-up (method B) and reacted with 6-chloro-9-(tetrahydro-2H-pyran-2-yl)-9H-purine **8** (48.7 mg, 0.20 mmol) and triethylamine (41.3 mg, 0.41 mmol, 57 μ L) in ethanol (0.3 mL). The remaining residue was purified by flash chromatography on silica gel using 0–5% MeOH (0.5% AcOH)/ DCM to afford the product 5-(2-((1*S*)-1-((9-(tetrahydro-2H-pyran-2-yl)-9H-purin-6-yl)amino)propyl)quinazolin-4-yl)pentanoic acid **9a** (27.7 mg, 0.057 mmol) in 56% yield. LC–MS (method 1): $t_R = 2.92$ min, m/z ($M + H$)⁺ = 490.3. Step 2. *Conversion of carboxylic acid to hydroxamic acid*. The general procedure GP4 (method A, without the LiOH hydrolysis step) was used with carboxylic acid, **9a** (16.3 mg, 0.033 mmol) to afford the final product, (*S*)-5-(2-(1-((9H-purin-6-yl)amino)propyl)quinazolin-4-yl)-*N*-hydroxypentanamide, TFA (**10a**) (7.5 mg, 0.014 mmol) in 55% yield. LC–MS (method 2): $t_R = 3.40$ min, m/z ($M + H$)⁺ = 421.2. ¹H NMR (400 MHz, DMSO-*d*₆) δ 10.50 (s, 1H), 8.40–8.28 (m, 3H), 8.03–7.94 (m, 2H), 7.76–7.67 (m, 1H), 3.32 (h, $J = 7.9$ Hz, 2H), 2.23–2.14 (m, 1H), 2.07 (dt, $J = 19.8, 6.9$ Hz, 3H), 1.85–1.76 (m, 2H), 1.76–1.66 (m, 2H), 1.62–1.57 (m, 1H), 0.93 (t, $J = 7.3$ Hz, 3H). HRMS (ESI) m/z : [$M + H$]⁺ calcd for C₂₁H₂₅N₈O₂ 421.2095, found 421.2087.

Compound 9b was synthesized using a similar procedure, as described above for 9a.—(*S*)-6-(2-(1-((9H-Purin-6-yl)amino)propyl)quinazolin-4-yl)-*N*-hydroxyhexanamide (**10b**). The general procedure GP4 (method A) was used with compound **9b** (70.4 mg, 0.14 mmol) to afford the final product, (*S*)-6-(2-(1-((9H-purin-6-yl)amino)propyl)quinazolin-4-

yl)-*N*-hydroxyhexanamide, TFA (**10b**) (45.0 mg, 0.082 mmol) in 60% yield. LC–MS (method 2): $t_R = 3.53$ min, m/z ($M + H$)⁺ = 435.3. ¹H NMR (400 MHz, DMSO-*d*₆) δ 10.35 (s, 1H), 8.39 (d, $J = 8.8$ Hz, 2H), 8.32 (dt, $J = 8.4, 1.1$ Hz, 1H), 7.99–7.95 (m, 2H), 7.76–7.70 (m, 1H), 5.59 (s, 1H), 3.29 (h, $J = 7.1$ Hz, 2H), 2.20 (dd, $J = 14.6, 7.7$ Hz, 1H), 2.08 (dt, $J = 13.6, 7.4$ Hz, 1H), 1.93 (t, $J = 7.3$ Hz, 2H), 1.79 (p, $J = 7.5$ Hz, 2H), 1.53 (p, $J = 7.3$ Hz, 2H), 1.34 (p, $J = 7.7$ Hz, 2H), 0.94 (t, $J = 7.3$ Hz, 3H). HRMS (ESI) m/z : [$M + H$]⁺ calcd for C₂₂H₂₇N₈O₂ 435.2251, found 435.2250.

(S)-4-((2-(1-((9*H*-Purin-6-yl)amino)propyl)quinazolin-4-yl)amino)-*N*-hydroxybutanamide (**14a**). Step 1. *N*-Alkylation. Compound **5** (103.0 mg, 0.32 mmol) was dissolved in ethanol (0.7 mL) in a 5 mL microwave vial equipped with a stir bar, and ethyl 4-aminobutyrate hydrochloride (107.0 mg, 0.64 mmol) and triethylamine (130.0 mg, 1.28 mmol, 0.18 mL) were added to it. The vial was sealed and heated at 100 1/2C for 1 h in a microwave. After completion of reaction (by LC-MS), the reaction mixture was concentrated in vacuo and the remaining residue was purified on silica using 0–30% EtOAc/hexanes to afford (*S*)-ethyl 4-((2-(1-((*tert*-butoxycarbonyl)-amino)propyl)quinazolin-4-yl)amino)butanoate **12a** (125.0 mg, 0.30 mmol) in 94% yield. LC–MS (method 1): $t_R = 2.85$ min, m/z ($M + H$)⁺ = 417.3. ¹H NMR (400 MHz, CDCl₃) δ 7.78 (d, $J = 8.4$ Hz, 1H), 7.75–7.63 (m, 2H), 7.40 (t, $J = 7.6$ Hz, 1H), 6.51 (s, 1H), 6.04 (d, $J = 7.9$ Hz, 1H), 4.75 (q, $J = 6.6$ Hz, 1H), 4.12 (q, $J = 7.2$ Hz, 2H), 3.71 (q, $J = 6.2$ Hz, 2H), 2.50 (t, $J = 6.7$ Hz, 2H), 2.07 (p, $J = 6.8$ Hz, 2H), 2.03–1.97 (m, 1H), 1.88 (dt, $J = 13.8, 7.0$ Hz, 1H), 1.47 (s, 9H), 1.22 (t, $J = 7.1$ Hz, 3H), 0.89 (t, $J = 7.5$ Hz, 3H). Step 2. Attachment of purine hinge binding group. The general procedure GP3 was used compound **12a** (120.0 mg, 0.29 mmol) and with trifluoroacetic acid (661.0 mg, 5.8 mmol, 0.44 mL) in DCM (3.0 mL). The crude Bocdeprotected amine was worked-up (method A) and reacted with 6-chloro-9-(tetrahydro-2*H*-pyran-2-yl)-9*H*-purine **8** (140.4 mg, 0.58 mmol) and triethylamine (118.0 mg, 1.16 mmol, 0.16 mL) in ethanol (0.7 mL). The remaining residue was purified by flash chromatography on silica gel using 0–5% MeOH/DCM to afford ethyl 4-((2-((1*S*)-1-((9-(tetrahydro-2*H*-pyran-2-yl)-9*H*-purin-6-yl)amino)-propyl)quinazolin-4-yl)amino)butanoate **13a** (113.0 mg, 0.22 mmol) in 77% yield. LC–MS (method 1): $t_R = 2.78$ min, m/z ($M + H$)⁺ = 519.3. Step 3. Conversion of alkyl ester to hydroxamic acid. The general procedure GP4 (method A) was used with compound **13a** (100.0 mg, 0.193 mmol) to afford the final product, (*S*)-4-((2-(1-((9*H*-purin-6-yl)amino)propyl)quinazolin-4-yl)amino)-*N*-hydroxybutanamide, TFA (**14a**) (39.0 mg, 0.073 mmol) in 38% yield. LC–MS (method 2): $t_R = 2.70$ min, m/z ($M + H$)⁺ = 422.1. ¹H NMR (400 MHz, DMSO-*d*₆) δ 10.56 (s, 1H), 8.38 (d, $J = 8.1$ Hz, 1H), 8.28 (d, $J = 16.0$ Hz, 2H), 8.05–7.96 (m, 1H), 7.88–7.81 (m, 1H), 7.74 (t, $J = 7.7$ Hz, 1H), 3.63 (ddd, $J = 35.6, 13.3, 6.7$ Hz, 3H), 2.20–2.02 (m, 4H), 2.02–1.88 (m, 1H), 1.78 (dq, $J = 13.4, 6.7$ Hz, 1H), 1.03 (t, $J = 7.4$ Hz, 3H). HRMS (ESI) m/z : [$M + H$]⁺ calcd for C₂₀H₂₄N₉O₂ 422.2047, found 422.2055.

Compound 13b was synthesized from 5 and 11b, using the similar procedure as described for 13a.—(*S*)-6-((2-(1-((9*H*-Purin-6-yl)amino)propyl)quinazolin-4-yl)amino)-*N*-hydroxyhexanamide (**14b**). The general procedure GP4 (method A) was used with compound **13b** (280.0 mg, 0.526 mmol) to afford the final product, (*S*)-6-((2-(1-((9*H*-purin-6-yl)amino)-propyl)quinazolin-4-yl)amino)-*N*-hydroxyhexanamide, TFA **14b** (112.5 mg, 0.200 mmol) in 38% yield. LC–MS (method 2): $t_R = 2.77$ min, m/z ($M + H$)⁺ = 450.3.

^1H NMR (400 MHz, DMSO- d_6) δ 10.09 (s, 1H), 8.38 (dd, J = 8.5, 1.2 Hz, 2H), 8.31 (s, 1H), 8.22 (s, 1H), 8.01 (ddd, J = 8.3, 7.1, 1.2 Hz, 1H), 7.85 (dd, J = 8.5, 1.1 Hz, 1H), 7.74 (ddd, J = 8.3, 7.2, 1.2 Hz, 1H), 5.24 (s, 1H), 3.69 (dq, J = 13.2, 6.6 Hz, 1H), 3.55 (dt, J = 13.1, 6.6 Hz, 1H), 2.14 (q, J = 7.2 Hz, 2H), 1.88 (t, J = 7.3 Hz, 2H), 1.56–1.41 (m, 2H), 1.41–1.34 (m, 2H), 1.17 (q, J = 7.7 Hz, 2H), 1.06 (t, J = 7.4 Hz, 3H). HRMS (ESI) m/z . $[\text{M} + \text{H}]^+$ calcd for $\text{C}_{22}\text{H}_{28}\text{N}_9\text{O}_2$ 450.2360, found 450.2377.

Procedure for Synthesis of C5-Substituted Quinazolinones (19a–c and 24a–c, Scheme 2).—

Sonogashira Cross-Coupling of Compound 15a with Alkynes 16a–c. tert-Butyl (S)-5-(2-(1-((tert-butoxycarbonyl)amino)propyl)-4-oxo-3-phenyl-3,4-dihydroquinazolin-5-yl)pent-4-ynoate (17a). The general procedure GP1 was used with *tert*-butyl (S)-1-(5-bromo-4-oxo-3-phenyl-3,4-dihydroquinazolin-2-yl)propyl)carbamate **15a** (150.0 mg, 0.33 mmol), allylpalladium(II) chloride dimer (5.9 mg, 0.02 mmol), tri-*tert*-butylphosphonium tetrafluoroborate (9.5 mg, 0.03 mmol), *tert*-butyl pent-4-ynoate **16a** (60.6 mg, 0.39 mmol), and DABCO (73.4 mg, 0.66 mmol) in 2.5 mL of dry 1,4-dioxane. The remaining residue was purified by flash chromatography on silica using 0–25% ethyl acetate/hexanes to afford *tert*-butyl (S)-5-(2-(1-((tert-butoxycarbonyl)amino)propyl)-4-oxo-3-phenyl-3,4-dihydroquinazolin-5-yl)pent-4-ynoate **17a** (130.0 mg, 0.245 mmol) as a yellow oil in 75% yield. LC–MS (method 1): t_R = 3.90 min, m/z ($\text{M} + \text{H}$) $^+$ = 532.4. ^1H NMR (400 MHz, CDCl_3) δ 7.67–7.48 (m, 6H), 7.37 (d, J = 8.0 Hz, 1H), 7.32–7.28 (m, 1H), 5.55 (s, 1H), 4.38 (s, 1H), 2.74 (dd, J = 8.4, 6.7 Hz, 2H), 2.55 (dd, J = 8.3, 6.7 Hz, 2H), 1.47–1.40 (m, 18H), 0.76 (t, J = 7.4 Hz, 3H).

Methyl (S)-6-(2-(1-((tert-butoxycarbonyl)amino)propyl)-4-oxo-3-phenyl-3,4-dihydroquinazolin-5-yl)hex-5-ynoate (17b). The general procedure GP1 was used with *tert*-butyl (S)-1-(5-bromo-4-oxo-3-phenyl-3,4-dihydroquinazolin-2-yl)propyl)carbamate **15a** (234.0 mg, 0.51 mmol), allylpalladium(II) chloride dimer (9.3 mg, 0.03 mmol), tri-*tert*-butylphosphonium tetrafluoroborate (15.0 mg, 0.05 mmol), methyl hex-5-ynoate **16b** (77.0 mg, 0.613 mmol), and DABCO (115.0 mg, 1.02 mmol) in 2.5 mL of dry 1,4-dioxane. The remaining residue was purified by flash chromatography on silica using 0–30% ethyl acetate/hexanes to afford methyl (S)-6-(2-(1-((tert-butoxycarbonyl)amino)propyl)-4-oxo-3-phenyl-3,4-dihydroquinazolin-5-yl)hex-5-ynoate **17b** (162.0 mg, 0.322 mmol) as a yellow oil in 63% yield. LC–MS (method 1): t_R = 3.60 min, m/z ($\text{M} + \text{H}$) $^+$ = 504.3. ^1H NMR (400 MHz, CDCl_3) δ 7.67–7.47 (m, 6H), 7.39–7.28 (m, 2H), 5.49 (d, J = 9.0 Hz, 1H), 4.38 (s, 1H), 3.65 (s, 3H), 2.53 (dt, J = 15.0, 7.2 Hz, 4H), 1.94 (p, J = 7.2 Hz, 2H), 1.79–1.66 (m, 1H), 1.57–1.45 (m, 2H), 1.43 (s, 9H), 0.75 (t, J = 7.4 Hz, 3H).

Methyl (S)-4-(2-(1-((tert-butoxycarbonyl)amino)propyl)-4-oxo-3-phenyl-3,4-dihydroquinazolin-5-yl)ethynyl)benzoate (17c). The general procedure GP1 was used with *tert*-butyl (S)-1-(5-bromo-4-oxo-3-phenyl-3,4-dihydroquinazolin-2-yl)propyl)carbamate **15a** (183.0 mg, 0.40 mmol), allylpalladium(II) chloride dimer (7.2 mg, 0.02 mmol), tri-*tert*-butylphosphonium tetrafluoroborate (12.0 mg, 0.04 mmol), methyl 4-ethynylbenzoate **17c** (77.0 mg, 0.48 mmol), and DABCO (90.0 mg, 0.80 mmol) in 2.0 mL of dry 1,4-dioxane. The resulting mixture was stirred at room temperature for 16 h and concentrated in vacuo. The remaining residue was purified by flash chromatography on silica using 0–25% ethyl

acetate/hexanes to afford methyl (*S*)-4-((2-(1-((*tert*-butoxycarbonyl)amino)propyl)-4-oxo-3-phenyl-3,4-dihydroquinazolin-5-yl)ethynyl)benzoate **17c** (200.0 mg, 0.37 mmol) as a yellow solid in 93% yield. LC–MS (method 1): $t_R = 3.78$ min, m/z ($M + H$)⁺ = 538.3. ¹H NMR (400 MHz, CDCl₃) δ 8.00–7.95 (m, 2H), 7.74–7.69 (m, 3H), 7.66–7.49 (m, 5H), 7.40 (d, $J = 7.9$ Hz, 1H), 7.36–7.30 (m, 1H), 5.49 (d, $J = 9.0$ Hz, 1H), 4.40 (s, 1H), 3.91 (s, 3H), 1.75 (ddd, $J = 13.9, 7.3, 4.6$ Hz, 1H), 1.55–1.48 (m, 1H), 1.43 (s, 9H), 0.77 (t, $J = 7.4$ Hz, 3H).

(*S*)-5-(2-(1-((9*H*-Purin-6-yl)amino)propyl)-4-oxo-3-phenyl-3,4-dihydroquinazolin-5-yl)-*N*-hydroxypentanamide (**19a**). Step 1. (i) *Alkyne hydrogenation*. The general procedure GP2 was used with compound **17a** (102.0 mg, 0.19 mmol) and 10 wt % Pd/C (10.0 mg) in dry ethyl acetate (1.9 mL). After completion of reaction (determined by LC–MS), the crude reaction mixture was filtered using Celite, concentrated in vacuo, and carried over to the next step without purification. (ii) *Attachment of purine hinge binding group*. The general procedure GP3 was used on the hydrogenated product (formed above) with trifluoroacetic acid (438.0 mg, 3.84 mmol, 0.29 mL) in DCM (1.9 mL). The crude Boc-protected amine was worked-up (method B) and reacted with 6-chloro-9-(tetrahydro-2*H*-pyran-2-yl)-9*H*-purine **8** (92.0 mg, 0.38 mmol) and triethylamine (78.0 mg, 0.77 mmol, 0.1 mL) in ethanol (0.5 mL). The remaining residue was purified by flash chromatography on silica gel using 0–100% EtOAc (0.5% AcOH by vol)/hexanes to afford 5-(4-oxo-3-phenyl-2-((1*S*)-1-((9-(tetrahydro-2*H*-pyran-2-yl)-9*H*-purin-6-yl)-amino)propyl)-3,4-dihydroquinazolin-5-yl)pentanoic acid **5.2n** (60.0 mg, 0.103 mmol) in 54% yield. LC–MS (method 1): $t_R = 3.17$ min, m/z ($M + H$)⁺ = 582.4. Step 2. *Conversion of carboxylic acid to hydroxamic acid*. The general procedure GP4 (method A, without the LiOH hydrolysis step) was used with carboxylic acid, **18a** (17.0 mg, 0.03 mmol), to afford the final product, (*S*)-5-(2-(1-((9*H*-purin-6-yl)amino)propyl)-4-oxo-3-phenyl-3,4-dihydroquinazolin-5-yl)-*N*-hydroxypentanamide, TFA **19a** (8.0 mg, 0.013 mmol) in 43% yield. LC–MS (method 2): $t_R = 3.74$ min, m/z ($M + H$)⁺ = 513.2. ¹H NMR (400 MHz, DMSO-*d*₆) δ 10.28 (s, 1H), 8.26 (s, 1H), 7.68 (t, $J = 7.7$ Hz, 1H), 7.56 (d, $J = 7.3$ Hz, 3H), 7.50 (d, $J = 1.2$ Hz, 1H), 7.48 (s, 1H), 7.28 (dd, $J = 7.6, 1.2$ Hz, 1H), 7.20 (s, 1H), 7.07 (s, 1H), 6.95 (s, 1H), 4.74 (s, 1H), 3.81 (s, 1H), 3.14 (s, 2H), 1.97–1.90 (m, 2H), 1.90–1.79 (m, 1H), 1.53–1.48 (m, 3H), 0.76 (t, $J = 7.3$ Hz, 3H). HRMS (ESI) m/z . [$M + H$]⁺ calcd for C₂₇H₂₉N₈O₃ 513.2357, found 513.2346.

Compounds 19b and 19c were synthesized using the similar procedure as described for 19a.—(*S*)-6-(2-(1-((9*H*-Purin-6-yl)amino)propyl)-4-oxo-3-phenyl-3,4-dihydroquinazolin-5-yl)-*N*-hydroxyhexanamide (**19b**). The general procedure GP4 (method B) was used with compound **18b** (60.0 mg, 0.098 mmol) to afford the final product (*S*)-6-(2-(1-((9*H*-purin-6-yl)amino)propyl)-4-oxo-3-phenyl-3,4-dihydroquinazolin-5-yl)-*N*-hydroxyhexanamide, TFA **19b** (15.0 mg, 0.023 mmol) in 24% yield. LC–MS (method 2): $t_R = 3.75$ min, m/z ($M + H$)⁺ = 527.3. ¹H NMR (400 MHz, DMSO-*d*₆) δ 10.27 (s, 1H), 8.32 (s, 2H), 7.73–7.64 (m, 1H), 7.59–7.46 (m, 5H), 7.29 (dd, $J = 7.5, 1.3$ Hz, 1H), 4.76 (s, 1H), 3.13 (t, $J = 7.7$ Hz, 2H), 2.04–1.95 (m, 1H), 1.94–1.78 (m, 3H), 1.47 (p, $J = 7.6$ Hz, 4H), 1.27 (dt, $J = 14.4, 7.6$ Hz, 2H), 0.77 (t, $J = 7.3$ Hz, 3H). HRMS (ESI) m/z . [$M + H$]⁺ calcd for C₂₈H₃₁N₈O₃ 527.2514, found 527.2524.

(*S*)-4-(2-(2-(1-((9*H*-Purin-6-yl)amino)propyl)-4-oxo-3-phenyl-3,4-dihydroquinazolin-5-yl)ethyl)-*N*-hydroxybenzamide (**19c**). The general procedure GP4 (method A) was used with

compound **18c** (12.0 mg, 0.019 mmol) to afford the final product (*S*)-4-(2-(2-(1-((9*H*-purin-6-yl)amino)propyl)-4-oxo-3-phenyl-3,4-dihydroquinazolin-5-yl)ethyl)-*N*-hydroxybenzamide, TFA **19c** (3.0 mg, 0.005 mmol) in 25% yield. LC-MS (method 2): $t_R = 3.94$ min, m/z ($M + H$)⁺ = 561.3. HRMS (ESI) m/z : [$M + H$]⁺ calcd for C₃₁H₂₉N₈O₃ 561.2357, found 561.2357.

(*S*)-4-(2-(1-((9*H*-Purin-6-yl)amino)propyl)-4-oxo-3-phenyl-3,4-dihydroquinazolin-5-yl)-*N*-hydroxybenzamide (**24a**). Step 1. *Suzuki cross-coupling reaction*. ((*S*)-*tert*-butyl (1-(5-chloro-4-oxo-3-phenyl-3,4-dihydroquinazolin-2-yl)propyl)carbamate **15a'** (261.0 mg, 0.63 mmol), chloro(crotyl)(2-dicyclohexylphosphino-2',4',6'-triisopropylbiphenyl)palladium(II) [Pd-170] (21.0 mg, 0.03 mmol), and (4-(ethoxycarbonyl)phenyl)boronic acid **20a** (147.0 mg, 0.76 mmol) were suspended in 1,4-dioxane/water (2.0 mL, 4:1 by vol) in a MW vial equipped with a stir bar under N₂ atmosphere, and potassium phosphate (402.0 mg, 1.89 mmol) was added to it. The MW vial was sealed and heated at 100 1/2C for 1 h in a MW reactor. The reaction mixture was allowed to cool to RT, quenched with water, and then extracted 3 times with ethyl acetate. The combined organic fractions were dried over MgSO₄ and then concentrated in vacuo. The remaining residue was purified by flash chromatography on silica using 0–35% ethyl acetate/hexanes to afford ethyl (*S*)-4-(2-(1-((*tert*-butoxycarbonyl)amino)propyl)-4-oxo-3-phenyl-3,4-dihydroquinazolin-5-yl)benzoate **22a** (320.0 mg, 0.61 mmol) as a colorless solid in 96% yield. LC-MS (method 1): $t_R = 3.82$ min, m/z ($M + H$)⁺ = 528.3. ¹H NMR (400 MHz, CDCl₃) δ 8.05–8.00 (m, 2H), 7.80–7.76 (m, 2H), 7.56–7.40 (m, 3H), 7.39–7.30 (m, 3H), 7.27 (t, $J = 4.4$ Hz, 1H), 7.22–7.16 (m, 1H), 5.57 (d, $J = 9.1$ Hz, 1H), 4.41 (d, $J = 8.6$ Hz, 1H), 4.36 (q, $J = 7.1$ Hz, 2H), 1.76 (ddd, $J = 14.2, 7.4, 4.6$ Hz, 1H), 1.62–1.53 (m, 1H), 1.45 (s, 9H), 0.78 (t, $J = 7.4$ Hz, 3H). Step 2. *Installation of purine hinge binding group*. The general procedure GP3 was used with **22a** (320.0 mg, 0.61 mmol) and trifluoroacetic acid (1.38 g, 12.13 mmol, 0.93 mL) in DCM (6.0 mL). The crude Boc-protected amine was worked-up (method A) and reacted with 6-chloro-9-(tetrahydro-2*H*-pyran-2-yl)-9*H*-purine (289.0 mg, 1.21 mmol) and triethylamine (245 mg, 2.42 mmol, 0.34 mL) in ethanol (1.2 mL). The remaining residue was purified by flash chromatography on silica gel using 0–5% MeOH/DCM to afford ethyl 4-(4-oxo-3-phenyl-2-((1*S*)-1-((9-(tetrahydro-2*H*-pyran-2-yl)-9*H*-purin-6-yl)amino)propyl)-3,4-dihydroquinazolin-5-yl)benzoate **23a** (348.0 mg, 0.55 mmol) in 91% yield. LC-MS (method 1): $t_R = 3.56$ min, m/z ($M + H$)⁺ = 630.3. Step 3. *Conversion of alkyl ester to hydroxamic acid*. The general procedure GP4 (method A) was used with compound **23a** (73.2 mg, 0.116 mmol) to afford the final product, (*S*)-4-(2-(1-((9*H*-purin-6-yl)amino)propyl)-4-oxo-3-phenyl-3,4-dihydroquinazolin-5-yl)-*N*-hydroxybenzamide, TFA **24a** (53.0 mg, 0.082 mmol) in 71% yield. LC-MS (method 2): $t_R = 3.56$ min, m/z ($M + H$)⁺ = 533.2. ¹H NMR (400 MHz, DMSO-*d*₆) δ 11.18 (s, 1H), 8.69 (s, 1H), 8.42 (s, 2H), 7.84 (dd, $J = 8.2, 7.4$ Hz, 1H), 7.74–7.64 (m, 3H), 7.57–7.37 (m, 5H), 7.34–7.24 (m, 3H), 5.75 (s, 1H), 4.80 (s, 1H), 2.03 (ddd, $J = 11.6, 7.4, 3.6$ Hz, 1H), 1.87 (dt, $J = 14.7, 7.6$ Hz, 1H), 0.79 (t, $J = 7.3$ Hz, 3H). HRMS (ESI) m/z : [$M + H$]⁺ calcd for C₂₉H₂₅N₈O₃ 533.2044, found 533.2044.

Compound 24b was synthesized using the similar procedure as described for 24a.—(*S*)-2-(4-(2-(1-((9*H*-Purin-6-yl)amino)propyl)-4-oxo-3-phenyl-3,4-dihydroquinazolin-5-yl)phenyl)-*N*-hydroxyacetamide (**24b**). The general procedure GP4

(method A) was used with compound **23b** (33.4 mg, 0.052 mmol) to afford the final product, (*S*)-2-(4-(2-(1-((9*H*-purin-6-yl)amino)propyl)-4-oxo-3-phenyl-3,4-dihydroquinazolin-5-yl)phenyl)-*N*-hydroxyacetamide, TFA **24b** (12.7 mg, 0.019 mmol) in 36% yield. LC–MS (method 2): $t_R = 3.66$ min, m/z ($M + H$)⁺ = 546.2. ¹H NMR (400 MHz, DMSO-*d*₆) δ 10.64 (s, 1H), 8.67 (s, 1H), 8.42 (s, 2H), 7.81 (t, $J = 7.8$ Hz, 1H), 7.67 (dd, $J = 8.1, 1.3$ Hz, 1H), 7.57–7.39 (m, 5H), 7.25 (dd, $J = 7.4, 1.3$ Hz, 1H), 7.21–7.14 (m, 4H), 5.75 (s, 2H), 4.81 (s, 1H), 2.03 (dd, $J = 12.1, 6.8$ Hz, 1H), 1.86 (dt, $J = 14.7, 7.7$ Hz, 1H), 0.79 (t, $J = 7.3$ Hz, 3H). HRMS (ESI) m/z : [$M + H$]⁺ calcd for C₃₀H₂₇N₈O₃ 547.2201, found 547.2203.

Ethyl (S)-2-(2-(1-((tert-Butoxycarbonyl)amino)propyl)-4-oxo-3-phenyl-3,4-dihydroquinazolin-5-yl)benzo[d]thiazole-6-carboxylate (22c). To a mixture of ((*S*)-*tert*-butyl (1-(5-bromo-4-oxo-3-phenyl-3,4-dihydroquinazolin-2-yl)propyl)carbamate **15a** (116.0 mg, 0.25 mmol) and 4,4,4',4',5,5,5',5'-octamethyl-2,2'-bi(1,3,2-dioxaborolane) [BPin]₂ (77.0 mg, 0.30 mmol) in 1,4-dioxane (1.0 mL) in a sealed tube, Pd(dppf)Cl₂ (9.3 mg, 13.0 μ mol) and potassium acetate (74.5 mg, 0.76 mmol) were added under N₂ bubbling through the solvent. The resulting mixture was stirred at 100 $^{\circ}$ C for 16 h. After completion of the reaction, the crude reaction mixture was filtered into a MW vial equipped with a stir bar, and ethyl 2-bromobenzo[d]thiazole-6-carboxylate **20c** (60.0 mg, 0.21 mmol) and 0.1 mL of water were added to it. [Pd-170] (10.6 mg, 7.1 μ mol) and potassium phosphate (134.0 mg, 0.63 mmol) were added to this mixture under nitrogen atmosphere. The MW vial was sealed and heated at 100 $^{\circ}$ C for 10 h. The reaction mixture was allowed to cool to room temperature, quenched with water, and then extracted 3 times with ethyl acetate. The combined organic fractions were dried over MgSO₄ and then concentrated in vacuo. The remaining residue was purified by flash chromatography on silica using 0–45% EtOAc/hexanes to afford the coupled product, ethyl (*S*)-2-(2-(1-((*tert*-butoxycarbonyl)amino)propyl)-4-oxo-3-phenyl-3,4-dihydroquinazolin-5-yl)benzo[d]thiazole-6-carboxylate (87.0 mg, 0.15 mmol) **22c** in 70% yield. LC–MS (method 1): $t_R = 3.80$ min, m/z ($M + H$)⁺ = 585.2. ¹H NMR (400 MHz, CDCl₃) δ 8.59 (d, $J = 1.6$ Hz, 1H), 8.14 (dd, $J = 8.6, 1.7$ Hz, 1H), 8.05 (d, $J = 8.6$ Hz, 1H), 7.94 (d, $J = 8.3$ Hz, 1H), 7.90–7.82 (m, 1H), 7.63–7.40 (m, 4H), 7.36 (d, $J = 8.0$ Hz, 1H), 7.23 (d, $J = 7.3$ Hz, 1H), 5.50 (d, $J = 9.1$ Hz, 1H), 4.42 (q, $J = 7.1$ Hz, 3H), 1.75 (dt, $J = 12.6, 6.9$ Hz, 1H), 1.58–1.52 (m, 1H), 1.44 (m, 9H), 0.78 (t, $J = 7.4$ Hz, 3H).

Compound 23c was synthesized from 22c using the similar procedure as described for 23a.—(*S*)-2-(2-(1-((9*H*-Purin-6-yl)amino)propyl)-4-oxo-3-phenyl-3,4-dihydroquinazolin-5-yl)-*N*-hydroxybenzo[d]thiazole-6-carboxamide (**24c**). The general procedure GP4 (method B) was used with compound **23c** (16.4 mg, 0.024 mmol) to afford the final product, (*S*)-2-(2-(1-((9*H*-purin-6-yl)amino)propyl)-4-oxo-3-phenyl-3,4-dihydroquinazolin-5-yl)-*N*-hydroxybenzo[d]thiazole-6-carboxamide, TFA **24c** (5.0 mg, 0.007 mmol) in 32% yield. LC–MS (method 2): $t_R = 3.64$ min, m/z ($M + H$)⁺ = 590.2. ¹H NMR (400 MHz, DMSO-*d*₆) δ 11.33 (s, 1H), 8.47 (d, $J = 1.7$ Hz, 1H), 8.27 (s, 2H), 8.02 (d, $J = 8.5$ Hz, 1H), 7.97–7.83 (m, 4H), 7.67–7.60 (m, 2H), 7.58–7.47 (m, 4H), 7.42 (s, 3H), 4.73 (s, 1H), 2.01 (s, 1H), 1.89 (s, 1H), 0.78 (t, $J = 7.3$ Hz, 3H). HRMS (ESI) m/z : [$M + H$]⁺ calcd for C₃₀H₂₄N₉O₃S 590.1717, found 590.1708.

General Procedure for Pd-Catalyzed Amination Reaction (GP5). Aryl bromide (1 equiv), methanesulfonato[9,9-dimethyl-4,5-bis-(diphenylphosphino)xanthene](2'-methylamino-1,1'-biphenyl-2-yl)-palladium(II) XantPhos Palladacycle (methanesulfonato[9,9-dimethyl-4,5-bis(diphenylphosphino)xanthene](2'-methylamino-1,1'-biphenyl-2-yl)palladium(II), Strem Chemicals Inc.) (0.025–0.05 equiv), and amine [if solid] (1.3 equiv) were weighed and added to a microwave vial equipped with a stir bar. The vial was covered with a rubber septum, evacuated, and then filled with nitrogen. Dry toluene or 1,4-dioxane (0.2 M) and amine [if oil at room temperature] (1.3 equiv) were added to the vial, followed by the addition of Cs₂CO₃ (3.0 equiv) under nitrogen bubbling through the solvent. The microwave vial was sealed and heated at 110 1/2C for 20 h. After 20 h, the crude reaction mixture was filtered through a short pad of Celite and concentrated in vacuo. The remaining residue was purified by flash chromatography on silica using forced flow of ethyl acetate/ hexanes system on Biotage KP-Sil prepacked cartridges and using the Biotage SP-1 automated chromatography system to afford the coupled product.

Procedure for Synthesis of C5-Substituted Quinazolinones (28a–h, Scheme 3).

—*Pd-Catalyzed Amination of Compounds 15a or 15b with Amines 25a–g.* Ethyl (*S*)-4-((2-(1-((*tert*-butoxycarbonyl)amino)propyl)-4-oxo-3-phenyl-3,4-dihydroquinazolin-5-yl)amino)butanoate (**26a**). The general procedure GP5 was used with *tert*-butyl (*S*)-(1-(5-bromo-4-oxo-3-phenyl-3,4-dihydroquinazolin-2-yl)propyl)carbamate **15a** (75.2 mg, 0.16 mmol), [XantPhos Palladacycle] (3.9 mg, 4.10 μmol), Cs₂CO₃ (160.0 mg, 0.49 mmol), and 4-ethoxy-4-oxobutan-1-aminium chloride **25a** (35.8 mg, 0.21 mmol) were combined in dry toluene (0.8 mL). The resulting mixture was heated at 110 1/2C for 20 h and concentrated in vacuo. The remaining residue was purified by flash chromatography on silica using 0–30% ethyl acetate/hexanes to afford the coupled product, ethyl (*S*)-4-((2-(1-((*tert*-butoxycarbonyl)amino)propyl)-4-oxo-3-phenyl-3,4-dihydroquinazolin-5-yl)amino)butanoate **26a** (58.4 mg, 0.115 mmol) in 70% yield. LC–MS (method 1): *t*_R = 3.77 min, *m/z* (M + H)⁺ = 509.4. ¹H NMR (400 MHz, CDCl₃) δ 8.49 (s, 1H), 7.62 (d, *J* = 7.1 Hz, 1H), 7.55 (q, *J* = 8.0, 7.6 Hz, 3H), 7.40 (s, 1H), 6.93 (d, *J* = 27.4 Hz, 1H), 6.56 (d, *J* = 8.4 Hz, 1H), 5.57 (s, 1H), 4.39–4.32 (m, 1H), 4.12 (q, *J* = 7.1 Hz, 2H), 3.25 (q, *J* = 6.5 Hz, 2H), 2.41 (t, *J* = 7.3 Hz, 2H), 1.97 (p, *J* = 7.2 Hz, 2H), 1.73 (s, 2H), 1.43 (s, 9H), 1.24 (t, *J* = 7.1 Hz, 3H), 0.77 (t, *J* = 7.4 Hz, 3H).

Methyl (S)-5-((2-(1-((tert-butoxycarbonyl)amino)propyl)-4-oxo-3-phenyl-3,4-dihydroquinazolin-5-yl)amino)pentanoate (26b). The general procedure GP5 was used with *tert*-butyl (*S*)-(1-(5-bromo-4-oxo-3-phenyl-3,4-dihydroquinazolin-2-yl)propyl)carbamate **15a** (218.4 mg, 0.48 mmol), [XantPhos Palladacycle] (13.7 mg, 14.0 μmol), Cs₂CO₃ (466.0 mg, 1.43 mmol), and 5-methoxy-5-oxopentan-1-aminium chloride **25b** (96.0 mg, 0.57 mmol) in dry toluene (2.4 mL). The remaining residue was purified by flash chromatography on silica using 0–50% ethyl acetate/hexanes to afford the coupled product, methyl (*S*)-5-((2-(1-((*tert*-butoxycarbonyl)amino)propyl)-4-oxo-3-phenyl-3,4-dihydroquinazolin-5-yl)amino)pentanoate **26b** (153.0 mg, 0.30 mmol) in 63% yield. LC–MS (method 1): *t*_R = 3.75 min, *m/z* (M + H)⁺ = 509.3. ¹H NMR (400 MHz, CDCl₃) δ 8.42 (s, 1H), 7.57 (td, *J* = 18.2, 14.9, 7.7 Hz, 4H), 7.41 (s, 1H), 7.26 (s, 1H), 6.53 (d, *J* = 8.4 Hz, 1H),

4.35 (s, 1H), 3.66 (s, 3H), 3.20 (q, $J = 6.2$ Hz, 2H), 2.34 (t, $J = 6.9$ Hz, 2H), 1.79–1.64 (m, 6H), 1.43 (s, 9H), 0.77 (t, $J = 7.3$ Hz, 3H).

Methyl (S)-6-((2-(1-((tert-Butoxycarbonyl)amino)propyl)-4-oxo-3-phenyl-3,4-dihydroquinazolin-5-yl)amino)hexanoate (26c). The general procedure GP5 was used with *tert*-butyl (S)-(1-(5-bromo-4-oxo-3-phenyl-3,4-dihydroquinazolin-2-yl)propyl)carbamate **15a** (121.2 mg, 0.26 mmol), [XantPhos Palladacycle] (6.3 mg, 6.61 μ mol), Cs₂CO₃ (258.0 mg, 0.79 mmol), and 6-methoxy-6-oxohexan-1-aminium chloride **25c** (62.4 mg, 0.34 mmol) in dry toluene (1.3 mL). The remaining residue was purified by flash chromatography on silica using 0–20% ethyl acetate/hexanes to afford the coupled product, methyl (S)-6-((2-(1-((tert-butoxycarbonyl)amino)propyl)-4-oxo-3-phenyl-3,4-dihydroquinazolin-5-yl)amino)hexanoate **26c** (126.0 mg, 0.24 mmol) in 91% yield. LC–MS (method 1): $t_R = 3.83$ min, m/z (M + H)⁺ = 523.3. ¹H NMR (400 MHz, CDCl₃) δ 8.44 (d, $J = 5.3$ Hz, 1H), 7.66–7.48 (m, 4H), 7.37 (d, $J = 7.9$ Hz, 1H), 6.84 (d, $J = 7.8$ Hz, 1H), 6.50 (d, $J = 8.4$ Hz, 1H), 4.40–4.30 (m, 1H), 3.65 (s, 3H), 3.17 (td, $J = 6.9, 5.1$ Hz, 2H), 2.31 (t, $J = 7.5$ Hz, 2H), 1.67 (ddt, $J = 17.5, 15.2, 7.6$ Hz, 6H), 1.58–1.45 (m, 2H), 1.43 (s, 9H), 0.76 (t, $J = 7.4$ Hz, 3H).

Methyl (S)-4-(((2-(1-((tert-Butoxycarbonyl)amino)propyl)-4-oxo-3-phenyl-3,4-dihydroquinazolin-5-yl)amino)methyl)benzoate (26d). The general procedure GP5 was used with *tert*-butyl (S)-(1-(5-bromo-4-oxo-3-phenyl-3,4-dihydroquinazolin-2-yl)propyl)carbamate **15a** (95.2 mg, 0.21 mmol), [XantPhos Palladacycle] (4.9 mg, 5.19 μ mol), Cs₂CO₃ (203.0 mg, 0.62 mmol), and methyl 4-(aminomethyl)benzoate hydrochloride **25d** (54.3 mg, 1.3 mmol) in dry toluene (1.0 mL). The remaining residue was purified by flash chromatography on silica using 0–30% ethyl acetate/hexanes to afford the coupled product, methyl (S)-4-(((2-(1-((tert-butoxycarbonyl)amino)propyl)-4-oxo-3-phenyl-3,4-dihydroquinazolin-5-yl)amino)methyl)benzoate **26d** (100.0 mg, 0.184 mmol) as an off-white solid in 89% yield. LC–MS (method 1): $t_R = 3.82$ min, m/z (M + H)⁺ = 542.3. ¹H NMR (400 MHz, CDCl₃) δ 9.03 (t, $J = 5.6$ Hz, 1H), 8.02–7.95 (m, 2H), 7.57 (td, $J = 17.2, 14.9, 8.1$ Hz, 3H), 7.49–7.37 (m, 4H), 7.31–7.28 (m, 1H), 6.91 (d, $J = 7.8$ Hz, 1H), 6.40 (d, $J = 8.4$ Hz, 1H), 5.54 (s, 1H), 4.49 (d, $J = 5.8$ Hz, 2H), 4.43–4.33 (m, 1H), 3.90 (s, 3H), 1.79–1.70 (m, 1H), 1.64–1.56 (m, 1H), 1.43 (s, 9H), 0.77 (t, $J = 7.4$ Hz, 3H).

Methyl (S)-4-(((2-(1-((tert-Butoxycarbonyl)amino)propyl)-4-oxo-3-phenyl-3,4-dihydroquinazolin-5-yl)amino)methyl)-2-methylbenzoate (26e). The general procedure GP5 was used with *tert*-butyl (S)-(1-(5-bromo-4-oxo-3-phenyl-3,4-dihydroquinazolin-2-yl)propyl)-carbamate **15a** (170.0 mg, 0.411 mmol), [XantPhos Palladacycle] (20.0 mg, 0.02 mmol), Cs₂CO₃ (401.0 mg, 1.23 mmol), and methyl 5-(aminomethyl)picolinate dihydrochloride **25e** (88.0 mg, 0.493 mmol) in dry toluene (2.0 mL). The remaining residue was purified by flash chromatography on silica using 0–50% ethyl acetate/hexanes to afford the coupled product, methyl (S)-4-(((2-(1-((tert-butoxycarbonyl)amino)propyl)-4-oxo-3-phenyl-3,4-dihydroquinazolin-5-yl)amino)methyl)-2-methylbenzoate **26e** (175.0 mg, 0.31 mmol) in 88% yield. LC–MS (method 1): $t_R = 3.88$ min, m/z (M + H)⁺ = 557.3.

Methyl (S)-5-(((2-(1-((tert-Butoxycarbonyl)amino)propyl)-4-oxo-3-phenyl-3,4-dihydroquinazolin-5-yl)amino)methyl)picolinate (26f). The general procedure GP5 was used with *tert*-butyl (S)-(1-(5-bromo-4-oxo-3-phenyl-3,4-dihydroquinazolin-2-

yl)propyl)carbamate **15a** (96.5 mg, 0.21 mmol), [XantPhos Palladacycle] (5.0 mg, 5.26 μ mol), Cs₂CO₃ (206.0 mg, 0.63 mmol), and methyl 5-(aminomethyl)picolinate dihydrochloride **25f** (54.3 mg, 1.3 mmol) in dry toluene (1.0 mL). The remaining residue was purified by flash chromatography on silica using 0–80% ethyl acetate/hexanes to afford the coupled product, methyl (*S*)-5-(((2-(1-((*tert*-butoxycarbonyl)amino)propyl)-4-oxo-3-phenyl-3,4-dihydroquinazolin-5-yl)amino)methyl) picolinate **26f** (67.5 mg, 0.124 mmol) in 59% yield. LC–MS (method 1): t_R = 3.56 min, m/z (M + H)⁺ = 544.3. ¹H NMR (400 MHz, CDCl₃) δ 9.07 (s, 1H), 8.73 (d, J = 2.1 Hz, 1H), 8.08 (d, J = 8.0 Hz, 1H), 7.82 (dd, J = 8.1, 2.2 Hz, 1H), 7.67–7.51 (m, 3H), 7.47 (t, J = 8.1 Hz, 1H), 7.41 (d, J = 8.2 Hz, 1H), 7.29 (s, 1H), 6.97 (s, 1H), 6.38 (d, J = 8.4 Hz, 1H), 4.54 (d, J = 5.8 Hz, 2H), 4.38 (s, 1H), 4.01 (d, J = 1.2 Hz, 3H), 1.78–1.72 (m, 1H), 1.63–1.53 (m, 1H) 1.43 (s, 9H), 0.78 (t, J = 7.3 Hz, 3H).

Methyl (S)-6-(((2-(1-((tert-Butoxycarbonyl)amino)propyl)-4-oxo-3-phenyl-3,4-dihydroquinazolin-5-yl)amino)methyl)nicotinate (26g). The general procedure GP5 was used with *tert*-butyl (*S*)-(1-(5-bromo-4-oxo-3-phenyl-3,4-dihydroquinazolin-2-yl)propyl)carbamate **15a** (109.0 mg, 0.24 mmol), [XantPhos Palladacycle] (6.8 mg, 0.007 mmol), Cs₂CO₃ (232.0 mg, 0.71 mmol), and methyl 5-(aminomethyl)picolinate dihydrochloride **25g** (58.0 mg, 0.29 mmol) in dry toluene (1.2 mL). The remaining residue was purified by flash chromatography on silica using 0–50% ethyl acetate/hexanes to afford the coupled product, methyl (*S*)-6-(((2-(1-((*tert*-butoxycarbonyl)amino)propyl)-4-oxo-3-phenyl-3,4-dihydroquinazolin-5-yl)amino)methyl)nicotinate **26g** (100.0 mg, 0.18 mmol) in 77% yield. LC–MS (method 1): t_R = 3.58 min, m/z (M + H)⁺ = 544.3. ¹H NMR (400 MHz, CDCl₃) δ 9.28–9.15 (m, 2H), 8.20 (dd, J = 8.2, 2.2 Hz, 1H), 7.67–7.50 (m, 3H), 7.44 (dt, J = 13.8, 9.0 Hz, 3H), 7.33–7.28 (m, 1H), 6.91 (d, J = 7.9 Hz, 1H), 6.37 (d, J = 8.3 Hz, 1H), 5.56–5.51 (m, 1H), 4.64 (d, J = 6.0 Hz, 2H), 4.39 (s, 1H), 3.94 (d, J = 1.6 Hz, 3H), 1.78–1.70 (m, 1H), 1.60–1.50 (m, 1H), 1.40 (s, 9H), 0.77 (t, J = 7.4 Hz, 3H).

Methyl (S)-5-(((2-(1-((tert-Butoxycarbonyl)amino)propyl)-4-oxo-3-phenyl-3,4-dihydroquinazolin-5-yl)amino)methyl)furan-2-carboxylate (26h). The general procedure GP5 was used with *tert*-butyl (*S*)-(1-(5-bromo-4-oxo-3-phenyl-3,4-dihydroquinazolin-2-yl)propyl)-carbamate **15a** (56.6 mg, 0.12 mmol) [XantPhos Palladacycle] (2.9 mg, 3.09 μ mol), Cs₂CO₃ (121.0 mg, 0.37 mmol), and methyl 5-(aminomethyl)furan-2-carboxylate hydrochloride **25h** (35.5 mg, 0.18 mmol) in dry toluene (0.6 mL). The remaining residue was purified by flash chromatography on silica using 0–55% ethyl acetate/hexanes to afford the coupled product, methyl (*S*)-5-(((2-(1-((*tert*-butoxycarbonyl)amino)propyl)-4-oxo-3-phenyl-3,4-dihydroquinazolin-5-yl)amino)methyl)furan-2-carboxylate **26h** (58.0 mg, 0.11 mmol) in 88% yield. LC–MS (method 1): t_R = 3.71 min, m/z (M + H)⁺ = 533.3. ¹H NMR (400 MHz, CDCl₃) δ 8.94 (t, J = 5.9 Hz, 1H), 7.66–7.48 (m, 4H), 7.38 (d, J = 7.9 Hz, 1H), 7.09 (d, J = 3.5 Hz, 1H), 6.94 (d, J = 7.9 Hz, 1H), 6.51 (d, J = 8.4 Hz, 1H), 6.34 (d, J = 3.3 Hz, 1H), 4.48 (d, J = 5.8 Hz, 2H), 4.39 (d, J = 11.2 Hz, 1H), 3.88 (s, 3H), 1.74 (ddd, J = 14.3, 7.4, 4.8 Hz, 1H), 1.55 (dt, J = 14.0, 7.1 Hz, 1H), 1.43 (s, 9H), 0.77 (t, J = 7.4 Hz, 3H).

Methyl (S)-4-(((2-(1-((tert-Butoxycarbonyl)amino)ethyl)-4-oxo-3-phenyl-3,4-dihydroquinazolin-5-yl)amino)methyl)benzoate (26i). The procedure mentioned in Scheme 1(3) was used with *tert*-butyl (*S*)-(1-(5-bromo-4-oxo-3-phenyl-3,4-dihydroquinazolin-2-yl)ethyl)-carbamate **15a** (300.0 mg, 0.675 mmol) [XantPhos Palladacycle] (19.0 mg, 0.02

mmol), Cs₂CO₃ (660.0 mg, 2.03 mmol), and methyl 4-(aminomethyl)benzoate hydrochloride (177.0 mg, 0.88 mmol) in dry toluene (3.4 mL). The remaining residue was purified by flash chromatography on silica using 0–50% ethyl acetate/hexanes to afford the coupled product, methyl (*S*)-4-(((2-(1-((*tert*-butoxycarbonyl)amino)ethyl)-4-oxo-3-phenyl-3,4-dihydroquinazolin-5-yl)amino)methyl)benzoate **26i** (274.0 mg, 0.52 mmol) as an off-white solid in 77% yield. LC–MS (method 1): *t*_R = 3.53 min, *m/z* (M + H)⁺ = 529.3. ¹H NMR (400 MHz, CDCl₃) δ 8.98 (s, 1H), 8.02–7.96 (m, 2H), 7.69–7.37 (m, 8H), 7.30 (d, *J* = 7.3 Hz, 1H), 6.42 (d, *J* = 8.4 Hz, 1H), 4.52 (m, 1H), 4.49 (d, *J* = 5.9 Hz, 2H), 3.91 (d, *J* = 1.2 Hz, 3H), 1.43 (s, 9H), 1.32 (m, 3H). (*S*)-4-((2-(1-((9*H*-Purin-6-yl)amino)propyl)-4-oxo-3-phenyl-3,4-dihydroquinazolin-5-yl)amino)-*N*-hydroxybutanamide (**28a**). Step 1. *Installation of purine hinge binding group*. The general procedure GP3 was used with **26a** (83.0 mg, 0.16 mmol) and trifluoroacetic acid (374.0 mg, 3.28 mmol, 0.25 mL) in DCM (1.6 mL). The crude Bocdeprotected amine was worked-up (method A) and reacted with 6-chloro-9-(tetrahydro-2*H*-pyran-2-yl)-9*H*-purine (78.0 mg, 0.33 mmol) and triethylamine (66.0 mg, 0.66 mmol, 91.0 μL) in ethanol (0.5 mL). The remaining residue was purified by flash chromatography on silica gel using 0–5% MeOH/DCM to afford ethyl 4-((4-oxo-3-phenyl-2-((1*S*)-1-((9-(tetrahydro-2*H*-pyran-2-yl)-9*H*-purin-6-yl)amino)propyl)-3,4-dihydroquinazolin-5-yl)amino)butanoate **27a** (53.0 mg, 0.09 mmol) in 53% yield. LC–MS (method 1): *t*_R = 3.46 min, *m/z* (M + H)⁺ = 611.4. Step 2. *Conversion of alkyl ester to hydroxamic acid*. The general procedure GP4 (method B) was used with compound **27a** (50.0 mg, 0.08 mmol) to afford the final product, (*S*)-4-((2-(1-((9*H*-purin-6-yl)amino)propyl)-4-oxo-3-phenyl-3,4-dihydroquinazolin-5-yl)amino)-*N*-hydroxybutanamide, TFA **28a** (8.8 mg, 0.02 mmol) in 21% yield. LC–MS (method 2): *t*_R = 3.50 min, *m/z* (M + H)⁺ = 514.2. ¹H NMR (400 MHz, DMSO-*d*₆) δ 10.39 (s, 1H), 8.49 (s, 1H), 8.38 (s, 2H), 7.59–7.47 (m, 5H), 6.70 (d, *J* = 7.9 Hz, 1H), 6.57 (d, *J* = 8.5 Hz, 1H), 5.75 (s, 1H), 4.74 (s, 1H), 3.16 (d, *J* = 4.9 Hz, 3H), 2.08–1.92 (m, 3H), 1.79 (h, *J* = 7.3, 6.9 Hz, 3H), 0.76 (t, *J* = 7.3 Hz, 3H). HRMS (ESI) *m/z*: [M + H]⁺ calcd for C₂₆H₂₈N₉O₃ 514.2310, found 514.2285 [Note: In addition to compound **28a**, a side product originating from the hydrolysis of ethyl ester in **27a** to carboxylic acid was also isolated after TFA deprotection step, in 7% yield].

Compounds 26b–g were converted to 27b–g using the similar procedure, as described above for 27a.—(*S*)-5-((2-(1-((9*H*-Purin-6-yl)amino)propyl)-4-oxo-3-phenyl-3,4-dihydroquinazolin-5-yl)amino)-*N*-hydroxypentanamide (**28b**). The procedure mentioned in Scheme 3 (method B) was used with compound **27b** (68.5 mg, 0.112 mmol) to afford the product, (*S*)-5-((2-(1-((9*H*-purin-6-yl)amino)propyl)-4-oxo-3-phenyl-3,4-dihydroquinazolin-5-yl)amino)-*N*-hydroxypentanamide, TFA **28b** (42.0 mg, 0.065 mmol) in 61% yield. LC–MS (method 2): *t*_R = 3.69 min, *m/z* (M + H)⁺ = 528.3. ¹H NMR (400 MHz, DMSO-*d*₆) δ 10.33 (s, 1H), 8.71 (s, 1H), 8.44 (s, 2H), 7.52 (td, *J* = 13.5, 5.2 Hz, 5H), 6.70 (d, *J* = 7.9 Hz, 1H), 6.56 (d, *J* = 8.4 Hz, 1H), 4.76 (s, 1H), 3.14 (d, *J* = 5.7 Hz, 2H), 2.10–1.93 (m, 3H), 1.82 (dt, *J* = 15.1, 7.6 Hz, 1H), 1.56 (dt, *J* = 7.0, 3.5 Hz, 4H), 0.77 (t, *J* = 7.3 Hz, 3H).

(*S*)-6-((2-(1-((9*H*-Purin-6-yl)amino)propyl)-4-oxo-3-phenyl-3,4-dihydroquinazolin-5-yl)amino)-*N*-hydroxyhexanamide (**28c**). The general procedure GP4 (method B) was used

with compound **27c** (135.0 mg, 0.216 mmol) to afford the final product, (*S*)-6-((2-(1-((9*H*-purin-6-yl)amino)propyl)-4-oxo-3-phenyl-3,4-dihydroquinazolin-5-yl)amino)-*N*-hydroxyhexanamide, TFA **28c** (30.2 mg, 0.056 mmol) in 32% yield. LC–MS (method 2): $t_R = 4.02$ min, m/z ($M + H$)⁺ = 542.3. ¹H NMR (400 MHz, DMSO-*d*₆) δ 10.33–10.28 (m, 1H), 8.89 (s, 1H), 8.48 (s, 2H), 7.53 (dq, $J = 13.3, 8.0, 4.8$ Hz, 5H), 6.70 (d, $J = 7.9$ Hz, 1H), 6.56 (d, $J = 8.5$ Hz, 1H), 4.77 (s, 1H), 3.13 (t, $J = 6.9$ Hz, 2H), 2.01 (ddd, $J = 14.2, 7.5, 4.5$ Hz, 1H), 1.93 (t, $J = 7.4$ Hz, 2H), 1.83 (h, $J = 7.4$ Hz, 1H), 1.53 (dp, $J = 22.8, 7.3$ Hz, 4H), 1.37–1.25 (m, 2H), 0.77 (t, $J = 7.3$ Hz, 3H). HRMS (ESI) m/z : [$M + H$]⁺ calcd for C₂₈H₃₂N₉O₃ 542.2623, found 542.2647 [Note: In addition to compound **28c**, a side product originating from the hydrolysis of methyl ester in **27c** to carboxylic acid was also isolated after TFA deprotection step, in 14% yield].

(*S*)-4-(((2-(1-((9*H*-Purin-6-yl)amino)propyl)-4-oxo-3-phenyl-3,4-dihydroquinazolin-5-yl)amino)methyl)-*N*-hydroxybenzamide (**28d**). The general procedure GP4 (method A) was used with compound **27d** (78.1 mg, 0.121 mmol) to afford the final product, (*S*)-4-(((2-(1-((9*H*-purin-6-yl)amino)propyl)-4-oxo-3-phenyl-3,4-dihydroquinazolin-5-yl)amino)methyl)-*N*-hydroxybenzamide, TFA **28d** (35.5 mg, 0.106 mmol) in 50% yield. LC–MS (method 2): $t_R = 3.88$ min, m/z ($M + H$)⁺ = 562.2. ¹H NMR (400 MHz, DMSO-*d*₆) δ 11.15 (s, 1H), 8.97 (s, 1H), 8.77 (s, 1H), 8.45 (s, 2H), 7.73–7.66 (m, 2H), 7.58 (s, 2H), 7.55 (t, $J = 1.6$ Hz, 1H), 7.52–7.36 (m, 5H), 6.73 (d, $J = 7.9$ Hz, 1H), 6.48 (d, $J = 8.4$ Hz, 1H), 4.77 (s, 1H), 4.52–4.46 (m, 2H), 2.01 (ddd, $J = 14.2, 7.6, 4.6$ Hz, 1H), 1.83 (dt, $J = 14.4, 7.5$ Hz, 1H), 0.77 (t, $J = 7.3$ Hz, 3H). HRMS (ESI) m/z : [$M + H$]⁺ calcd for C₃₀H₂₈N₉O₃ 562.2310, found 562.2322.

(*S*)-4-(((2-(1-((9*H*-Purin-6-yl)amino)propyl)-4-oxo-3-phenyl-3,4-dihydroquinazolin-5-yl)amino)methyl)-*N*-hydroxy-2-methylbenzamide (**28e**). The general procedure GP4 (method B) was used with compound **27e** (105.0 mg, 0.159 mmol) to afford the final product (*S*)-4-(((2-(1-((9*H*-purin-6-yl)amino)propyl)-4-oxo-3-phenyl-3,4-dihydroquinazolin-5-yl)amino)methyl)-*N*-hydroxy-2-methylbenzamide, TFA **28e** (60.0 mg, 0.087 mmol) in 55% yield. LC–MS (method 2): $t_R = 4.18$ min, m/z ($M + H$)⁺ = 576.2. ¹H NMR (400 MHz, DMSO-*d*₆) δ 10.76 (s, 1H), 8.88 (s, 1H), 8.74 (s, 1H), 8.44 (s, 2H), 7.61–7.52 (m, 3H), 7.56–7.43 (m, 4H), 7.26–7.13 (m, 3H), 6.73 (d, $J = 7.9$ Hz, 1H), 6.51 (dd, $J = 8.5, 1.0$ Hz, 1H), 4.78 (s, 1H), 4.41 (s, 2H), 2.30 (s, 3H), 2.01 (ddd, $J = 14.0, 7.4, 4.4$ Hz, 1H), 1.83 (dt, $J = 14.8, 8.0$ Hz, 1H), 0.77 (t, $J = 7.3$ Hz, 3H). HRMS (ESI) m/z : [$M + H$]⁺ calcd for C₃₁H₃₀N₉O₃; 576.2466, found 576.2471 [Note: In addition to compound **28e**, a side product originating from the hydrolysis of methyl ester in **27e** to carboxylic acid was also isolated after TFA deprotection step, in 13% yield].

(*S*)-5-(((2-(1-((9*H*-Purin-6-yl)amino)propyl)-4-oxo-3-phenyl-3,4-dihydroquinazolin-5-yl)amino)methyl)-*N*-hydroxypicolinamide (**28f**). The general procedure GP4 (method A) was used with compound **28f** (60.5 mg, 0.094 mmol) to afford the final product, (*S*)-5-(((2-(1-((9*H*-purin-6-yl)amino)propyl)-4-oxo-3-phenyl-3,4-dihydroquinazolin-5-yl)amino)methyl)-*N*-hydroxypicolinamide, TFA **28f** (20.0 mg, 0.03 mmol) in 32% yield. LC–MS (method 2): $t_R = 3.77$ min, m/z ($M + H$)⁺ = 563.2. ¹H NMR (400 MHz, DMSO-*d*₆) δ 11.35 (s, 1H), 9.02 (s, 1H), 8.85 (s, 1H), 8.58 (d, $J = 2.0$ Hz, 1H), 8.47 (s, 2H), 7.96–7.83 (m, 2H), 7.66–7.40 (m, 6H), 6.75 (d, $J = 7.9$ Hz, 1H), 6.53 (d, $J = 8.4$ Hz, 1H), 4.78 (s, 1H),

4.58 (d, $J = 3.4$ Hz, 2H), 2.02 (ddd, $J = 14.4, 7.5, 4.5$ Hz, 1H), 1.82 (dt, $J = 14.7, 7.7$ Hz, 1H), 0.77 (t, $J = 7.3$ Hz, 3H). HRMS (ESI) m/z : $[M + H]^+$ calcd for $C_{29}H_{27}N_{10}O_3$ 563.2262, found 563.2273.

(*S*)-6-(((2-(1-((9*H*-Purin-6-yl)amino)propyl)-4-oxo-3-phenyl-3,4-dihydroquinazolin-5-yl)amino)methyl)-*N*-hydroxynicotinamide (**28g**). The general procedure GP4 (method B) was used with compound **28g** (79.1 mg, 0.122 mmol) to afford the final product, (*S*)-6-(((2-(1-((9*H*-purin-6-yl)amino)propyl)-4-oxo-3-phenyl-3,4-dihydroquinazolin-5-yl)amino)methyl)-*N*-hydroxynicotinamide, TFA **28g** (30.0 mg, 0.044 mmol) in 36% yield. LC–MS (method 2): $t_R = 3.54$ min, m/z ($M + H$)⁺ = 563.3. ¹H NMR (400 MHz, DMSO- d_6) δ 11.32 (s, 1H), 9.22 (s, 1H), 8.96 (s, 1H), 8.85 (dd, $J = 2.2, 0.8$ Hz, 1H), 8.51 (s, 2H), 8.06 (dd, $J = 8.1, 2.3$ Hz, 1H), 7.63–7.42 (m, 6H), 6.76 (d, $J = 7.9$ Hz, 1H), 6.54–6.49 (m, 1H), 4.81 (s, 1H), 4.59 (s, 2H), 2.08–1.98 (m, 1H), 1.83 (dt, $J = 14.7, 7.8$ Hz, 1H), 0.79 (t, $J = 7.3$ Hz, 3H). HRMS (ESI) m/z : $[M + H]^+$ calcd for $C_{29}H_{27}N_{10}O_3$ 563.2262, found 563.2283.

(*S*)-5-(((2-(1-((9*H*-Purin-6-yl)amino)propyl)-4-oxo-3-phenyl-3,4-dihydroquinazolin-5-yl)amino)methyl)-*N*-hydroxyfuran-2-carbox-amide (**28h**). The general procedure GP4 (method A) was used with compound **28h** (61.5 mg, 0.097 mmol) to afford the final product, (*S*)-5-(((2-(1-((9*H*-purin-6-yl)amino)propyl)-4-oxo-3-phenyl-3,4-dihydroquinazolin-5-yl)amino)methyl)-*N*-hydroxyfuran-2-carboxamide, TFA **28h** (41.0 mg, 0.076 mmol) in 78% yield. LC–MS (method 2): $t_R = 3.73$ min, m/z ($M + H$)⁺ = 552.2. ¹H NMR (400 MHz, DMSO- d_6) δ 11.09 (s, 2H), 8.83 (s, 3H), 8.46 (d, $J = 2.9$ Hz, 2H), 7.65–7.42 (m, 6H), 6.95 (d, $J = 3.4$ Hz, 1H), 6.77 (d, $J = 7.9$ Hz, 1H), 6.69 (d, $J = 8.4$ Hz, 1H), 6.45 (d, $J = 3.4$ Hz, 1H), 4.76 (dd, $J = 10.5, 4.9$ Hz, 1H), 4.48 (d, $J = 3.7$ Hz, 2H), 2.00 (ddd, $J = 14.3, 7.4, 4.3$ Hz, 1H), 1.82 (dt, $J = 14.5, 7.6$ Hz, 1H), 0.76 (t, $J = 7.3$ Hz, 3H). HRMS (ESI) m/z : $[M + H]^+$ calcd for $C_{28}H_{26}N_9O_4$ 552.2102, found 552.2106.

(*S*)-4-(((2-(1-((9*H*-Purin-6-yl)amino)propyl)-4-oxo-3-phenyl-3,4-dihydroquinazolin-5-yl)amino)methyl)-*N*-hydroxy-*N*-methylbenzamide (**28i**). Compound **27d** (40.6 mg, 0.063) was suspended in MeOH/water (1.2 mL, 1:1) in a vial equipped with a stir bar, and LiOH·H₂O (5.3 mg, 0.13 mmol) was added to it. The resulting mixture was stirred at room temperature for 10 h and concentrated in vacuo. This crude product was dissolved in DMF (1.2 mL), and *N*-methylhydroxylamine hydrochloride (8.0 mg, 0.95 mmol), DIPEA (18.0 mg, 0.16 mmol), and 2-(3*H*-[1,2,3]triazolo[4,5-*b*]pyridin-3-yl)-1,1,3,3-tetramethylisouronium hexafluorophosphate(V) [HATU] (36.0 mg, 0.095 mmol) were added to it. The resulting mixture was stirred at room temperature for 16 h, concentrated in vacuo, and redissolved in DCM (1.2 mL) in a vial followed by dropwise addition of TFA (144.0 mg, 1.26 mmol, 0.10 mL) into it. The resulting mixture was stirred for 10 h, concentrated in vacuo, and purified on preparative HPLC to afford the final compound, (*S*)-4-(((2-(1-((9*H*-purin-6-yl)amino)propyl)-4-oxo-3-phenyl-3,4-dihydroquinazolin-5-yl)amino)methyl)-*N*-hydroxy-*N*-methylbenzamide, TFA **28i** (13.0 mg, 0.019 mmol) in 30% yield. LC–MS (method 2): $t_R = 4.15$ min, m/z ($M + H$)⁺ = 576.3. ¹H NMR (400 MHz, DMSO- d_6) δ 9.95 (s, 1H), 8.96 (s, 1H), 8.54 (s, 1H), 8.39 (s, 1H), 7.57 (dt, $J = 6.6, 1.9$ Hz, 4H), 7.47 (dd, $J = 10.6, 5.7$ Hz, 3H), 7.40–7.32 (m, 2H), 6.73 (d, $J = 7.8$ Hz, 1H), 6.50 (dd, $J = 8.5, 1.0$ Hz, 1H), 4.77 (s, 1H), 4.48 (s, 2H), 3.22 (s, 3H), 1.99 (ddd, $J = 11.7, 7.4, 3.7$ Hz, 1H), 1.87–1.78

(m, 1H), 0.77 (t, $J = 7.3$ Hz, 3H). HRMS (ESI) m/z : $[M + H]^+$ calcd for $C_{31}H_{30}N_9O_3$ 576.2466, found 576.2494.

Procedure for Synthesis of C5-Substituted Quinazolinones (33, 37, 40a,b, 47, Scheme 4).—*tert*-Butyl (*S*)-(1-(5-Cyano-4-oxo-3-phenyl-3,4-dihydroquinazolin-2-yl)propyl)carbamate (**29a**). *tert*-Butyl (*S*)-(1-(5-bromo-4-oxo-3-phenyl-3,4-dihydroquinazolin-2-yl)-ethyl)carbamate **15a** (181.0 mg, 0.40 mmol), zinc cyanide (58.0 mg, 0.49 mmol), and tetrakis(triphenylphosphine)Pd(0) (23.0 mg, 0.02 mmol) were suspended in dry DMF (2.0 mL) in a MW vial equipped with a stir bar under nitrogen atmosphere. The mixture was bubbled with N_2 gas for 2 min, sealed and heated at 100 $1/2C$ for 16 h. After 16 h, the crude reaction mixture was filtered through a short pad of Celite and concentrated in vacuo. The remaining residue was purified by flash chromatography on silica using 0–45% ethyl acetate/hexanes to afford *tert*-butyl (*S*)-(1-(5-cyano-4-oxo-3-phenyl-3,4-dihydroquinazolin-2-yl)propyl)carbamate **29a** (154.0 mg, 0.38 mmol) as a colorless solid in 96% yield. LC–MS (method 1): $t_R = 3.64$ min, m/z ($M + H$) $^+ = 405.2$. 1H NMR (400 MHz, $CDCl_3$) δ 7.99–7.92 (m, 1H), 7.91–7.79 (m, 2H), 7.65–7.50 (m, 3H), 7.42 (d, $J = 7.8$ Hz, 1H), 7.30 (d, $J = 7.1$ Hz, 1H), 5.39 (d, $J = 9.0$ Hz, 1H), 4.46 (s, 1H), 1.75 (ddd, $J = 12.2, 7.3, 4.6$ Hz, 1H), 1.55–1.49 (m, 1H), 1.43 (s, 9H), 0.78 (t, $J = 7.4$ Hz, 3H).

tert-Butyl (*S*)-(1-(5-(Aminomethyl)-4-oxo-3-phenyl-3,4-dihydroquinazolin-2-yl)propyl)carbamate (**30a**). Compound **29a** (180.0 mg, 0.44 mmol) was dissolved in methanolic ammonia (2.2 mL, 7N in MeOH) in a 20 mL scintillation vial, and Raney Ni (20.0 mg (approx)) was added to it. The reaction vial was evacuated and then kept under hydrogen atmosphere using a balloon. The resulting suspension was stirred at room temperature for 20 h. After completion of reaction (by LC–MS), the crude reaction mixture was carefully filtered under nitrogen and concentrated in vacuo to afford *tert*-butyl (*S*)-(1-(5-(aminomethyl)-4-oxo-3-phenyl-3,4-dihydroquinazolin-2-yl)propyl)carbamate **30a**. LC–MS (method 1): $t_R = 2.85$ min, m/z ($M + H$) $^+ = 409.3$, that was carried to the next step without purification.

Compound 30b was synthesized from 15a' using the similar procedure as described for 30a.—Ethyl (*S*)-2-(((2-(1-((*tert*-Butoxycarbonyl)amino)propyl)-4-oxo-3-phenyl-3,4-dihydroquinazolin-5-yl)methyl)amino)thiazole-4-carboxylate (**32a**). Compound **30a** (102.0 mg, 0.25 mmol) was dissolved in dry DMF (0.6 mL) in a microwave vial, and ethyl 2-bromothiazole-4-carboxylate **31** (118.0 mg, 0.5 mmol) and *N*-ethyl-*N*-isopropylpropan-2-amine [DIPEA] (129.0 mg, 1.00 mmol) were added to it. The microwave vial was sealed and heated at 180 $1/2C$ for 30 min in a microwave. After completion of the reaction, the reaction mixture was concentrated in vacuo and the remaining residue was purified using 0–5% MeOH/DCM to afford ethyl (*S*)-2-(((2-(1-((*tert*-butoxycarbonyl)amino)propyl)-4-oxo-3-phenyl-3,4-dihydroquinazolin-5-yl)methyl)amino)thiazole-4-carboxylate **32a** (52.8 mg, 0.094 mmol) in 38% yield. LC–MS (method 1): $t_R = 3.55$ min, m/z ($M + H$) $^+ = 564.3$.

(*S*)-2-(((2-(1-((9*H*-Purin-6-yl)amino)propyl)-4-oxo-3-phenyl-3,4-dihydroquinazolin-5-yl)methyl)amino)-*N*-hydroxythiazole-4-carboxamide (**33**). The general procedure GP3 was used with compound **32a** (78.8 mg, 0.14 mmol) and trifluoroacetic acid (319.0 mg, 2.80

mmol, 0.21 mL) in DCM (1.4 mL). The crude Bocdeprotected amine was worked-up (method A) and reacted with 6-chloro-9-(tetrahydro-2*H*-pyran-2-yl)-9*H*-purine 8 (66.8 mg, 0.28 mmol) and triethylamine (56.7 mg, 0.56 mmol, 78.0 μ L) in ethanol (0.3 mL). The remaining residue was purified by flash chromatography on silica gel using 0–5% MeOH/DCM to afford ethyl 2-(((4-oxo-3-phenyl-2-((1*S*)-1-((9-(tetrahydro-2*H*-pyran-2-yl)-9*H*-purin-6-yl)amino)propyl)-3,4-dihydroquinazolin-5-yl)methyl)amino)thiazole-4-carboxylate (68.1 mg, 0.102 mmol) in 73% yield. LC–MS (method 1): t_R = 3.35 min, m/z (M + H)⁺ = 666.3.

The general procedure GP4 (method A) was used with compound **32a** (62.4 mg, 0.09 mmol) to afford the final product, (*S*)-2-(((2-((1-((9*H*-purin-6-yl)amino)propyl)-4-oxo-3-phenyl-3,4-dihydroquinazolin-5-yl)methyl)amino)-*N*-hydroxythiazole-4-carboxamide, TFA **33** (17.6 mg, 0.03 mmol) in 33% yield. LC–MS (method 2): t_R = 3.71 min, m/z (M + H)⁺ = 569.2. ¹H NMR (400 MHz, DMSO-*d*₆) δ 10.62 (s, 1H), 8.50 (s, 1H), 8.37 (s, 2H), 8.05 (t, *J* = 6.2 Hz, 1H), 7.76 (t, *J* = 7.8 Hz, 1H), 7.65–7.55 (m, 5H), 7.52 (s, 2H), 7.17 (s, 1H), 5.03 (d, *J* = 6.0 Hz, 2H), 4.79 (s, 1H), 2.00 (d, *J* = 11.7 Hz, 1H), 1.90–1.82 (m, 1H), 0.78 (t, *J* = 7.3 Hz, 3H). HRMS (ESI) m/z : [M + H]⁺ calcd for C₂₇H₂₅N₁₀O₃S 569.1826, found 569.1805.

*4-Oxo-3-phenyl-2-((1*S*)-1-((9-(tetrahydro-2*H*-pyran-2-yl)-9*H*-purin-6-yl)amino)propyl)-3,4-dihydroquinazolin-5-carbonitrile (34)*. The general procedure GP3 was used with compound **29a** (250.0 mg, 0.63 mmol) and trifluoroacetic acid (1.44 g, 12.7 mmol, 0.97 mL) in DCM (6.3 mL). The crude Boc-deprotected amine was worked-up (method B) and reacted with 6-chloro-9-(tetrahydro-2*H*-pyran-2-yl)-9*H*-purine 8 (300.0 mg, 1.26 mmol) and triethylamine (256.0 mg, 2.52 mmol, 0.35 mL) in ethanol (1.6 mL). The remaining residue was purified by flash chromatography on silica gel using 0–5% MeOH/DCM to afford 4-oxo-3-phenyl-2-((1*S*)-1-((9-(tetrahydro-2*H*-pyran-2-yl)-9*H*-purin-6-yl)amino)propyl)-3,4-dihydroquinazolin-5-carbonitrile **34** (258.4 mg, 0.51 mmol) in 81% yield. LC–MS (method 1): t_R = 3.18 min, m/z (M + H)⁺ = 507.3.

*Methyl 4-(((4-Oxo-3-phenyl-2-((1*S*)-1-((9-(tetrahydro-2*H*-pyran-2-yl)-9*H*-purin-6-yl)amino)propyl)-3,4-dihydroquinazolin-5-yl)-methyl)carbamoyl)benzoate (36)*. Compound **34** (136.7 mg, 0.27 mmol) was dissolved in ammonia (1.5 mL, 7*N* in MeOH) in a 20 mL scintillation vial, and Raney Ni (20.0 mg (approx)) was added to it. The reaction vial was evacuated and then kept under hydrogen atmosphere using a balloon. The resulting suspension was stirred at room temperature for 20 h. After completion of reaction (by LC–MS), the crude reaction mixture was carefully filtered under nitrogen, concentrated in vacuo to afford the hydrogenated product, 5-(aminomethyl)-3-phenyl-2-((1*S*)-1-((9-(tetrahydro-2*H*-pyran-2-yl)-9*H*-purin-6-yl)amino)propyl)quinazolin-4(3*H*)-one [LC–MS (method 1): t_R = 2.67 min, m/z (M + H)⁺ = 511.3]. This hydrogenated product was dissolved in DMF (1.3 mL) in a 20 mL scintillation vial, and 4-(methoxycarbonyl)benzoic acid **35** (68.0 mg, 0.41 mmol), DIPEA (106.0 mg, 0.82 mmol, 0.14 mL), and HATU (125.0 mg, 0.33 mmol) were added to it. The resulting mixture was stirred at room temperature for 16 h and concentrated in vacuo. The remaining residue was purified using 0–10% MeOH/DCM to afford methyl 4-(((4-oxo-3-phenyl-2-((1*S*)-1-((9-(tetrahydro-2*H*-pyran-2-yl)-9*H*-purin-6-yl)amino)propyl)-3,4-dihydroquinazolin-5-yl)methyl)-carbamoyl)benzoate

36 (160.0 mg, 0.24 mmol) in 87% yield. LC–MS (method 1): $t_R = 3.32$ min, m/z (M + H)⁺ = 673.3.

(*S*)-*N*1-((2-(1-((9*H*-Purin-6-yl)amino)propyl)-4-oxo-3-phenyl-3,4-dihydroquinazolin-5-yl)methyl)-*N*4-hydroxyterephthalamide (**37**). The general procedure GP4 (method A) was used with compound **36** (80.0 mg, 0.119 mmol) to afford the final product, (*S*)-*N*1-((2-(1-((9*H*-purin-6-yl)amino)propyl)-4-oxo-3-phenyl-3,4-dihydroquinazolin-5-yl)methyl)-*N*4-hydroxyterephthalamide, TFA **37** (26.0 mg, 0.037 mmol) in 31% yield. LC–MS (method 2): $t_R = 3.54$ min, m/z (M + H)⁺ = 590.3. ¹H NMR (400 MHz, DMSO-*d*₆) δ 11.35 (s, 1H), 9.04 (t, $J = 6.0$ Hz, 1H), 8.56 (s, 1H), 8.39 (s, 2H), 7.98–7.94 (m, 2H), 7.86–7.82 (m, 2H), 7.76 (t, $J = 7.9$ Hz, 1H), 7.65–7.48 (m, 6H), 7.41 (d, $J = 7.6$ Hz, 1H), 5.02 (d, $J = 5.8$ Hz, 2H), 4.79 (s, 1H), 2.03 (ddd, $J = 14.3, 7.5, 4.5$ Hz, 1H), 1.89–1.82 (m, 1H), 0.78 (t, $J = 7.3$ Hz, 3H). HRMS (ESI) m/z : [M + H]⁺ calcd for C₃₁H₂₈N₉O₄ 590.2259, found 590.2265.

(*S*)-2-(((2-(1-((9*H*-Purin-6-yl)amino)propyl)-4-oxo-3-phenyl-3,4-dihydroquinazolin-5-yl)methyl)amino)methyl)-*N*-hydroxythiazole-4-carboxamide (**40a**). 5-(Aminomethyl)-3-phenyl-2-((1*S*)-1-((9-(tetrahydro-2*H*-pyran-2-yl)-9*H*-purin-6-yl)amino)propyl)quinazolin-4(3*H*)-one (20.0 mg, 0.04 mmol) was dissolved in DCE (1 mL), and ethyl 2-formylthiazole-4-carboxylate **38a** (7.3 mg, 0.04 mmol) and a drop of acetic acid were added to it. The resulting mixture was stirred at room temperature for 2 h. After 2 h, sodium triacetoxy borohydride (24.9 mg, 0.12 mmol) was added and the reaction mixture was stirred at room temperature for 2 h. After completion of the reaction (by LCMS), a saturated aqueous solution of sodium bicarbonate was added. The product was extracted three times with DCM. The combined organic layers were washed, dried over MgSO₄, filtered, and concentrated in vacuo. The remaining residue was purified by flash chromatography on silica gel using 0–5% MeOH (with 1% triethylamine)/DCM to afford ethyl 2-(((4-oxo-3-phenyl-2-((1*S*)-1-((9-(tetrahydro-2*H*-pyran-2-yl)-9*H*-purin-6-yl)amino)propyl)-3,4-dihydroquinazolin-5-yl)methyl)amino)methyl)thiazole-4-carboxylate **39a** (17.4 mg, 0.026 mmol) in 65% yield. LC–MS (method 1): $t_R = 2.96$ min, m/z (M + H)⁺ = 680.3. The general procedure GP4 (method B) was used with compound **39a** (11.0 mg, 0.018 mmol) to afford the final product, (*S*)-2-(((2-(1-((9*H*-purin-6-yl)amino)-propyl)-4-oxo-3-phenyl-3,4-dihydroquinazolin-5-yl)methyl)amino)-methyl)-*N*-hydroxythiazole-4-carboxamide, TFA **40a** (5.0 mg, 0.007 mmol) in 39% yield. LC–MS (method 2): $t_R = 3.14$ min, m/z (M + H)⁺ = 583.2. ¹H NMR (400 MHz, DMSO-*d*₆) δ 11.13 (s, 1H), 10.08 (s, 1H), 9.22 (s, 2H), 8.30 (s, 1H), 8.21 (s, 2H), 7.87 (dd, $J = 8.3, 7.3$ Hz, 1H), 7.78–7.73 (m, 1H), 7.68 (dt, $J = 6.6, 2.2$ Hz, 1H), 7.62 (dd, $J = 7.4, 1.3$ Hz, 2H), 7.55 (d, $J = 7.4$ Hz, 2H), 4.76 (d, $J = 15.8$ Hz, 4H), 4.64 (s, 2H), 1.96–1.89 (m, 2H), 0.77 (t, $J = 7.3$ Hz, 3H). HRMS (ESI) m/z : [M + 2H]²⁺ (M + z/z, z = 2) calcd for C₂₈H₂₈N₁₀O₃S 292.1028, found 292.1042.

(*S*)-4-(((2-(1-((9*H*-Purin-6-yl)amino)propyl)-4-oxo-3-phenyl-3,4-dihydroquinazolin-5-yl)methyl)amino)methyl)-*N*-hydroxybenzamide (**40b**). 5-(Aminomethyl)-3-phenyl-2-((1*S*)-1-((9-(tetrahydro-2*H*-pyran-2-yl)-9*H*-purin-6-yl)amino)propyl)quinazolin-4(3*H*)-one (44.1 mg, 0.09 mmol) was dissolved in DCE (2 mL), and ethyl 2-formylthiazole-4-carboxylate **38b** (14.1 mg, 0.09 mmol) and a drop of acetic acid were added to it. The resulting mixture was stirred at room temperature for 2 h. After 2

h of stirring, sodium triacetoxy borohydride (54.9 mg, 0.26 mmol) was added and the reaction mixture was stirred at room temperature for 2 h. After completion of the reaction (by LC-MS), a saturated aqueous solution of sodium bicarbonate was added. The product was extracted three times with DCM. The combined organic layers were washed, dried over MgSO₄, filtered, and concentrated in vacuo. The remaining residue was purified by flash chromatography on silica gel using 0–5% MeOH (with 1% triethylamine)/DCM to afford methyl 4-(((4-oxo-3-phenyl-2-((1*S*)-1-((9-(tetrahydro-2*H*-pyran-2-yl)-9*H*-purin-6-yl)-amino)propyl)-3,4-dihydroquinazolin-5-yl)methyl)amino)methyl)-benzoate **39b** (53.3 mg, 0.08 mmol) in 94% yield. LC-MS (method 1): $t_R = 2.98$ min, m/z (M + H)⁺ = 659.3. The general procedure GP4 (method A) was used with compound **39b** (53.3 mg, 0.081 mmol) to afford the final product, (*S*)-4-(((2-(1-((9*H*-purin-6-yl)amino)-propyl)-4-oxo-3-phenyl-3,4-dihydroquinazolin-5-yl)methyl)amino)-methyl)-*N*-hydroxybenzamide, TFA **40b** (33.5 mg, 0.049 mmol) in 41% yield. LC-MS (method 2): $t_R = 3.09$ min, m/z (M + H)⁺ = 576.3. ¹H NMR (400 MHz, DMSO-*d*₆) δ 11.27 (s, 1H), 8.99 (s, 2H), 8.26 (d, $J = 5.8$ Hz, 2H), 8.18 (s, 1H), 7.85 (dd, $J = 8.3, 7.3$ Hz, 1H), 7.81–7.71 (m, 3H), 7.67 (qt, $J = 6.2, 3.5$ Hz, 2H), 7.59–7.50 (m, 5H), 4.78 (s, 1H), 4.58 (dd, $J = 11.5, 5.8$ Hz, 2H), 4.29 (t, $J = 5.8$ Hz, 2H), 1.97–1.85 (m, 2H), 0.77 (t, $J = 7.3$ Hz, 3H). HRMS (ESI) m/z : [M + 2H]²⁺ (M + z/z , $z = 2$) calcd for C₃₁H₃₁N₉O₃ 288.6269, found 288.6270.

(*S*)-2-(((2-(1-((9*H*-Purin-6-yl)amino)propyl)-4-oxo-3-phenyl-3,4-dihydroquinazolin-5-yl)methyl)amino)-*N*-hydroxypyrimidine-5-carboxamide (**43**). 5-(Aminomethyl)-3-phenyl-2-((1*S*)-1-((9-(tetrahydro-2*H*-pyran-2-yl)-9*H*-purin-6-yl)amino)propyl)quinazolin-4(3*H*)-one (160.0 mg, 0.31 mmol) was dissolved in ethanol (0.7 mL) in a microwave vial equipped with a stir bar, and ethyl 2-chloropyrimidine-5-carboxylate **41** (117.0 mg, 0.63 mmol) and triethylamine (127.0 mg, 1.25 mmol, 0.18 mL) were added to it. The microwave vial was sealed, and the resulting mixture was heated at 90 °C for 3 h in a microwave. After completion of the reaction, the reaction mixture was concentrated in vacuo, and the remaining residue was purified using 0–5% MeOH/DCM to afford ethyl 2-(((4-oxo-3-phenyl-2-((1*S*)-1-((9-(tetrahydro-2*H*-pyran-2-yl)-9*H*-purin-6-yl)amino)propyl)-3,4-dihydroquinazolin-5-yl)methyl)amino)-pyrimidine-5-carboxylate **42** (170.0 mg, 0.26 mmol) in 82% yield. LC-MS (method 1): $t_R = 3.41$ min, m/z (M + H)⁺ = 661.3.

The general procedure GP4 (method A) was used with compound **42** (72.0 mg, 0.11 mmol) to afford the final product, (*S*)-2-(((2-(1-((9*H*-purin-6-yl)amino)propyl)-4-oxo-3-phenyl-3,4-dihydroquinazolin-5-yl)methyl)amino)-*N*-hydroxypyrimidine-5-carboxamide, TFA **43** (42.0 mg, 0.062 mmol) in 57% yield. LC-MS (method 2): $t_R = 3.84$ min, m/z (M + H)⁺ = 564.3. ¹H NMR (400 MHz, DMSO-*d*₆) δ 11.05 (s, 1H), 10.01 (d, $J = 6.8$ Hz, 1H), 8.73–8.53 (m, 4H), 8.17 (d, $J = 6.6$ Hz, 1H), 7.72 (t, $J = 7.9$ Hz, 1H), 7.66–7.45 (m, 6H), 7.37 (d, $J = 7.6$ Hz, 1H), 5.08 (d, $J = 4.8$ Hz, 2H), 4.77 (ddd, $J = 10.7, 6.9, 3.8$ Hz, 2H), 2.15–2.02 (m, 1H), 1.97–1.82 (m, 1H), 0.86 (t, $J = 7.3$ Hz, 3H). HRMS (ESI) m/z : [M + H]⁺ calcd for C₂₈H₂₆N₁₁O₃ 564.2215, found 564.2207.

General Procedure for Attachment of Pyrimidine Hinge Binding Group (GP6).

—The Boc-protected amine (1.0 equiv) was dissolved in DCM (0.1 M) in a vial, and trifluoroacetic acid (20 equiv) was added dropwise to it. The resulting mixture was stirred at

room temperature for 3 h. After completion of reaction (by LC-MS), the reaction mixture was worked-up by either of the following two methods. Method A: The crude reaction was quenched with aqueous saturated NaHCO₃ solution and extracted three times with DCM. The combined organic layers were dried over anhydrous MgSO₄, filtered, and concentrated in vacuo to afford the free amine. Method B: The crude reaction mixture was concentrated in vacuo, redissolved in 1–2 mL of DCM, and passed through preconditioned PL-HCO₃ MP SPE device (bicarbonate resin solid phase extraction) and washed with 2 mL of DCM. The filtrate was concentrated in vacuo to afford the free amine. The free amine was dissolved in *n*-butanol (0.4 M) in a microwave vial equipped with a stir bar followed by the addition of substituted chloro-pyrimidine (1.5–2.0 equiv) and DIPEA (3.0–4.0 equiv) to it. The vial was sealed and heated for 1–5 h at 130 1/2C in a microwave. After completion of reaction (by LC-MS), the reaction mixture was concentrated in vacuo and the remaining residue was purified by flash chromatography on silica gel using forced flow of indicated solvent system on Biotage KP-Sil prepacked cartridges and using the Biotage SP-1 automated chromatography system to afford the coupled product.

Procedure for Synthesis of C5-Substituted quinazolinones (46a–d and 48a–o, Scheme 5).—Methyl (*S*)-6-(2-(1-((2,6-Diamino-5-cyanopyrimidin-4-yl)amino)propyl)-4-oxo-3-phenyl-3,4-dihydroquinazolin-5-yl)hexanoate (**45a**). The general procedure GP2 was used with compound **17b** (96.0 mg, 0.19 mmol) and 10 wt % Pd/C (9.6 mg). After completion of reaction (determined by LC-MS), the crude reaction mixture was filtered using Celite and concentrated in vacuo. The general procedure GP6 was used on the hydrogenated product (formed above) with trifluoroacetic acid (440.0 mg, 3.86 mmol, 0.30 mL) in DCM (2.0 mL). The crude reaction was worked-up (method B) and heated with 2,4-diamino-6-chloropyrimidine-5-carbonitrile **44a** (49.0 mg, 0.29 mmol) and DIPEA (75.0 mg, 0.58 mmol, 0.10 mL) in *n*-butanol (0.5 mL) at 130 1/2C for 5 h in a MW reactor. The remaining residue was purified by flash chromatography on silica gel using 0–70% EtOAc/hexanes to afford methyl (*S*)-6-(2-(1-((2,6-diamino-5-cyanopyrimidin-4-yl)amino)propyl)-4-oxo-3-phenyl-3,4-dihydroquinazolin-5-yl)hexanoate **45a** (66.0 mg, 0.12 mmol) in 63% yield. LC–MS (method 1): $t_R = 3.13$ min, m/z (M + H)⁺ = 541.3.

Methyl (*S*)-6-(2-(1-((2-Amino-5-cyano-6-methylpyrimidin-4-yl)amino)propyl)-4-oxo-3-phenyl-3,4-dihydroquinazolin-5-yl)-hexanoate (**45b**). The general procedure GP2 was used with compound **17b** (141.0 mg, 0.28 mmol) and 10 wt % Pd/C (9.6 mg). After completion of reaction (determined by LC-MS), the crude reaction mixture was filtered using Celite and concentrated in vacuo. The general procedure GP6 was used on the hydrogenated product (formed above) with trifluoroacetic acid (643.0 mg, 5.64 mmol, 0.43 mL) in DCM (2.8 mL). The crude reaction was worked-up (method B) and heated with 2-amino-4-chloro-6-methylpyrimidine-5-carbonitrile **44b** (71.0 mg, 0.42 mmol) and DIPEA (109.0 mg, 0.85 mmol, 0.15 mL) in *n*-butanol (0.7 mL) at 130 1/2C for 1 h in a MW reactor. The remaining residue was purified by flash chromatography on silica gel using 0–70% EtOAc/hexanes to afford methyl (*S*)-6-(2-(1-((2-amino-5-cyano-6-methylpyrimidin-4-yl)amino)propyl)-4-oxo-3-phenyl-3,4-dihydroquinazolin-5-yl)hexanoate **45b** (76.0 mg, 0.14 mmol) in 50% yield. LC–MS (method 1): $t_R = 3.19$ min, m/z (M + H)⁺ = 540.3.

Methyl (S)-6-(2-(1-((2-Amino-5-methylpyrimidin-4-yl)amino)propyl)-4-oxo-3-phenyl-3,4-dihydroquinazolin-5-yl)hexanoate (45c). The general procedure GP2 was used with compound **17b** (96.0 mg, 0.19 mmol) and 10 wt % Pd/C (9.6 mg). After completion of reaction (determined by LC-MS), the crude reaction mixture was filtered using Celite and concentrated in vacuo. The general procedure GP6 was used on the hydrogenated product (formed above) with trifluoroacetic acid (440.0 mg, 3.86 mmol, 0.30 mL) in DCM (2.0 mL). The crude reaction was worked-up (method B) and heated with 4-chloro-5-methylpyrimidin-2-amine **45c** (42.0 mg, 0.29 mmol) and DIPEA (75.0 mg, 0.58 mmol, 0.10 mL) in *n*-butanol (0.5 mL) at 130 1/2C for 5 h in a MW reactor. The remaining residue was purified by flash chromatography on silica gel using 0–10% MeOH/DCM to afford the product methyl (*S*)-6-(2-(1-((2-amino-5-methylpyrimidin-4-yl)amino)propyl)-4-oxo-3-phenyl-3,4-dihydroquinazolin-5-yl)hexanoate **45c** (38.0 mg, 0.07 mmol) in 38% yield. LC-MS (method 1): $t_R = 3.2$ min, m/z (M + H)⁺ = 515.3.

Methyl (S)-4-(2-(2-(1-((2,6-Diamino-5-cyanopyrimidin-4-yl)amino)propyl)-4-oxo-3-phenyl-3,4-dihydroquinazolin-5-yl)ethyl)benzoate (45d). The general procedure GP2 was used with compound **17c** (81.2 mg, 0.15 mmol) and 10 wt % Pd/C (8.0 mg). After completion of reaction (determined by LC-MS), the crude reaction mixture was filtered using Celite and concentrated in vacuo. The general procedure GP6 was used on the hydrogenated product (formed above) with trifluoroacetic acid (333.0 mg, 2.92 mmol, 0.22 mL) in DCM (1.5 mL). The crude reaction was worked-up (method B) and heated with 2,4-diamino-6-chloropyrimidine-5-carbonitrile **44a** (50.0 mg, 0.29 mmol) and DIPEA (75.0 mg, 0.58 mmol, 0.1 mL) in *n*-butanol (0.4 mL) at 130 1/2C for 5 h in a MW reactor. The remaining residue was purified by flash chromatography on silica gel using 0–100% EtOAc/hexanes to afford methyl (*S*)-4-(2-(2-(1-((2,6-diamino-5-cyanopyrimidin-4-yl)amino)propyl)-4-oxo-3-phenyl-3,4-dihydroquinazolin-5-yl)ethyl)benzoate **45d** (64.0 mg, 0.11 mmol) in 76% yield. LC-MS (method 1): $t_R = 3.23$ min, m/z (M + H)⁺ = 575.3.

(S)-6-(2-(1-((2,6-Diamino-5-cyanopyrimidin-4-yl)amino)propyl)-4-oxo-3-phenyl-3,4-dihydroquinazolin-5-yl)-N-hydroxyhexanamide (46a). The general procedure GP4 (method B) was used with compound **45a** (54.0 mg, 0.10 mmol) to afford the final product, (*S*)-6-(2-(1-((2,6-diamino-5-cyanopyrimidin-4-yl)amino)propyl)-4-oxo-3-phenyl-3,4-dihydroquinazolin-5-yl)-*N*-hydroxyhexanamide, TFA **46a** (40.0 mg, 0.061 mmol) in 61% yield. LC-MS (method 2): $t_R = 3.91$ min, m/z (M + H)⁺ = 542.3. ¹H NMR (400 MHz, DMSO-*d*₆) δ 10.29 (s, 1H), 8.05 (s, 3H), 7.74 (t, $J = 7.8$ Hz, 2H), 7.57–7.42 (m, 7H), 7.33 (dd, $J = 7.6, 1.3$ Hz, 1H), 4.77 (td, $J = 7.6, 4.9$ Hz, 1H), 3.14 (ddq, $J = 12.4, 8.0, 5.5, 4.2$ Hz, 2H), 1.90 (t, $J = 7.2$ Hz, 3H), 1.82–1.71 (m, 1H), 1.49 (dp, $J = 15.0, 7.4$ Hz, 4H), 1.28 (q, $J = 8.1$ Hz, 2H), 0.71 (t, $J = 7.3$ Hz, 3H). HRMS (ESI) m/z : [M + H]⁺ calcd for C₂₈H₃₂N₉O₃ 542.2623, found 542.2635.

(S)-6-(2-(1-((2-Amino-5-cyano-6-methylpyrimidin-4-yl)amino)propyl)-4-oxo-3-phenyl-3,4-dihydroquinazolin-5-yl)-N-hydroxyhexanamide (46b). The general procedure GP4 (method B) was used with compound **45b** (54.0 mg, 0.10 mmol) to afford the final product, (*S*)-6-(2-(1-((2-amino-5-cyano-6-methylpyrimidin-4-yl)amino)propyl)-4-oxo-3-phenyl-3,4-dihydroquinazolin-5-yl)-*N*-hydroxyhexanamide, TFA **46b** (45.0 mg, 0.069 mmol) in 69% yield. LC-MS (method 2): $t_R = 4.04$ min, m/z (M + H)⁺ = 541.3. ¹H NMR

(400 MHz, DMSO- d_6) δ 10.28 (s, 1H), 8.09 (s, 1H), 7.73 (t, J = 7.8 Hz, 1H), 7.59–7.45 (m, 6H), 7.45–7.36 (m, 2H), 7.32 (dd, J = 7.5, 1.3 Hz, 1H), 4.77 (td, J = 7.6, 4.8 Hz, 1H), 3.14 (t, J = 7.7 Hz, 2H), 2.54 (s, 1H), 2.34 (s, 3H), 2.00–1.86 (m, 3H), 1.79 (dp, J = 14.7, 7.4 Hz, 1H), 1.49 (dq, J = 15.1, 7.6 Hz, 4H), 1.28 (p, J = 7.7 Hz, 2H), 0.72 (t, J = 7.3 Hz, 3H). HRMS (ESI) m/z : $[M + H]^+$ calcd for $C_{29}H_{33}N_8O_3$ 541.2670, found 541.2680.

(*S*)-6-(2-(1-((2-Amino-5-methylpyrimidin-4-yl)amino)propyl)-4-oxo-3-phenyl-3,4-dihydroquinazolin-5-yl)-*N*-hydroxyhexanamide (**46c**). The general procedure GP4 (method B) was used with compound **45c** (35.0 mg, 0.068 mmol) to afford the final product, (*S*)-6-(2-(1-((2-amino-5-methylpyrimidin-4-yl)amino)propyl)-4-oxo-3-phenyl-3,4-dihydroquinazolin-5-yl)-*N*-hydroxyhexanamide, TFA **46c** (30.0 mg, 0.048 mmol) in 70% yield. LC–MS (method 2): t_R = 4.06 min, m/z ($M + H$) $^+$ = 516.3. 1H NMR (400 MHz, DMSO- d_6) δ 11.72 (s, 1H), 10.29 (s, 1H), 8.09 (d, J = 7.7 Hz, 1H), 7.73 (t, J = 7.8 Hz, 1H), 7.57–7.50 (m, 4H), 7.42–7.31 (m, 5H), 4.85 (td, J = 7.9, 5.2 Hz, 1H), 3.14 (t, J = 7.7 Hz, 2H), 2.08–1.78 (m, 8H), 1.47 (dt, J = 14.9, 7.0 Hz, 4H), 1.27 (p, J = 7.5, 7.1 Hz, 2H), 0.76 (t, J = 7.3 Hz, 3H). HRMS (ESI) m/z : $[M + H]^+$ calcd for $C_{28}H_{34}N_7O_3$ 516.2718, found 516.2717.

(*S*)-4-(2-(2-(1-((2,6-Diamino-5-cyanopyrimidin-4-yl)amino)-propyl)-4-oxo-3-phenyl-3,4-dihydroquinazolin-5-yl)ethyl)-*N*-hydroxybenzamide (**46d**). The general procedure GP4 (method B) was used with compound **45d** (56.0 mg, 0.097 mmol) to afford the final product, (*S*)-4-(2-(2-(1-((2,6-diamino-5-cyanopyrimidin-4-yl)amino)propyl)-4-oxo-3-phenyl-3,4-dihydroquinazolin-5-yl)ethyl)-*N*-hydroxybenzamide, TFA **46d** (27.2 mg, 0.039 mmol) in 40% yield. LC–MS (method 2): t_R = 4.34 min, m/z ($M + H$) $^+$ = 576.2. 1H NMR (400 MHz, DMSO- d_6) δ 11.10 (s, 1H), 7.77–7.71 (m, 1H), 7.67–7.61 (m, 3H), 7.60–7.44 (m, 6H), 7.36–7.25 (m, 4H), 4.76 (q, J = 7.3 Hz, 1H), 2.91–2.82 (m, 2H), 1.94–1.85 (m, 1H), 1.75 (dt, J = 14.5, 7.4 Hz, 1H), 0.74–0.65 (m, 3H). HRMS (ESI) m/z : $[M + H]^+$ calcd for $C_{31}H_{30}N_9O_3$ 576.2466, found 576.2475 [Note: In addition to compound **46d**, a side product originating from the hydrolysis of methyl ester in **45d** to carboxylic acid was also isolated in 7% yield].

(*S*)-5-((2-(1-((2-Amino-5-cyano-6-methylpyrimidin-4-yl)amino)-propyl)-4-oxo-3-phenyl-3,4-dihydroquinazolin-5-yl)amino)-*N*-hydroxypentanamide (**48a**). The general procedure GP6 was used with compound **26b** (98.0 mg, 0.193 mmol) and trifluoroacetic acid (439.0 mg, 3.85 mmol, 0.3 mL) in DCM (2.0 mL). The crude reaction was worked-up (method B) and heated with 2-amino-4-chloro-6-methylpyrimidine-5-carbonitrile **44b** (49.0 mg, 0.29 mmol) and DIPEA (75.0 mg, 0.56 mmol, 0.1 mL) in *n*-butanol (0.5 mL) at 130 $^{\circ}C$ for 2 h in a MW reactor. The remaining residue was purified by flash chromatography on silica gel using 0–100% EtOAc/hexanes to afford methyl (*S*)-5-((2-(1-((2-amino-5-cyano-6-methylpyrimidin-4-yl)amino)propyl)-4-oxo-3-phenyl-3,4-dihydroquinazolin-5-yl)amino)-pentanoate **47a** (89.0 mg, 0.164 mmol) in 85% yield. LC–MS (method 1): t_R = 3.18 min, m/z ($M + H$) $^+$ = 541.3.

The general procedure GP4 (method B) was used with compound **47a** (74.0 mg, 0.14 mmol) to afford the final product, (*S*)-5-((2-(1-((2-amino-5-cyano-6-methylpyrimidin-4-yl)amino)propyl)-4-oxo-3-phenyl-3,4-dihydroquinazolin-5-yl)amino)-*N*-

hydroxypentanamide, TFA **48a** (73.5 mg, 0.112 mmol) in 82% yield. LC–MS (method 2): $t_R = 4.02$ min, m/z ($M + H$)⁺ = 542.3. ¹H NMR (400 MHz, DMSO-*d*₆) δ 10.30 (s, 1H), 8.03 (s, 1H), 7.63–7.51 (m, 3H), 7.51–7.46 (m, 3H), 7.46–7.37 (m, 2H), 6.74 (dd, $J = 7.9, 1.0$ Hz, 1H), 6.59 (d, $J = 8.5$ Hz, 1H), 4.74 (td, $J = 7.6, 4.8$ Hz, 1H), 3.18 (d, $J = 6.1$ Hz, 2H), 2.54 (s, 1H), 2.35 (s, 3H), 2.02–1.85 (m, 3H), 1.76 (dp, $J = 14.6, 7.4$ Hz, 1H), 1.57 (q, $J = 4.1$ Hz, 4H), 0.70 (t, $J = 7.3$ Hz, 3H). HRMS (ESI) m/z : [$M + H$]⁺ calcd for C₂₈H₃₂N₉O₃ 542.2623, found 542.2626 [Note: In addition to compound **48a**, a side product originating from the hydrolysis of methyl ester in **47a** to carboxylic acid was also isolated in 7% yield].

(*S*)-4-(((2-(1-((2,6-Diamino-5-cyanopyrimidin-4-yl)amino)-propyl)-4-oxo-3-phenyl-3,4-dihydroquinazolin-5-yl)amino)-methyl)-*N*-hydroxybenzamide (**48b**). The general procedure GP6 was used with compound **26d** (80.0 mg, 0.15 mmol) and trifluoroacetic acid (336.0 mg, 2.95 mmol, 0.23 mL) in DCM (1.7 mL). The crude reaction was worked-up (method B) and heated with 2,4-diamino-6-chloropyrimidine-5-carbonitrile **44a** (50.0 mg, 0.29 mmol) and DIPEA (76.0 mg, 0.59 mmol, 0.1 mL) in 2-propanol (0.7 mL) at 130 1/2C for 1 h in a MW reactor. The remaining residue was purified by flash chromatography on silica gel using 0–100% EtOAc/ hexanes to afford the product methyl (*S*)-4-(((2-(1-((2,6-diamino-5-cyanopyrimidin-4-yl)amino)propyl)-4-oxo-3-phenyl-3,4-dihydroquinazolin-5-yl)amino)methyl)benzoate **47b** (70.0 mg, 0.10 mmol) in 69% yield. LC–MS (method 1): $t_R = 3.18$ min, m/z ($M + H$)⁺ = 576.3. The general procedure GP4 (method B) was used with compound **47b** (41.7 mg, 0.072 mmol) to afford the final product, (*S*)-4-(((2-(1-((2,6-diamino-5-cyanopyrimidin-4-yl)amino)propyl)-4-oxo-3-phenyl-3,4-dihydroquinazolin-5-yl)amino)methyl)-*N*-hydroxybenzamide, TFA **48b** (21.2 mg, 0.031 mmol) in 42% yield. LC–MS (method 2): $t_R = 3.98$ min, m/z ($M + H$)⁺ = 577.3. ¹H NMR (400 MHz, DMSO-*d*₆) δ 11.12 (s, 1H), 8.96 (s, 1H), 7.70 (dd, $J = 8.2, 1.7$ Hz, 2H), 7.55 (t, $J = 7.3$ Hz, 2H), 7.52–7.43 (m, 5H), 7.40 (dd, $J = 8.2, 1.7$ Hz, 2H), 6.76 (d, $J = 7.8$ Hz, 1H), 6.51 (d, $J = 8.4$ Hz, 1H), 4.72 (q, $J = 7.1$ Hz, 1H), 4.50 (d, $J = 4.4$ Hz, 2H), 1.85 (q, $J = 6.4, 5.8$ Hz, 1H), 1.71 (dt, $J = 14.5, 7.4$ Hz, 1H), 0.72–0.64 (m, 3H). HRMS (ESI) m/z : [$M + H$]⁺ calcd for C₃₀H₂₉N₁₀O₃ 577.2419, found 577.2407.

(*S*)-4-(((2-(1-((2-Amino-5-cyano-6-methylpyrimidin-4-yl)amino)-propyl)-4-oxo-3-phenyl-3,4-dihydroquinazolin-5-yl)amino)-methyl)-*N*-hydroxybenzamide (**48c**). The general procedure GP6 was used with compound **26d** (68.0 mg, 0.125 mmol) and trifluoroacetic acid (286.0 mg, 2.51 mmol, 0.19 mL) in DCM (1.2 mL). The crude reaction was worked-up (method B) and heated with 2-amino-4-chloro-6-methylpyrimidine-5-carbonitrile **44b** (32.0 mg, 0.19 mmol) and DIPEA (48.0 mg, 0.38 mmol, 65.0 μ L) in *n*-butanol (0.3 mL) at 130 1/2C for 1 h in a MW reactor. The remaining residue was purified by flash chromatography on silica gel using 0–70% EtOAc/hexanes to afford the product methyl (*S*)-4-(((2-(1-((2-amino-5-cyano-6-methylpyrimidin-4-yl)amino)propyl)-4-oxo-3-phenyl-3,4-dihydroquinazolin-5-yl)amino)methyl)benzoate **47c** (60.0 mg, 0.10 mmol) in 84% yield. LC–MS (method 1): $t_R = 3.24$ min, m/z ($M + H$)⁺ = 575.3. The general procedure GP4 (method B) was used with compound **47c** (54.0 mg, 0.094 mmol) to afford the final product, (*S*)-4-(((2-(1-((2-amino-5-cyano-6-methylpyrimidin-4-yl)-amino)propyl)-4-oxo-3-phenyl-3,4-dihydroquinazolin-5-yl)amino)-methyl)-*N*-hydroxybenzamide, TFA **48c** (34.0 mg, 0.05 mmol) in 52% yield. LC–MS (method 2): $t_R = 4.18$ min, m/z ($M + H$)⁺ = 576.3. ¹H

NMR (400 MHz, DMSO- d_6) δ 11.13 (s, 1H), 8.97 (s, 1H), 8.00 (s, 1H), 7.73–7.66 (m, 2H), 7.59–7.45 (m, 5H), 7.45–7.36 (m, 4H), 6.76 (dd, J = 7.9, 0.8 Hz, 1H), 6.51 (dd, J = 8.5, 0.9 Hz, 1H), 4.74 (td, J = 7.7, 4.7 Hz, 1H), 4.50 (s, 2H), 2.33 (s, 3H), 1.90 (dtd, J = 14.2, 7.2, 4.7 Hz, 1H), 1.82–1.71 (m, 1H), 0.70 (t, J = 7.3 Hz, 3H). HRMS (ESI) m/z : $[M + H]^+$ calcd for $C_{31}H_{30}N_9O_3$ 576.2466, found 576.2481 [Note: For PK studies, **48c** was converted to a free base].

(*S*)-4-(((2-(1-((2-Amino-6-methylpyrimidin-4-yl)amino)propyl)-4-oxo-3-phenyl-3,4-dihydroquinazolin-5-yl)amino)methyl)-*N*-hydroxybenzamide (**48d**). The general procedure GP6 was used with compound **26d** (52.0 mg, 0.096 mmol) and trifluoroacetic acid (219.0 mg, 1.92 mmol, 0.15 mL) in DCM (1.0 mL). The crude reaction was worked-up (method B) and heated with 4-chloro-6-methylpyrimidin-2-amine **44d** (21.0 mg, 0.14 mmol) and DIPEA (37.0 mg, 0.29 mmol, 50.0 μ L) in *n*-butanol (0.3 mL) at 130 1/2C for 5 h in a MW reactor. The remaining residue was purified by flash chromatography on silica gel using 0–10% MeOH/DCM to afford methyl (*S*)-4-(((2-(1-((2-amino-6-methylpyrimidin-4-yl)amino)propyl)-4-oxo-3-phenyl-3,4-dihydroquinazolin-5-yl)amino)methyl)-benzoate **47d** (29.0 mg, 0.053 mmol) in 55% yield. LC–MS (method 1): t_R = 2.97 min, m/z ($M + H$)⁺ = 550.3. The general procedure GP4 (method B) was used with compound **47d** (35.0 mg, 0.064 mmol) to afford the final product, (*S*)-4-(((2-(1-((2-amino-6-methylpyrimidin-4-yl)amino)propyl)-4-oxo-3-phenyl-3,4-dihydroquinazolin-5-yl)amino)methyl)-*N*-hydroxybenzamide, TFA **48d** (18.0 mg, 0.027 mmol) in 42% yield. LC–MS (method 2): t_R = 4.23 min, m/z ($M + H$)⁺ = 551.2. ¹H NMR (400 MHz, DMSO- d_6) δ 12.08 (s, 1H), 11.14 (s, 1H), 8.96 (d, J = 7.2 Hz, 2H), 7.72–7.68 (m, 2H), 7.60–7.45 (m, 6H), 7.42–7.37 (m, 3H), 6.73 (d, J = 7.8 Hz, 1H), 6.51 (d, J = 8.4 Hz, 1H), 5.99 (s, 1H), 4.51 (ddd, J = 11.5, 5.5, 2.7 Hz, 3H), 2.20 (s, 3H), 1.88 (ddd, J = 14.2, 7.4, 4.1 Hz, 1H), 1.64 (ddd, J = 13.9, 9.0, 7.0 Hz, 1H), 0.67 (t, J = 7.3 Hz, 3H). HRMS (ESI) m/z : $[M + H]^+$ calcd for $C_{30}H_{31}N_8O_3$ 551.2514, found 551.2532 [Note: In addition to compound **48d**, a side product originating from the hydrolysis of methyl ester in **47d** to carboxylic acid was also isolated in 7% yield].

(*S*)-4-(((2-(1-((6-Amino-5-cyanopyrimidin-4-yl)amino)propyl)-4-oxo-3-phenyl-3,4-dihydroquinazolin-5-yl)amino)methyl)-*N*-hydroxybenzamide (**48e**). The general procedure GP6 was used with compound **26d** (48.3 mg, 0.09 mmol) and trifluoroacetic acid (203.0 mg, 1.78 mmol, 0.14 mL) in DCM (1.0 mL). The crude reaction was worked-up (method B) and heated with 4-amino-6-chloropyrimidine-5-carbonitrile **44e** (27.5 mg, 0.18 mmol) and DIPEA (46.0 mg, 0.36 mmol, 62.0 μ L) in *n*-butanol (0.3 mL) at 130 1/2C for 1 h in a MW reactor. The remaining residue was purified by flash chromatography on silica gel using 0–100% EtOAc/hexanes to afford methyl (*S*)-4-(((2-(1-((6-amino-5-cyanopyrimidin-4-yl)amino)propyl)-4-oxo-3-phenyl-3,4-dihydroquinazolin-5-yl)amino)methyl)benzoate **47e** (25.0 mg, 0.045 mmol) in 50% yield. LC–MS (method 1): t_R = 3.39 min, m/z ($M + H$)⁺ = 561.3. The general procedure GP4 (method B) was used with compound **47e** (72.0 mg, 0.13 mmol) to afford the final product, (*S*)-4-(((2-(1-((6-amino-5-cyanopyrimidin-4-yl)amino)propyl)-4-oxo-3-phenyl-3,4-dihydroquinazolin-5-yl)amino)methyl)-*N*-hydroxybenzamide, TFA **48e** (34.0 mg, 0.05 mmol) in 39% yield. LC–MS (method 2): t_R = 4.36 min, m/z ($M + H$)⁺ = 562.2. ¹H NMR (400 MHz, DMSO- d_6) δ 11.13 (s, 1H), 8.96 (s, 1H), 7.93 (s, 1H), 7.73–7.66 (m, 2H), 7.60–7.45 (m, 6H), 7.42–7.32 (m, 3H), 6.78–6.70 (m, 1H), 6.49 (d, J =

8.4 Hz, 1H), 4.65 (td, $J = 7.9, 4.8$ Hz, 1H), 4.49 (s, 2H), 2.54 (s, 1H), 1.86 (tq, $J = 12.2, 7.4, 6.2$ Hz, 1H), 1.80–1.72 (m, 1H), 0.70 (t, $J = 7.3$ Hz, 3H). HRMS (ESI) m/z : $[M + H]^+$ calcd for $C_{30}H_{28}N_9O_3$ 562.2310, found 562.2330. [Note: In addition to compounds **48e**, a side product originating from the hydrolysis of methyl ester in **47e** to carboxylic acid was also isolated in 2% yield].

(S)-4-(((2-(1-((6-Amino-5-chloropyrimidin-4-yl)amino)propyl)-4-oxo-3-phenyl-3,4-dihydroquinazolin-5-yl)amino)methyl)-*N*-hydroxybenzamide (**48f**). The general procedure GP6 was used with compound **26d** (61.8 mg, 0.114 mmol) and trifluoroacetic acid (260.0 mg, 2.28 mmol, 0.17 mL) in DCM (1.2 mL). The crude reaction was worked-up (method B) and heated with 5,6-dichloropyrimidin-4-amine **44f** (37.0 mg, 0.23 mmol) and DIPEA (59.0 mg, 0.46 mmol, 79.0 μ L) in *n*-butanol (0.3 mL) at 130 1/2C for 5 h in a MW reactor. The remaining residue was purified by flash chromatography on silica gel using 0–100% EtOAc/hexanes to afford methyl (*S*)-4-(((2-(1-((6-amino-5-chloropyrimidin-4-yl)amino)-propyl)-4-oxo-3-phenyl-3,4-dihydroquinazolin-5-yl)amino)methyl)-benzoate **47f** (55.0 mg, 0.096 mmol) in 85% yield. LC–MS (method 1): $t_R = 3.25$ min, m/z ($M + H$) $^+ = 570.2$. The general procedure GP4 (method B) was used with compound **47f** (55.0 mg, 0.096 mmol) to afford the final product, (*S*)-4-(((2-(1-((6-amino-5-chloropyrimidin-4-yl)amino)propyl)-4-oxo-3-phenyl-3,4-dihydroquinazolin-5-yl)-amino)methyl)-*N*-hydroxybenzamide, TFA **48f** (53.0 mg, 0.077 mmol) in 80% yield. LC–MS (method 2): $t_R = 4.50$ min, m/z ($M + H$) $^+ = 571.1$. 1H NMR (400 MHz, DMSO- d_6) δ 11.13 (s, 1H), 8.95 (s, 1H), 8.03 (s, 1H), 7.73–7.66 (m, 2H), 7.60–7.51 (m, 2H), 7.51–7.44 (m, 5H), 7.40 (d, $J = 8.1$ Hz, 3H), 6.75 (d, $J = 7.8$ Hz, 1H), 6.49 (d, $J = 8.4$ Hz, 1H), 4.63 (td, $J = 8.1, 4.2$ Hz, 1H), 4.49 (s, 2H), 1.93–1.75 (m, 2H), 0.70 (t, $J = 7.3$ Hz, 3H). HRMS (ESI) m/z : $[M + H]^+$ calcd for $C_{29}H_{28}ClN_8O_3$ 571.1967, found 571.1972 [Note: In addition to compound **48f**, a side product originating from the hydrolysis of methyl ester in **47f** to carboxylic acid was also isolated in 9% yield].

(S)-6-(((2-(1-((6-Amino-5-chloropyrimidin-4-yl)amino)propyl)-4-oxo-3-phenyl-3,4-dihydroquinazolin-5-yl)amino)methyl)-*N*-hydroxynicotinamide (**48g**). The general procedure GP6 was used with compound **26g** (66.0 mg, 0.12 mmol) and trifluoroacetic acid (277.0 mg, 2.45 mmol, 0.19 mL) in DCM (1.2 mL). The crude reaction was worked-up (method B) and heated with 5,6-dichloropyrimidin-4-amine **44f** (40.0 mg, 0.24 mmol) and DIPEA (63.0 mg, 0.48 mmol, 83.0 μ L) in *n*-butanol (0.3 mL) at 130 1/2C for 2 h in a MW reactor. The remaining residue was purified by flash chromatography on silica gel using 0–100% EtOAc/hexanes to afford methyl (*S*)-6-(((2-(1-((6-amino-5-chloropyrimidin-4-yl)amino)propyl)-4-oxo-3-phenyl-3,4-dihydroquinazolin-5-yl)amino)methyl)nicotinate **47g** (30.0 mg, 0.053 mmol) in 43% yield. LC–MS (method 1): $t_R = 3.06$ min, m/z ($M + H$) $^+ = 571.2$. The general procedure GP4 (method B) was used with compound **47g** (30.0 mg, 0.053 mmol) to afford the final product, (*S*)-6-(((2-(1-((6-amino-5-chloropyrimidin-4-yl)amino)-propyl)-4-oxo-3-phenyl-3,4-dihydroquinazolin-5-yl)amino)methyl)-*N*-hydroxynicotinamide, TFA **48g** (13.0 mg, 0.019 mmol) in 36% yield. LC–MS (method 2): $t_R = 3.89$ min, m/z ($M + H$) $^+ = 572.3$. 1H NMR (400 MHz, DMSO- d_6) δ 11.31 (s, 1H), 9.21 (s, 1H), 8.84 (d, $J = 2.1$ Hz, 1H), 8.05 (dd, $J = 8.1, 2.2$ Hz, 1H), 7.89 (s, 1H), 7.60–7.42 (m, 6H), 6.93 (d, $J = 22.9$ Hz, 2H), 6.76 (d, $J = 7.6$ Hz, 1H), 6.50 (d, $J = 8.5$ Hz, 1H), 5.75 (s,

1H), 4.64–4.55 (m, 2H), 3.10 (qd, $J = 7.3, 4.8$ Hz, 1H), 1.90–1.72 (m, 2H), 0.70 (t, $J = 7.2$ Hz, 3H). HRMS (ESI) m/z : $[M + H]^+$ calcd for $C_{28}H_{27}ClN_9O_3$ 572.1920, found 572.1936.

(S)-4-(((2-(1-((2-Amino-5-chloro-6-methylpyrimidin-4-yl)amino)-propyl)-4-oxo-3-phenyl-3,4-dihydroquinazolin-5-yl)amino)-methyl)-*N*-hydroxybenzamide (**48f**). The general procedure GP6 was used with compound **26d** (72.0 mg, 0.133 mmol) and trifluoroacetic acid (303.0 mg, 2.65 mmol, 0.20 mL) in DCM (1.3 mL). The crude reaction was worked-up (method B) and heated with 4,5-dichloro-6-methylpyrimidin-2-amine **44g** (36.0 mg, 0.20 mmol) and DIPEA (52.0 mg, 0.40 mmol, 70.0 μ L) in *n*-butanol (0.3 mL) at 130 $^{\circ}$ C for 5 h in a MW reactor. The remaining residue was purified by flash chromatography on silica gel using 0–100% EtOAc/hexanes to afford the product methyl (*S*)-4-(((2-(1-((2-amino-5-chloro-6-methylpyrimidin-4-yl)amino)propyl)-4-oxo-3-phenyl-3,4-dihydroquinazolin-5-yl)amino)methyl)benzoate **47h** (68.0 mg, 0.116 mmol) in 88% yield. LC–MS (method 1): $t_R = 3.15$ min, m/z ($M + H$) $^+ = 584.2$. The general procedure GP4 (method B) was used with compound **47h** (68.0 mg, 0.116 mmol) to afford the final product, (*S*)-4-(((2-(1-((2-amino-5-chloro-6-methylpyrimidin-4-yl)amino)-propyl)-4-oxo-3-phenyl-3,4-dihydroquinazolin-5-yl)amino)methyl)-*N*-hydroxybenzamide, TFA **48h** (62.0 mg, 0.089 mmol) in 76% yield. LC–MS (method 2): $t_R = 4.19$ min, m/z ($M + H$) $^+ = 585.2$. 1H NMR (400 MHz, DMSO- d_6) δ 11.13 (s, 1H), 8.97 (t, $J = 5.8$ Hz, 1H), 8.39 (d, $J = 7.4$ Hz, 1H), 7.70 (d, $J = 8.0$ Hz, 2H), 7.61–7.46 (m, 4H), 7.46–7.36 (m, 5H), 6.78 (d, $J = 7.8$ Hz, 1H), 6.53 (d, $J = 8.4$ Hz, 1H), 4.78 (td, $J = 7.7, 4.8$ Hz, 1H), 4.51 (d, $J = 4.8$ Hz, 2H), 2.33 (s, 3H), 2.03–1.91 (m, 1H), 1.83 (dq, $J = 14.4, 7.4$ Hz, 1H), 0.72 (t, $J = 7.3$ Hz, 3H). HRMS (ESI) m/z : $[M + H]^+$ calcd for $C_{30}H_{30}ClN_8O_3$ 585.2124, found 585.2151 [Note: In addition to compound **48h**, a side product originating from the hydrolysis of methyl ester in **47h** to carboxylic acid, was also isolated in 4% yield].

(S)-4-(((2-(1-((6-Amino-5-cyano-2-methylpyrimidin-4-yl)amino)-propyl)-4-oxo-3-phenyl-3,4-dihydroquinazolin-5-yl)amino)-methyl)-*N*-hydroxybenzamide (**48i**). The general procedure GP6 was used with compound **26d** (86.0 mg, 0.158 mmol) and trifluoroacetic acid (361.0 mg, 3.17 mmol, 0.24 mL) in DCM (1.6 mL). The crude reaction was worked-up (method B) and heated with 4-amino-6-chloro-2-methylpyrimidine-5-carbonitrile **44h** (40.0 mg, 0.24 mmol) and DIPEA (61.0 mg, 0.47 mmol, 84.0 μ L) in *n*-butanol (0.3 mL) at 130 $^{\circ}$ C for 2 h in a MW reactor. The remaining residue was purified by flash chromatography on silica gel using 0–100% EtOAc/hexanes to afford methyl (*S*)-4-(((2-(1-((6-amino-5-cyano-2-methylpyrimidin-4-yl)amino)propyl)-4-oxo-3-phenyl-3,4-dihydroquinazolin-5-yl)amino)methyl)benzoate **47i** (75.0 mg, 0.131 mmol) in 83% yield. LC–MS (method 1): $t_R = 3.33$ min, m/z ($M + H$) $^+ = 575.3$. The general procedure GP4 (method B) was used with compound **47i** (73.0 mg, 0.13 mmol) to afford the final product, (*S*)-4-(((2-(1-((6-amino-5-cyano-2-methylpyrimidin-4-yl)amino)propyl)-4-oxo-3-phenyl-3,4-dihydroquinazolin-5-yl)amino)methyl)-*N*-hydroxybenzamide, TFA **48i** (56.0 mg, 0.08 mmol) in 64% yield. LC–MS (method 2): $t_R = 4.17$ min, m/z ($M + H$) $^+ = 576.3$. 1H NMR (400 MHz, DMSO- d_6) δ 11.13 (s, 1H), 8.96 (s, 1H), 7.69 (d, $J = 8.1$ Hz, 2H), 7.59–7.42 (m, 8H), 7.40 (d, $J = 8.0$ Hz, 2H), 6.76 (d, $J = 7.9$ Hz, 1H), 6.49 (d, $J = 8.4$ Hz, 1H), 4.78 (td, $J = 8.3, 4.3$ Hz, 1H), 4.50 (s, 2H), 2.17 (s, 3H), 1.92–1.75 (m, 2H), 0.68 (t, $J = 7.3$ Hz, 3H). HRMS (ESI) m/z : $[M + H]^+$ calcd for $C_{31}H_{30}CN_9O_3$ 576.2466, found 576.2470 [Note: In addition to compound **48i**, a

side product originating from the hydrolysis of methyl ester in **47i** to carboxylic acid, was also isolated in 3% yield].

(S)-4-(((2-(1-((2,6-Diamino-5-chloropyrimidin-4-yl)amino)propyl)-4-oxo-3-phenyl-3,4-dihydroquinazolin-5-yl)amino)methyl)-*N*-hydroxybenzamide (**48j**). The general procedure GP6 was used with compound **26d** (64.0 mg, 0.12 mmol) and trifluoroacetic acid (269.0 mg, 2.36 mmol, 0.18 mL) in DCM (1.2 mL). The crude reaction was worked-up (method B) and heated with 5,6-dichloropyrimidine-2,4-diamine **44i** (32.0 mg, 0.18 mmol) and DIPEA (46.0 mg, 0.35 mmol, 63.0 μ L) in *n*-butanol (0.5 mL) at 130 $^{\circ}$ C for 3 h in a MW reactor. The remaining residue was purified by flash chromatography on silica gel using 0–100% EtOAc/hexanes to afford methyl (*S*)-4-(((2-(1-((2,6-diamino-5-chloropyrimidin-4-yl)amino)propyl)-4-oxo-3-phenyl-3,4-dihydroquinazolin-5-yl)amino)methyl)benzoate **47j** (32.0 mg, 0.06 mmol) in 46% yield. LC–MS (method 1): $t_R = 3.78$ min, m/z ($M + H$)⁺ = 585.2. The general procedure GP4 (method B) was used with compound **47j** (31.0 mg, 0.05 mmol) to afford the final product, (*S*)-4-(((2-(1-((2,6-diamino-5-chloropyrimidin-4-yl)amino)propyl)-4-oxo-3-phenyl-3,4-dihydroquinazolin-5-yl)amino)methyl)-*N*-hydroxybenzamide, TFA **48j** (15.0 mg, 0.02 mmol) in 40% yield. LC–MS (method 2): $t_R = 4.29$ min, m/z ($M + H$)⁺ = 586.3. ¹H NMR (400 MHz, DMSO-*d*₆) δ 11.13 (s, 1H), 8.96 (d, $J = 6.4$ Hz, 1H), 7.70 (d, $J = 8.0$ Hz, 2H), 7.61–7.46 (m, 7H), 7.46–7.36 (m, 3H), 7.27 (s, 1H), 6.77 (d, $J = 7.9$ Hz, 1H), 6.51 (d, $J = 8.4$ Hz, 1H), 4.69 (td, $J = 7.7, 4.4$ Hz, 1H), 4.50 (d, $J = 4.7$ Hz, 2H), 1.88 (ddd, $J = 12.9, 7.4, 4.9$ Hz, 1H), 1.76 (p, $J = 7.4$ Hz, 1H), 0.68 (t, $J = 7.3$ Hz, 3H). HRMS (ESI) m/z : [$M + H$]⁺ calcd for C₂₉H₂₉CN₉O₃ 586.2076, found 586.2087.

(S)-4-(((2-(1-((2-Amino-5-cyano-6-(trifluoromethyl)pyrimidin-4-yl)amino)propyl)-4-oxo-3-phenyl-3,4-dihydroquinazolin-5-yl)amino)methyl)-*N*-hydroxybenzamide (**48k**). The general procedure GP6 was used with compound **26d** (85.0 mg, 0.16 mmol) and trifluoroacetic acid (361.0 mg, 3.17 mmol, 0.24 mL) in DCM (1.6 mL). The crude reaction was worked-up (method B) and heated with 2-amino-4-chloro-6-(trifluoromethyl)pyrimidine-5-carbonitrile **44j** (52.0 mg, 0.24 mmol) and DIPEA (61.0 mg, 0.47 mmol, 82.0 μ L) in *n*-butanol (0.5 mL) at 130 $^{\circ}$ C for 2 h in a MW reactor. The remaining residue was purified by flash chromatography on silica gel using 0–100% EtOAc/hexanes to afford methyl (*S*)-4-(((2-(1-((2-amino-5-cyano-6-(trifluoromethyl)pyrimidin-4-yl)amino)propyl)-4-oxo-3-phenyl-3,4-dihydroquinazolin-5-yl)amino)methyl)benzoate **47k** (94.0 mg, 0.15 mmol) in 95% yield. LC–MS (method 1): $t_R = 3.71$ min, m/z ($M + H$)⁺ = 629.3. The general procedure GP4 (method B) was used with compound **47k** (94.0 mg, 0.15 mmol) to afford the final product, (*S*)-4-(((2-(1-((2-amino-5-cyano-6-(trifluoromethyl)pyrimidin-4-yl)amino)propyl)-4-oxo-3-phenyl-3,4-dihydroquinazolin-5-yl)amino)methyl)-*N*-hydroxybenzamide, TFA **48k** (45.0 mg, 0.06 mmol) in 41% yield. LC–MS (method 2): $t_R = 5.39$ min, m/z ($M + H$)⁺ = 630.3. ¹H NMR (400 MHz, DMSO-*d*₆) δ 11.13 (s, 1H), 8.97 (s, 1H), 7.83 (d, $J = 7.3$ Hz, 1H), 7.70 (d, $J = 8.0$ Hz, 2H), 7.55–7.45 (m, 3H), 7.40 (d, $J = 7.4$ Hz, 3H), 7.29 (s, 1H), 6.76 (d, $J = 7.9$ Hz, 1H), 6.51 (d, $J = 8.4$ Hz, 1H), 4.80 (td, $J = 7.3, 4.8$ Hz, 1H), 4.50 (s, 2H), 1.92 (dq, $J = 13.3, 7.0$ Hz, 1H), 1.76 (hept, $J = 7.4$ Hz, 1H), 0.72 (t, $J = 7.3$ Hz, 3H). HRMS (ESI) m/z : [$M + H$]⁺ calcd for C₃₁H₂₇F₃N₉O₃ 630.2183, found 630.2205.

(S)-4-(((2-(1-((2-Amino-5-cyano-6-cyclopropylpyrimidin-4-yl)-amino)propyl)-4-oxo-3-phenyl-3,4-dihydroquinazolin-5-yl)amino)-methyl)-*N*-hydroxybenzamide (**48l**). The general procedure GP6 was used with compound **26d** (92.0 mg, 0.17 mmol) and trifluoroacetic acid (387.0 mg, 3.4 mmol, 0.26 mL) in DCM (1.7 mL). The crude reaction was worked-up (method B) and heated with 2-amino-4-chloro-6-cyclopropylpyrimidine-5-carbonitrile **44k** (50.0 mg, 0.26 mmol) and DIPEA (66.0 mg, 0.51 mmol, 89.0 μ L) in *n*-butanol (0.5 mL) at 130 $^{\circ}$ C for 2 h in a MW reactor. The remaining residue was purified by flash chromatography on silica gel using 0–100% EtOAc/hexanes to afford methyl (*S*)-4-(((2-(1-((2-amino-5-cyano-6-cyclopropylpyrimidin-4-yl)amino)propyl)-4-oxo-3-phenyl-3,4-dihydroquinazolin-5-yl)amino)methyl)benzoate **47l** (40.0 mg, 0.07 mmol) in 39% yield. LC–MS (method 1): t_R = 3.51 min, m/z (M + H)⁺ = 601.3. The general procedure GP4 (method B) was used with compound **47l** (40.0 mg, 0.07 mmol) to afford the final product, (*S*)-4-(((2-(1-((2-amino-5-cyano-6-cyclopropylpyrimidin-4-yl)-amino)propyl)-4-oxo-3-phenyl-3,4-dihydroquinazolin-5-yl)amino)-methyl)-*N*-hydroxybenzamide, TFA **48l** (28.0 mg, 0.04 mmol) in 59% yield. LC–MS (method 2): t_R = 4.74 min, m/z (M + H)⁺ = 602.3. ¹H NMR (400 MHz, DMSO-*d*₆) δ 11.18–11.06 (m, 1H), 8.96 (s, 1H), 8.01–7.90 (m, 1H), 7.72–7.66 (m, 2H), 7.58–7.44 (m, 6H), 7.40 (d, J = 8.1 Hz, 2H), 7.21 (d, J = 7.1 Hz, 1H), 6.75 (d, J = 7.9 Hz, 2H), 6.50 (d, J = 8.4 Hz, 1H), 4.66 (td, J = 7.7, 4.2 Hz, 1H), 4.50 (s, 2H), 2.05 (p, J = 6.3 Hz, 1H), 1.84 (ddd, J = 14.1, 7.3, 4.6 Hz, 1H), 1.72 (dt, J = 14.4, 7.2 Hz, 1H), 1.00 (d, J = 6.0 Hz, 4H), 0.66 (t, J = 7.3 Hz, 3H). HRMS (ESI) m/z : [M + H]⁺ calcd for C₃₃H₃₂N₉O₃ 602.2623, found 602.2617.

(S)-4-(((2-(1-((2-Amino-5-cyano-6-(difluoromethyl)pyrimidin-4-yl)amino)propyl)-4-oxo-3-phenyl-3,4-dihydroquinazolin-5-yl)amino)methyl)-*N*-hydroxybenzamide (**48m**). The general procedure GP6 was used with compound **26d** (50.5 mg, 0.114 mmol) and trifluoroacetic acid (260.0 mg, 2.28 mmol, 0.17 mL) in DCM (1.1 mL). The crude reaction was worked-up (method B) and heated with 5-bromo-4-chloro-6-(difluoromethyl)pyrimidin-2-amine **44l** (44.0 mg, 0.17 mmol) and DIPEA (44.0 mg, 0.34 mmol, 60.0 μ L) in *n*-butanol (0.5 mL) at 130 $^{\circ}$ C for 2 h in a MW reactor. The remaining residue was purified by flash chromatography on silica gel using 0–100% EtOAc/hexanes to afford methyl (*S*)-4-(((2-(1-((2-amino-5-bromo-6-(difluoromethyl)pyrimidin-4-yl)amino)propyl)-4-oxo-3-phenyl-3,4-dihydroquinazolin-5-yl)amino)methyl)benzoate (65.0 mg, 0.098 mmol) in 86% yield. LC–MS (method 1): t_R = 3.70 min, m/z (M + H)⁺ = 664.2. Methyl (*S*)-4-(((2-(1-((2-amino-5-bromo-6-(difluoromethyl)pyrimidin-4-yl)amino)propyl)-4-oxo-3-phenyl-3,4-dihydroquinazolin-5-yl)amino)methyl)benzoate (65.0 mg, 0.098 mmol) and zinc cyanide (14.0 mg, 0.12 mmol) were suspended in DMF (1.0 mL) under nitrogen atmosphere in a MW vial, and tris(dibenzylideneacetone)dipalladium(0) (9.0 mg, 9.8 μ mol) and 1,1'-Bis(diphenylphosphino)ferrocene [dppf] (10.9 mg, 0.02 mmol) were added to it. The resulting mixture was bubbled with nitrogen for 5 min, followed by sealing the MW vial and heating at 1/2C in microwave for 2 h. After completion of reaction, the crude reaction mixture was concentrated in vacuo and purified by silica gel chromatography using 0–60% EtOAc/hexanes to afford methyl (*S*)-4-(((2-(1-((2-amino-5-cyano-6-(difluoromethyl)pyrimidin-4-yl)-amino)propyl)-4-oxo-3-phenyl-3,4-dihydroquinazolin-5-yl)amino)-methyl)benzoate **47m** (50.0 mg, 0.08 mmol) in 84% yield. LC–MS (method 1): t_R = 3.42 min, m/z (M + H)⁺ = 611.2. The general procedure GP4 (method B) was used with

compound **47m** (50.0 mg, 0.08 mmol) to afford the final product, (*S*)-4-(((2-(1-((2-amino-5-cyano-6-(difluoromethyl)pyrimidin-4-yl)amino)propyl)-4-oxo-3-phenyl-3,4-dihydroquinazolin-5-yl)amino)methyl)-*N*-hydroxybenzamide, TFA **48m** (18.0 mg, 0.0258 mmol) in 30% yield. LC–MS (method 2): $t_R = 4.82$ min, m/z ($M + H$)⁺ 612.2. ¹H NMR (400 MHz, DMSO-*d*₆) δ 11.13 (s, 1H), 8.97 (s, 1H), 7.69 (d, $J = 7.9$ Hz, 2H), 7.64 (d, $J = 7.3$ Hz, 1H), 7.55–7.38 (m, 6H), 7.08 (s, 1H), 6.81–6.73 (m, 1H), 6.66 (s, 1H), 6.54–6.48 (m, 1H), 4.75 (q, $J = 6.7$ Hz, 1H), 4.50 (s, 2H), 1.94–1.84 (m, 1H), 1.75 (dt, $J = 14.1, 7.2$ Hz, 1H), 0.70 (t, $J = 7.3$ Hz, 3H). HRMS (ESI) m/z : [$M + H$]⁺ calcd for C₃₁H₂₈F₂N₉O₃ 612.2278, found 612.2262 [Note: In addition to compound **48m**, a side product originating from the hydrolysis of methyl ester in **47m** to carboxylic acid was also isolated in 4% yield].

(*S*)-4-(((2-(1-((2,6-Diamino-5-cyanopyrimidin-4-yl)amino)ethyl)-4-oxo-3-phenyl-3,4-dihydroquinazolin-5-yl)amino)methyl)-*N*-hydroxybenzamide (**48n**). The general procedure GP6 was used with compound **26i** (103.0 mg, 0.195 mmol) and trifluoroacetic acid (444.0 mg, 3.9 mmol, 0.29 mL) in DCM (2.0 mL). The crude reaction was worked-up (method B) and heated with 2,4-diamino-6-chloropyrimidine-5-carbonitrile **44a** (50.0 mg, 0.29 mmol) and DIPEA (76.0 mg, 0.59 mmol, 102.0 μ L) in *n*-butanol (0.5 mL) at 130 1/2C for 2 h in a MW reactor. The remaining residue was purified by flash chromatography on silica gel using 0–100% EtOAc/hexanes to afford methyl (*S*)-4-(((2-(1-((2,6-diamino-5-cyanopyrimidin-4-yl)amino)ethyl)-4-oxo-3-phenyl-3,4-dihydroquinazolin-5-yl)amino)methyl)benzoate **47n** (88.0 mg, 0.16 mmol) in 80% yield. LC–MS (method 1): $t_R = 3.11$ min, m/z ($M + H$)⁺ = 562.2. The general procedure GP4 (method B) was used with compound **47n** (88.0 mg, 0.16 mmol) to afford the final product, (*S*)-4-(((2-(1-((2,6-diamino-5-cyanopyrimidin-4-yl)amino)ethyl)-4-oxo-3-phenyl-3,4-dihydroquinazolin-5-yl)amino)methyl)-*N*-hydroxybenzamide, TFA **48n** (38.0 mg, 0.06 mmol) in 64% yield. LC–MS (method 2): $t_R = 3.90$ min, m/z ($M + H$)⁺ = 563.2. ¹H NMR (400 MHz, DMSO-*d*₆) δ 11.14 (s, 1H), 8.97 (s, 1H), 8.09 (d, $J = 6.5$ Hz, 1H), 7.96 (s, 2H), 7.73–7.68 (m, 2H), 7.54–7.48 (m, 3H), 7.46–7.38 (m, 5H), 6.78 (dd, $J = 7.8, 0.9$ Hz, 1H), 6.52 (dd, $J = 8.6, 1.1$ Hz, 1H), 5.75 (s, 2H), 4.89 (p, $J = 6.6$ Hz, 1H), 4.51 (s, 2H), 1.34 (d, $J = 6.6$ Hz, 3H). HRMS (ESI) m/z : [$M + H$]⁺ calcd for C₂₉H₂₇N₁₀O₃ 563.2262, found 563.2257 [Note: In addition to compound **48n**, a side product originating from the hydrolysis of methyl ester in **47n** to carboxylic acid was also isolated in 5% yield].

(*S*)-4-(((2-(1-((2-Amino-5-cyano-6-methylpyrimidin-4-yl)amino)-ethyl)-4-oxo-3-phenyl-3,4-dihydroquinazolin-5-yl)amino)methyl)-*N*-hydroxybenzamide (**48o**). The general procedure GP6 was used with compound **26i** (134.0 mg, 0.25 mmol) and trifluoroacetic acid (579.0 mg, 5.1 mmol, 0.39 mL) in DCM (2.5 mL). The crude reaction was worked-up (method B) and heated with 2-amino-4-chloro-6-methylpyrimidine-5-carbonitrile **44b** (64.2 mg, 0.38 mmol) and DIPEA (98.0 mg, 0.76 mmol, 133.0 μ L) in *n*-butanol (0.5 mL) at 130 1/2C for 2 h in a MW reactor. The remaining residue was purified by flash chromatography on silica gel using 0–100% EtOAc/hexanes to afford methyl (*S*)-4-(((2-(1-((2-amino-5-cyano-6-methylpyrimidin-4-yl)amino)ethyl)-4-oxo-3-phenyl-3,4-dihydroquinazolin-5-yl)amino)methyl)benzoate **47o** (90.0 mg, 0.16 mmol) in 63% yield. LC–MS (method 1): $t_R = 3.12$ min, m/z ($M + H$)⁺ = 561.2. The general procedure GP4 (method B) was used with compound **47o** (84.0 mg, 0.15 mmol) to afford the final product, (*S*)-4-(((2-(1-((2-amino-5-

cyano-6-methylpyrimidin-4-yl)amino)ethyl)-4-oxo-3-phenyl-3,4-dihydroquinazolin-5-yl)amino)methyl)-*N*-hydroxybenzamide, TFA **48o** (53.0 mg, 0.08 mmol) in 52% yield. LC-MS (method 2): $t_R = 3.99$ min, m/z ($M + H$)⁺ = 562.1. ¹H NMR (400 MHz, DMSO-*d*₆) δ 11.14 (s, 1H), 8.98 (s, 1H), 8.37 (s, 1H), 7.70 (d, $J = 7.9$ Hz, 2H), 7.54–7.48 (m, 3H), 7.45–7.35 (m, 5H), 6.79 (d, $J = 7.9$ Hz, 1H), 6.52 (d, $J = 8.4$ Hz, 1H), 4.91 (p, $J = 5.8, 4.9$ Hz, 1H), 4.51 (s, 2H), 2.35 (s, 3H), 1.36 (d, $J = 6.5$ Hz, 3H). HRMS (ESI) m/z : [$M + H$]⁺ calcd for C₂₉H₂₈N₉O₃ 562.2310, found 562.2301 [Note: In addition to compound 480, a side product originating from the hydrolysis of methyl ester in **47o** to carboxylic acid was also isolated in 3% yield].

Procedure for Synthesis of C5-Substituted Quinazolinones (**51** and **54**,

Scheme 6).—(*S*)-*N*1-((2-(1-((2,6-Diamino-5-cyanopyrimidin-4-yl)amino)ethyl)-4-oxo-3-phenyl-3,4-dihydroquinazolin-5-yl)-methyl)-*N*4-hydroxyterephthalamide (**51**). Compound **29b** (36.0 mg, 0.09 mmol) was dissolved in ammonia (1.0 mL, 7N in MeOH) in a 20 mL scintillation vial and Raney Ni (10.0 mg (approx.)) was added to it. The reaction vial was evacuated and then kept under hydrogen atmosphere using a balloon. The resulting suspension was stirred at room temperature for 20 h. After completion of reaction (by LC-MS), the crude reaction mixture was carefully filtered under nitrogen and concentrated in vacuo. This hydrogenated product was dissolved in DMF (1.0 mL) in a 20 mL scintillation vial, and 4-(methoxycarbonyl)benzoic acid **35** (18.2 mg, 0.10 mmol), DIPEA (24.0 mg, 0.18 mmol, 32.0 μ L), and HATU (38.0 mg, 0.10 mmol) were added to it. The resulting mixture was stirred at room temperature for 16 h and concentrated in vacuo. The remaining residue was purified using 0–10% MeOH/DCM to afford methyl (*S*)-4-(((2-(1-((*tert*-butoxycarbonyl)amino)ethyl)-4-oxo-3-phenyl-3,4-dihydroquinazolin-5-yl)methyl)carbamoyl)benzoate **49** (49.0 mg, 0.088 mmol) in 96% yield. LC-MS (method 1): $t_R = 3.45$ min, m/z ($M + H$)⁺ = 557.1. The general procedure GP6 was used with compound **49** (49.0 mg, 0.09 mmol) and trifluoroacetic acid (201.0 mg, 1.76 mmol, 0.14 mL) in DCM (1.0 mL). The crude reaction was worked-up (method B) and heated with 2,4-diamino-6-chloropyrimidine-5-carbonitrile **44a** (22.3 mg, 0.13 mmol) and DIPEA (34.1 mg, 0.26 mmol, 46.0 μ L) in *n*-butanol (0.5 mL) at 130 1/2C for 5 h in a MW reactor. The remaining residue was purified by flash chromatography on silica gel using 0–5% MeOH/DCM to afford methyl (*S*)-4-(((2-(1-((2,6-diamino-5-cyanopyrimidin-4-yl)amino)ethyl)-4-oxo-3-phenyl-3,4-dihydroquinazolin-5-yl)methyl)carbamoyl)benzoate **50** (40.0 mg, 0.07 mmol) in 77% yield. LC-MS (method 1): $t_R = 2.85$ min, m/z ($M + H$)⁺ = 590.0. The general procedure GP4 (method B) was used with compound **50** (40.0 mg, 0.07 mmol) to afford the final product, (*S*)-*N*1-((2-(1-((2,6-diamino-5-cyanopyrimidin-4-yl)-amino)ethyl)-4-oxo-3-phenyl-3,4-dihydroquinazolin-5-yl)methyl)-*N*4-hydroxyterephthalamide, TFA **51** (11.0 mg, 0.016 mmol) in 23% yield. LC-MS (method 2): $t_R = 3.55$ min, m/z ($M + H$)⁺ = 591.3. ¹H NMR (400 MHz, DMSO-*d*₆) δ 11.36 (s, 1H), 9.07 (t, $J = 6.0$ Hz, 1H), 8.01–7.94 (m, 2H), 7.89–7.76 (m, 4H), 7.64–7.53 (m, 4H), 7.53–7.40 (m, 5H), 5.03 (d, $J = 5.9$ Hz, 2H), 4.88 (t, $J = 6.8$ Hz, 1H), 1.35 (d, $J = 6.7$ Hz, 3H). HRMS (ESI) m/z : [$M + H$]⁺ calcd for C₃₀H₂₇N₁₀O₄ 591.2211, found 591.2210.

(*S*)-2-(((2-(1-((2,6-Diamino-5-cyanopyrimidin-4-yl)amino)ethyl)-4-oxo-3-phenyl-3,4-dihydroquinazolin-5-yl)methyl)amino)-*N*-hydroxypyrimidine-5-carboxamide (**54**).

Compound **29b** (125.0 mg, 0.32 mmol) was dissolved in ammonia (2.0 mL, 7N in MeOH) in a 20 mL scintillation vial, and Raney Ni (20.0 mg (approx) was added to it. The reaction vial was evacuated and then kept under hydrogen atmosphere using a balloon. The resulting suspension was stirred at room temperature for 20 h. After completion of reaction (by LC-MS), the crude reaction mixture was carefully filtered under nitrogen, concentrated in vacuo, and redissolved in *n*-BuOH (0.5 mL) in a MW vial. Ethyl 2-chloropyrimidine-5-carboxylate **41** (85.0 mg, 0.46 mmol) and DIPEA (118.0 mg, 0.91 mmol, 0.16 mL) were added to the MW vial, and the vial was sealed and heated at 130 1/2C for 1 h in a MW reactor. After completion of the reaction, the reaction mixture was concentrated in vacuo, and the remaining residue was purified using 0–100% EtOAc/hexanes to afford ethyl (*S*)-2-(((2-(1-((*tert*-butoxycarbonyl)amino)ethyl)-4-oxo-3-phenyl-3,4-dihydroquinazolin-5-yl)methyl)amino)pyrimidine-5-carboxylate **52** (138.0 mg, 0.25 mmol) in 83% yield. LC–MS (method 1): $t_R = 3.75$ min, m/z ($M + H$)⁺ = 545.3. The general procedure GP6 was used with compound **52** (138.0 mg, 0.25 mmol) and trifluoroacetic acid (579.0 mg, 5.1 mmol, 0.39 mL) in DCM (2.5 mL). The crude reaction was worked-up (method B) and heated with 2,4-diamino-6-chloropyrimidine-5-carbonitrile **44a** (64.0 mg, 0.38 mmol) and DIPEA (98.0 mg, 0.76 mmol, 133.0 μ L) in *n*-butanol (0.5 mL) at 130 1/2C for 2 h in a MW reactor. The remaining residue was purified by flash chromatography on silica gel using 0–5% MeOH/DCM to afford ethyl (*S*)-2-(((2-(1-((2,6-diamino-5-cyanopyrimidin-4-yl)amino)ethyl)-4-oxo-3-phenyl-3,4-dihydroquinazolin-5-yl)methyl)amino)pyrimidine-5-carboxylate **53** (116.0 mg, 0.20 mmol) in 79% yield. LC–MS (method 1): $t_R = 3.11$ min, m/z ($M + H$)⁺ = 578.1. The general procedure GP4 (method B) was used with compound **53** (116.0 mg, 0.20 mmol) to afford the final product, (*S*)-2-(((2-(1-((2,6-diamino-5-cyanopyrimidin-4-yl)amino)ethyl)-4-oxo-3-phenyl-3,4-dihydroquinazolin-5-yl)-methyl)amino)-*N*-hydroxypyrimidine-5-carboxamide, TFA **54** (68.0 mg, 0.10 mmol) in 50% yield. LC–MS (method 2): $t_R = 3.38$ min, m/z ($M + H$)⁺ = 565.0. ¹H NMR (400 MHz, DMSO-*d*₆) δ 11.36 (s, 1H), 9.07 (t, $J = 6.0$ Hz, 1H), 8.01–7.94 (m, 2H), 7.89–7.76 (m, 4H), 7.64–7.53 (m, 4H), 7.53–7.40 (m, 5H), 5.03 (d, $J = 5.9$ Hz, 2H), 4.88 (t, $J = 6.8$ Hz, 1H), 2.54 (s, 2H), 1.35 (d, $J = 6.7$ Hz, 3H). HRMS (ESI) m/z : [$M + H$]⁺ calcd for C₂₇H₂₅N₁₂O₃ 565.2167, found 565.2164.

Molecular Modeling.

All structure visualizations and computations were performed using molecular operating environment (MOE).⁶⁹ The images of Idelalisib bound to PI3K δ (Figure 3B) and SAHA (Vorinostat) bound to HDAC-2 (Figure 3D) are based on the protein data bank entries 4LXZ.pdb³⁹ and 5XE0.pdb⁴⁰ respectively. The structure of HDAC-6 bound to **19b** (Figure 4) was derived from 5EDU.pdb (Trichostatin A bound to HDAC-6).⁵⁷ In this derivation, 5EDU.pdb was loaded into MOE, protein prep was run, and hydrogens were added. The structure was then minimized, using the MMFF94 potential,⁷⁰ to a local minimum associated with the crystal structure coordinates. Then Trichostatin A was truncated all the way to the hydroxamic acid headgroup. **19b** was grown out from the hydroxamic acid headgroup one atom at a time. If the placement of an atom resulted in a new torsion angle, the torsion was searched to find a local minimum before the next atom was added. Once **19b** was completely grown into the HDAC-6 binding pocket, the whole structure was minimized to 0.001 RMS.

HDAC-6 Selectivity Carboxamide Compounds.—The sequences of HDACs-1, 2, 3, 4, 5, 6, 7, 8, 9, 10, and 11 were downloaded from UNIPROT⁷¹ and aligned. Using the structure that we modeled of **19b** bound to HDAC-6 we determined all HDAC-6 residues within 4.5 Å of **19b**. These residue positions were then marked on the HDAC-6 sequence, and their counterpart residues on the other aligned HDACs were determined. All marked HDAC-6 residue positions that were not conserved across the other kinases were identified. Then one at a time each nonconserved residue position in HDAC-6 was mutated to its value in each of the other HDACs, and the effect of the mutation on **19b** interactions with the protein was determined.

Biological Assay Protocols.

PI3K Assay Protocol (HTRF Assay Platform). (1) *Assay Principle.* The PIP3 product is detected by displacement of biotin-PIP3 from an energy transfer complex consisting of europium-labeled anti-GST monoclonal antibody, a GST-tagged pleckstrin homology (PH) domain, biotinylated PIP3 and streptavidin–allophycocyanin (APC). Excitation of europium in the complex results in an energy transfer to the APC and a fluorescent emission at 665 nm. The PIP3 product formed by PI3-kinase(h) activity displaces biotin-PIP3 from the complex, resulting in a loss of energy transfer, and thus, a decrease in signal. *This is a 3-step reaction:* First, the kinase reaction with PIP2 substrate is carried out in the presence of ATP, and the reaction is quenched with stop solution, and then, finally detect by adding detection mixture followed by incubation. (2) *Reaction Conditions. Assay Buffer:* HEPES 50 mM (pH7.0), NaN3 0.02%, BSA 0.01%, orthovanadate 0.1 mM, 1% DMSO. *Detection Buffer:* HEPES 10 mM (pH7.0), BSA 0.02%, KF 0.16 M, EDTA 4 mM. *Substrate:* 10 μM PIP2 substrate (PI(4,5)P2). *ATP:* 10 μM ATP under standard conditions. *Control Inhibitor:* PI-103. (3) *Assay Procedure.* (A) Prepare substrate in freshly prepared reaction buffer. (B) Deliver kinase into the substrate solution and gently mix. (C) Deliver compounds in 100% DMSO into the kinase reaction mixture by Acoustic Technology (Echo550; nanoliter range), incubate for 10 min at room temperature. (D) Deliver ATP into the reaction mixture to initiate the reaction. (E) Incubate for 30 min at 30 1/2C. (F) Quench the reaction with stop solution. (G) Add detection mixture and incubate for overnight. (H) Measure HTRF: Ex = 320 nm, ratio of Em = 615 nm and Em = 665 nm. (4) *Data Analysis.* The emission ratio is converted into μM PIP3 production based on PIP3 standard curves. The nonlinear regression to obtain the standard curve and IC₅₀ values are performed using Graphpad Prism software.

HDAC Fluorescent Activity Assay.—*Assay Description:* The HDAC fluorescent activity assay is based on the unique fluorogenic substrate and developer combination. This assay is a highly sensitive and validated. The assay procedure has two steps (Figure 1, Howitz, 2015 Drug Discovery Today: Technologies). First, the fluorogenic substrate, which comprises an acetylated lysine side chain, is incubated with a purified HDAC enzyme. Deacetylation of the substrate sensitizes the substrate so that, in the second step, treatment with the Developer produces a fluorophore. *Compound Handling:* Testing compounds were dissolved in 100% DMSO to specific concentration. The serial dilution was conducted by epMotion 5070 in DMSO. *Materials and Reagents:* HDAC reaction buffer: 50 mM Tris-HCl, pH 8.0, 137 mM NaCl, 2.7 mM KCl, and 1 mM MgCl₂, add fresh 1 mg/mL BSA, 1% DMSO. *Substrate:* HDAC1,2,3,6,10: Fluorogenic peptide from p53 residues 379–382

(RHKK(Ac)AMC). HDAC4,5,7, 9 and 11: Fluorogenic HDAC class2a substrate (trifluoroacetyl lysine). HDAC 8: fluorogenic peptide from p53 residues 379–382 (RHK(Ac)K(Ac)AMC). *General Reaction Procedure*: standard IC₅₀ determination. *Deacetylation Step*: (A) Deliver 2X enzyme in wells of reaction plate except no enzyme control wells. Add buffer in No En wells. (B) Deliver compounds in 100% DMSO into the enzyme mixture by Acoustic technology (Echo550; nanoliter range). Spin down and preincubation. (C) Deliver 2× substrate mixture (fluorogenic HDAC substrate and co-factor if applicable) in all reaction wells to initiate the reaction. Spin and shake. (D) Incubate for 1–2 h at 30 1/2C with seal. *Development Step*: (E) Add developer with Trichostatin A (or TMP269) to stop the reaction and to generate fluorescent color. (F) Fluorescence was read (excitatory, 360; emission, 460) using the EnVision Multilabel Plate Reader (PerkinElmer). (G) Take end point reading for analysis after the development reaches plateau. *Data Analysis*: The percentages of enzyme activity (relative to DMSO controls) and IC₅₀ values were calculated using the GraphPad Prism 4 program based on a sigmoidal dose–response equation.

NCI-60 Cellular Assays.—Assay Protocols and Data Analysis procedures are available at: https://dtp.cancer.gov/discovery_development/nci-60/methodology.htm

CETSA Protocol. K-562 (chronic myelogenous leukemia), MV-4–11 (B-myelomonocytic leukemia) and THP-1 (acute monocytic leukemia) were cultured in RPMI 1640 (ThermoFisher, cat. no, 11835) supplemented with 10% FBS (Hyclone) and 0.5× penicillin/streptomycin (ThermoFisher). Then 2 × 10⁶ cells were rinsed with PBS and resuspended in 200 μL of DPBS (+Ca, +Mg) + 1 g/L D-glucose + 1× Halt protease inhibitor cocktail (ThermoFisher). Four freeze–thaw cycles (dry ice/EtOH, 37 1/2C water bath) were performed, and lysates were centrifuged at 17 000g for 15 min (4 1/2C). The soluble fraction was separated on a 4–12% Bis-Tris gel using MOPS running buffer and transferred to a nitrocellulose membrane. Primary antibodies were anti-HDAC6 (ab133493, 1:10 000), anti-HDAC6 (ab82557, 1:1000), and anti-PI3kδ (ab109006, 1:1000). Secondary antibodies were HRP conjugated, and SuperSignal West Pico chemiluminescent substrate was used for detection. Membranes were imaged on a ChemiDoc imaging system (BioRad). CETSA melt curves were determined by collecting MV-4–11 cells in DPBS (+Ca, +Mg) supplemented 1 g/L D-glucose, 1× protease inhibitors, and 0.5% DMSO at 15 × 10⁶ cells/mL. Cell suspensions were distributed to 0.2 mL PCR tubes, and samples were heated for 3.5 min to various temperatures. After allowing samples to equilibrate to room temperature, samples were processed by freeze–thaw for immunoblot as outlined above. Isothermal dose–response CETSA was performed by collecting MV-4–11 cells in DPBS (+Ca, +Mg) supplemented 1 g/L D-glucose, 0.5× protease inhibitors, 10 × 10⁶ cells/mL. Then 1 μL of compound (at 100× final concentration; 1% DMSO final) was added to 99 μL of cell suspension and cells were incubated at 37 1/2C for 1 h. Samples were then heated for 3.5 min at either 52 1/2C (PI3Kδ) or 58 1/2C (HDAC6). Cells were lysed by freeze–thaw cycles and processed for immunoblot as outlined above. Densitometry analysis was performed using ImageQuant TL and a rolling ball radius 80 for background subtraction.

Cell Culture and Reagents.—Human MOLM-14 AML, Mv4–11, HL-60, THP-1, MOLM-13 wt, MOLM-13 FLT3 inhibitor resistant, and U-937 cells were maintained in RPMI1640 medium containing 10% heat-inactivated fetal bovine serum (FBS), 100 units/mL penicillin, 100 µg/mL streptomycin, and 2 mM *L*-glutamine. MOLM-13 cells were selected for resistance to FLT3 inhibitor HG-7-85-01 as described (Weisberg, 2011). Cells were treated with different dual inhibitor compounds (NCATS, NIH).

Cell Viability Assays. RPMI 8226 and U266B1 cells obtained from ATCC and were cultured in RPMI1640 (Gibco, cat. no. 11875093) supplemented with 10% FBS (HyClone), 50 U/mL penicillin, and 50 µg/mL streptomycin (Life Technologies). For cell viability assays, RPMI 8226 and U266B1 cells were seeded at 5×10^4 cells/mL (50 µL volume) into white, tissue culture-treated 384-well plates (Corning, cat. no. 3570BC). 63 nL of compound solutions in DMSO were immediately added using a Wako Pin-tool. Plates were covered with BreatheEasy seals (Diversified Biotech) and incubated at 37 °C, 5% CO₂ for 5 days. Then 25 µL of CellTiter-Glo (Promega) was then added to each well, and plates were incubated at RT for 10 min. Luminescence was measured on a ViewLux plate reader.

Human MOLM-14, MOLM-13 wt, MOLM-13 FLT3 inhibitor resistant, MV4–11, HL-60, THP-, and U-937 cell lines were treated with different concentrations of dual inhibitors for the indicated times. Cell viability was determined by trypan blue exclusion. For studies with primary AML blasts, cells were obtained pretherapy from AML patients under an approved protocol (DFCI 01–206). Normal PBMCs were obtained from normal donors under consent. Cells were left untreated or treated with test compound for the indicated times. Cell death was determined by staining with propidium iodide (PI) alone or PI/Annexin V and then analyzed by flow cytometry.

Necrosis Assays.—For analysis of cell death by necrosis, cells were stained with propidium iodide (PI) alone or PI/Annexin V, and then analyzed by flow cytometry as described.⁶⁷

Immunoblot Analysis.—Cells were harvested and rinsed with ice-cold phosphate buffered saline (PBS). Ice-cold lysis buffer [0.5 mL; 20 mM Tris (pH 7.5), 150 mM NaCl, 1 mM EDTA, 1% Triton X-100, 2.5 mM sodium pyrophosphate, 1 mM β-glycerophosphate, 1 mM Na₃VO₄, 1 mg/mL leupeptin, 1 mM PMSF] was added to 1×10^7 cells and sonicated on ice four times for 5 s each followed by microcentrifugation for 10 min at 4 °C. Soluble proteins were separated on gels and transferred to nitrocellulose filters. The lysates were immunoblotted with antiphospho AKT, total AKT and b-actin antibodies (Cell Signaling Technology), Antigen–antibody complexes were visualized by enhanced chemiluminescence (GE Healthcare).

Pharmacokinetic Analyses.

Parallel Artificial Membrane Permeability Assay (PAMPA).—Stirring double-sink PAMPA method (patented by pION Inc.) was employed to determine the permeability of compounds via PAMPA. The PAMPA lipid membrane consisted of an artificial membrane of a proprietary lipid mixture and dodecane (Pion Inc.), optimized to predict gastrointestinal tract (GIT) passive permeability. The lipid was immobilized on a plastic matrix of a 96-well

“donor” filter plate placed above a 96-well “acceptor” plate. pH 7.4 solution was used in both donor and acceptor wells. The test articles, stocked in 10 mM DMSO solutions, were diluted to 0.05 mM in aqueous buffer (pH 7.4), and the concentration of DMSO was 0.5% in the final solution. During the 30 min permeation period at room temperature, the test samples in the donor compartment were stirred using the Gutbox technology (Pion Inc.) to reduce the aqueous boundary layer. The test article concentrations in the donor and acceptor compartments were measured using a UV plate reader (Nano Quant, Infinite 200 PRO, Tecan Inc., Männedorf, Switzerland). Permeability calculations were performed using Pion Inc. software and were expressed in units of 10^{-6} cm/s. Compounds with low or weak UV signal we analyzed using high resolution LC/MS (Thermo QExactive). The three controls used were ranitidine (low permeability), dexamethasone (moderate permeability), and verapamil (high permeability). Method has been previously published.⁷²

Multispecies Multitime Point Assays.—*Microsome Stability Assay:* Briefly, each reaction mixture (110 μ L) consisted of a test article (1 μ M), human, SD rat, or CD-1 mouse microsomal fractions (0.5 mg/mL), and NADPH regenerating system (1 μ M) in phosphate buffer at pH 7.4. *Cytosol Stability Assay:* Briefly, each reaction mixture (110 μ L) consisted of a test article (1 μ M) and either human, SD rat, or CD-1 mouse cytosol fractions (2 mg/mL) in phosphate buffer (100 mM) at pH 7.4. Samples were incubated in 384-well plates at 37 1/2C for 0, 5, 10, 15, 30, and 60 min. Sample analysis and half-life calculations were performed using a previously described method.⁷³ The three controls used were Buspirone (short half-life), Loperamide (moderate half-life), and Antipyrine (long half-life).

Pharmacokinetics (PK) [NCATS].—Adult female Balb/c mice ($n = 3$ /sampling time point) were obtained from Charles River Laboratory (Frederick, MD). All experimental procedures were approved by the Animal Care and Use Committee (ACUC) of the NIH Division of Veterinary Resources (DVR). Pharmacokinetics (PK) was evaluated after a single dose of 3 mg/kg intravenous (IV) and 10 mg/kg oral gavage (PO) administration. Dosing solutions were freshly prepared on the day of administration in 70% PEG-300/30% H₂O/10% ethanol. The blood samples (~80 μ L) were collected in K2EDTA tubes after drug administration based on the PK study protocols, and plasma (~30 μ L) was harvested after centrifugation at 3000 rpm for 10 min. All plasma samples were stored at -80 1/2C until analysis. Ultraperformance liquid chromatography–tandem mass spectrometry (UPLC-MS/MS) methods were developed to determine compounds’ concentrations in mouse plasma samples. Mass spectrometric analysis was performed on a Waters Xevo TQ-S triple quadrupole instrument using electrospray ionization in positive mode with the selected reaction monitoring. The separation of test compounds from endogenous components was performed on an Acquity BEH C18 column (50 mm \times 2.1 mm, 1.7 μ) using a Waters Acquity UPLC system with 0.6 mL/min flow rate and gradient elution. The mobile phases were 0.1% formic acid in water and 0.1% formic acid in acetonitrile. The calibration standards and quality control samples were prepared in the blank mouse plasma. Aliquots of 10 μ L plasma samples were mixed with 200 μ L of internal standard in acetonitrile to precipitate proteins in a 96-well plate. Then 1 μ L of supernatant was injected for the UPLC-MS/MS analysis. Data were analyzed using TargetLynx V4.1 (Waters Corp., Milford, MA). The pharmacokinetic parameters, e.g., plasma clearance (CL_p) and volume of distribution at

steady-state (Vd_{ss}), were calculated using the noncompartmental approach (models 200 and 201) of the pharmacokinetic software Phoenix WinNonlin, version 8.0 (Certara, St. Louis, MO). The area under the plasma concentration versus time curve (AUC) was calculated using the linear trapezoidal method. The slope of the apparent terminal phase was estimated by log linear regression using at least 3 data points, and the terminal rate constant (λ) was derived from the slope. $AUC_{0-\infty}$ was estimated as the sum of the AUC_{0-t} (where “ t ” is the time of the last measurable concentration) and C/λ . The apparent terminal half-life ($t_{1/2}$) was calculated as $0.693/\lambda$.

Pharmacokinetics (PK) [Pharmaron].—Female Balb/c mice (sourced from Si Bei Fu Laboratory Animal Technology Co. Ltd.), approximately 6–8 weeks of age, and a weight of approximately 20–30 g, were dosed with **48c** at 50 and 150 mg/kg via IP injection. The formulations, [DMSO/PEG300/sterile water (10:40:50)] and [DMSO/PEG300/20% HP- β -CD in water (1:4)] (10:40:50), adjusted pH 3–4 with 1 M HCl) was prepared on the day of dosing. Each cohort had three mice, and plasma was collected at pre, 5 min, 15 min, 30 min, 1 h, 2 h, 4 h, 8 h, 12 h, and 24 h post dose for IP. Approximately 0.025 mL of blood was collected by the dorsal metatarsal vein at each time point. All blood samples were transferred into plastic microcentrifuge tubes containing Heparin-Na as anticoagulant. Collection tubes with blood samples and anticoagulant were inverted several times for proper mixing of the tube contents and then placed on wet ice prior to centrifugation for plasma. Blood samples will be centrifuged at 4000g for 5 min at 4 °C to obtain plasma. Plasma samples will be stored in polypropylene tubes, quickly frozen in a freezer, and kept at -75 ± 15 °C until analyzed by LCMS/MS. The following pharmacokinetic parameters were measured: $t_{1/2}$, C_{max} , T_{max} , and AUC_{0-t} .

Supplementary Material

Refer to Web version on PubMed Central for supplementary material.

ACKNOWLEDGMENTS

We gratefully acknowledge the funding from Intramural Research Program, National Center for Advancing Translational Sciences (NCATS), National Institutes of Health (NIH). We thank Paul Shinn and his team for the assistance with compound management and Christopher Leclair and his team for analytical chemistry and purification support. We also thank Reaction Biology Corporation for screening compounds in enzymatic assays and Pharmaron Inc. for conducting the pharmacokinetic studies.

ABBREVIATIONS USED

PI3K	phosphoinositide 3-kinase
PIP2	phosphatidylinositol 4,5-diphosphate
PIP3	phosphatidylinositol 3,4,5-triphosphate
RTK	receptor tyrosine kinase
GPCR	G protein-coupled receptor
HDAC	histone deacetylase

SAHA	suberanolhydroxamic acid
Akt	protein kinase B
mTOR	mammalian target of rapamycin
AML	acute monocytic leukemia
CNS	central nervous system
SAR	structure– activity relationship
DCM	dichloromethane
DMF	N, N-dimethylformamide
DCE	1,2-dichloroethane
DMSO	dimethyl sulfoxide
DABCO	(1,4-diazabicyclo[2.2.2]octane)
THF	tetrahydrofuran
TFA	trifluoroacetic acid
DIPEA	N, N-diisopropylethylamine
Boc	tert-butyloxycarbonyl
rt	room temperature
HATU	N-[(dimethylamino)-1H-1,2,3-triazolo-[4,5-b]pyridin-1-ylmethylene]-N-methylmethanaminium hexa-fluorophosphate N-oxide
PAMPA	parallel artificial membrane permeability assay
CETSA	cellular thermal shift assay

REFERENCES

- (1). Kamb A; Wee S; Lengauer C Why Is Cancer Drug Discovery So Difficult? *Nat. Rev. Drug Discovery* 2007, 6, 115–120. [PubMed: 17159925]
- (2). Hanahan D; Weinberg RA Hallmarks of Cancer: The Next Generation. *Cell* 2011, 144, 646–674. [PubMed: 21376230]
- (3). Anighoro A; Bajorath J; Rastelli G Polypharmacology: Challenges and Opportunities in Drug Discovery. *J. Med. Chem* 2014, 57, 7874–7887. [PubMed: 24946140]
- (4). Shang E; Yuan Y; Chen X; Liu Y; Pei J; Lai L De Novo Design of Multitarget Ligands with an Iterative Fragment-Growing Strategy. *J. Chem. Inf. Model* 2014, 54, 1235–1241. [PubMed: 24611712]
- (5). Morphy R; Rankovic Z Designed Multiple Ligands. An Emerging Drug Discovery Paradigm. *J. Med. Chem* 2005, 48, 6523–6543. [PubMed: 16220969]
- (6). O’Boyle NM; Meegan MJ Designed Multiple Ligands for Cancer Therapy. *Curr. Med. Chem* 2011, 18, 4722–4737. [PubMed: 21919848]

- (7). Costantino L; Barlocco D Designed Multiple Ligands: Basic Research vs Clinical Outcomes. *Curr. Med. Chem* 2012, 19, 3353–3387. [PubMed: 22680630]
- (8). Talevi A Multi-Target Pharmacology: Possibilities and Limitations of the “Skeleton Key Approach” from a Medicinal Chemist Perspective. *Front. Pharmacol* 2015, 6, 205. [PubMed: 26441661]
- (9). Fu RG; Sun Y; Sheng WB; Liao DF Designing Multi-Targeted Agents: An Emerging Anticancer Drug Discovery Paradigm. *Eur. J. Med. Chem* 2017, 136, 195–211. [PubMed: 28494256]
- (10). Anastasio TJ Editorial: Computational and Experimental Approaches in Multi-Target Pharmacology. *Front. Pharmacol* 2017, 8, 443. [PubMed: 28713280]
- (11). Proschak E; Stark H; Merk D Polypharmacology by Design: A Medicinal Chemist’s Perspective on Multitargeting Compounds. *J. Med. Chem* 2019, 62, 420–444. [PubMed: 30035545]
- (12). Bolognesi ML Harnessing Polypharmacology with Medicinal Chemistry. *ACS Med. Chem. Lett* 2019, 10, 273–275.
- (13). Toker A; Cantley LC Signalling through the Lipid Products of Phosphoinositide-3-OH Kinase. *Nature* 1997, 387, 673–676. [PubMed: 9192891]
- (14). Vanhaesebroeck B; Guillermet-Guibert J; Graupera M; Bilanges B The Emerging Mechanisms of Isoform-Specific PI3K Signalling. *Nat. Rev. Mol. Cell Biol* 2010, 11, 329–341. [PubMed: 20379207]
- (15). Liu P; Cheng H; Roberts TM; Zhao JJ Targeting the Phosphoinositide 3-Kinase Pathway in Cancer. *Nat. Rev. Drug Discovery* 2009, 8, 627–644. [PubMed: 19644473]
- (16). Fruman DA; Rommel C PI3K and Cancer: Lessons, Challenges and Opportunities. *Nat. Rev. Drug Discovery* 2014, 13, 140–156. [PubMed: 24481312]
- (17). Stark AK; Sriskantharajah S; Hessel EM; Okkenhaug K PI3K Inhibitors in Inflammation, Autoimmunity and Cancer. *Curr. Opin. Pharmacol* 2015, 23, 82–91. [PubMed: 26093105]
- (18). Garces AE; Stocks MJ Class 1 PI3K Clinical Candidates and Recent Inhibitor Design Strategies: A Medicinal Chemistry Perspective. *J. Med. Chem* 2019, 62, 4815–4850. [PubMed: 30582807]
- (19). Yang J; Nie J; Ma X; Wei Y; Peng Y; Wei X Targeting PI3K in Cancer: Mechanisms and Advances in Clinical Trials. *Mol. Cancer* 2019, 18, 26. [PubMed: 30782187]
- (20). Markham A Alpelisib: First Global Approval. *Drugs* 2019, 79, 1249–1253. [PubMed: 31256368]
- (21). Pons-Tostivint E; Thibault B; Guillermet-Guibert J Targeting PI3K Signaling in Combination Cancer Therapy. *Trends Cancer* 2017, 3, 454–469. [PubMed: 28718419]
- (22). West AC; Johnstone RW New and Emerging HDAC Inhibitors for Cancer Treatment. *J. Clin. Invest* 2014, 124, 30–39. [PubMed: 24382387]
- (23). Zhang L; Han Y; Jiang Q; Wang C; Chen X; Li X; Xu F; Jiang Y; Wang Q; Xu W Trend of Histone Deacetylase Inhibitors in Cancer Therapy: Isoform Selectivity or Multitargeted Strategy. *Med. Res. Rev* 2015, 35, 63–84. [PubMed: 24782318]
- (24). Eckschlagler T; Plch J; Stiborova M; Hrabeta J Histone Deacetylase Inhibitors as Anticancer Drugs. *Int. J. Mol. Sci* 2017, 18, 1414.
- (25). Suraweera A; O’Byrne KJ; Richard DJ Combination Therapy with Histone Deacetylase Inhibitors (HDACi) for the Treatment of Cancer: Achieving the Full Therapeutic Potential of HDACi. *Front. Oncol* 2018, 8, 92. [PubMed: 29651407]
- (26). Subramanian S; Bates SE; Wright JJ; Espinoza-Delgado I; Piekarz RL Clinical Toxicities of Histone Deacetylase Inhibitors. *Pharmaceuticals* 2010, 3, 2751–2767. [PubMed: 27713375]
- (27). Yee AJ; Raje NS Panobinostat and Multiple Myeloma in 2018. *Oncologist* 2018, 23, 516–517. [PubMed: 29445026]
- (28). Thurn KT; Thomas S; Moore A; Munster PN Rational Therapeutic Combinations with Histone Deacetylase Inhibitors for the Treatment of Cancer. *Future Oncol.* 2011, 7, 263–283. [PubMed: 21345145]
- (29). Bodo J; Zhao X; Sharma A; Hill BT; Portell CA; Lannutti BJ; Almasan A; Hsi ED The Phosphatidylinositol 3-Kinases (PI3K) Inhibitor GS-1101 Synergistically Potentiates Histone Deacetylase Inhibitor-Induced Proliferation Inhibition and Apoptosis through the Inactivation of PI3K and Extracellular Signal-Regulated Kinase Pathways. *Br. J. Haematol* 2013, 163, 72–80. [PubMed: 23889282]

- (30). Pei Y; Liu KW; Wang J; Garancher A; Tao R; Esparza LA; Maier DL; Udaka YT; Murad N; Morrissy S; Seker-Cin H; Brabetz S; Qi L; Kogiso M; Schubert S; Olson JM; Cho YJ; Li XN; Crawford JR; Levy ML; Kool M; Pfister SM; Taylor MD; Wechsler-Reya RJ HDAC and PI3K Antagonists Cooperate to Inhibit Growth of MYC-Driven Medulloblastoma. *Cancer Cell* 2016, 29, 311–323. [PubMed: 26977882]
- (31). Luan Y; Li J; Bernatchez JA; Li R Kinase and Histone Deacetylase Hybrid Inhibitors for Cancer Therapy. *J. Med. Chem* 2019, 62, 3171–3183. [PubMed: 30418766]
- (32). Wu Y; Dai W; Chen X; Geng A; Chen Y; Lu T; Zhu Y Design, Synthesis and Biological Evaluation of 2,3-Dihydroimidazo-[1,2-C]Quinazoline Derivatives as Novel Phosphatidylinositol 3-Kinase and Histone Deacetylase Dual Inhibitors. *RSC Adv.* 2017, 7, 52180–52186.
- (33). Chen D; Soh CK; Goh WH; Wang H Design, Synthesis, and Preclinical Evaluation of Fused Pyrimidine-Based Hydroxamates for the Treatment of Hepatocellular Carcinoma. *J. Med. Chem* 2018, 61, 1552–1575. [PubMed: 29360358]
- (34). Zhang K; Lai F; Lin S; Ji M; Zhang J; Zhang Y; Jin J; Fu R; Wu D; Tian H; Xue N; Sheng L; Zou X; Li Y; Chen X; Xu H Design, Synthesis, and Biological Evaluation of 4-Methyl Quinazoline Derivatives as Anticancer Agents Simultaneously Targeting Phosphoinositide 3-Kinases and Histone Deacetylases. *J. Med. Chem* 2019, 62, 6992–7014. [PubMed: 31117517]
- (35). Sun K; Atoyan R; Borek MA; Dellarocca S; Samson ME; Ma AW; Xu GX; Patterson T; Tuck DP; Viner JL; Fattaey A; Wang J Dual HDAC and PI3K Inhibitor CUDC-907 Downregulates MYC and Suppresses Growth of MYC-Dependent Cancers. *Mol. Cancer Ther* 2017, 16, 285–299. [PubMed: 27980108]
- (36). Sermer D; Pasqualucci L; Wendel HG; Melnick A; Younes A Emerging Epigenetic-Modulating Therapies in Lymphoma. *Nat. Rev. Clin. Oncol* 2019, 16, 494–507. [PubMed: 30837715]
- (37). Younes A; Berdeja JG; Patel MR; Flinn I; Gerecitano JF; Neelapu SS; Kelly KR; Copeland AR; Akins A; Clancy MS; Gong L; Wang J; Ma A; Viner JL; Oki Y Safety, Tolerability, and Preliminary Activity of CUDC-907, a First-in-Class, Oral, Dual Inhibitor of HDAC and PI3K, in Patients with Relapsed or Refractory Lymphoma or Multiple Myeloma: An Open-Label, Dose-Escalation, Phase 1 Trial. *Lancet Oncol.* 2016, 17, 622–631. [PubMed: 27049457]
- (38). Shah RR Safety and Tolerability of Histone Deacetylase (HDAC) Inhibitors in Oncology. *Drug Saf.* 2019, 42, 235–245. [PubMed: 30649740]
- (39). Somoza JR; Koditek D; Villasenor AG; Novikov N; Wong MH; Licican A; Xing W; Lagpacan L; Wang R; Schultz BE; Papalia GA; Samuel D; Lad L; McGrath ME Structural, Biochemical, and Biophysical Characterization of Idelalisib Binding to Phosphoinositide 3-Kinase Delta. *J. Biol. Chem* 2015, 290, 8439–8446. [PubMed: 25631052]
- (40). Lauffer BE; Mintzer R; Fong R; Mukund S; Tam C; Zilberleyb I; Flicke B; Ritscher A; Fedorowicz G; Vallero R; Ortwine DF; Gunzner J; Modrusan Z; Neumann L; Koth CM; Lupardus PJ; Kaminker JS; Heise CE; Steiner P Histone Deacetylase (HDAC) Inhibitor Kinetic Rate Constants Correlate with Cellular Histone Acetylation but Not Transcription and Cell Viability. *J. Biol. Chem* 2013, 288, 26926–26943. [PubMed: 23897821]
- (41). Zhang L; Zhang J; Jiang Q; Zhang L; Song W Zinc Binding Groups for Histone Deacetylase Inhibitors. *J. Enzyme Inhib. Med. Chem* 2018, 33, 714–721. [PubMed: 29616828]
- (42). Zhang K; Lai F; Lin S; Ji M; Zhang J; Zhang Y; Jin J; Fu R; Wu D; Tian H; Xue N; Sheng L; Zou X; Li Y; Chen X; Xu H Design, Synthesis, and Biological Evaluation of 4-Methyl Quinazoline Derivatives as Anticancer Agents Simultaneously Targeting Phosphoinositide 3-Kinases and Histone Deacetylases. *J. Med. Chem* 2019, 62, 6992–7014. [PubMed: 31117517]
- (43). Yao L; Mustafa N; Tan EC; Poulsen A; Singh P; Duong-Thi MD; Lee JXT; Ramanujulu PM; Chng WJ; Yen JY; Ohlson S; Dymock BW Design and Synthesis of Ligand Efficient Dual Inhibitors of Janus Kinase (JAK) and Histone Deacetylase (HDAC) Based on Ruxolitinib and Vorinostat. *J. Med. Chem* 2017, 60, 8336–8357. [PubMed: 28953386]
- (44). Huang Y; Dong G; Li H; Liu N; Zhang W; Sheng C Discovery of Janus Kinase 2 (JAK2) and Histone Deacetylase (HDAC) Dual Inhibitors as a Novel Strategy for the Combinational Treatment of Leukemia and Invasive Fungal Infections. *J. Med. Chem* 2018, 61, 6056–6074. [PubMed: 29940115]

- (45). Bhatia S; Krieger V; Groll M; Osko JD; Rensing N; Ahlert H; Borkhardt A; Kurz T; Christianson DW; Hauer J; Hansen FK Discovery of the First-in-Class Dual Histone Deacetylase-Proteasome Inhibitor. *J. Med. Chem* 2018, 61, 10299–10309. [PubMed: 30365892]
- (46). He S; Dong G; Wu S; Fang K; Miao Z; Wang W; Sheng C Small Molecules Simultaneously Inhibiting P53-Murine Double Minute 2 (MDM2) Interaction and Histone Deacetylases (HDACs): Discovery of Novel Multitargeting Antitumor Agents. *J. Med. Chem* 2018, 61, 7245–7260. [PubMed: 30045621]
- (47). Zang J; Liang X; Huang Y; Jia Y; Li X; Xu W; Chou CJ; Zhang Y Discovery of Novel Pazopanib-Based HDAC and VEGFR Dual Inhibitors Targeting Cancer Epigenetics and Angiogenesis Simultaneously. *J. Med. Chem* 2018, 61, 5304–5322. [PubMed: 29787262]
- (48). Li Y; Luo X; Guo Q; Nie Y; Wang T; Zhang C; Huang Z; Wang X; Liu Y; Chen Y; Zheng J; Yang S; Fan Y; Xiang R Discovery of N1-(4-((7-Cyclopentyl-6-(Dimethylcarbamoyl)-7H-Pyrrolo[2,3-d]Pyrimidin-2-yl)Amino)Phenyl)-N8-Hydroxyoctanediamide as a Novel Inhibitor Targeting Cyclin-Dependent Kinase 4/9 (CDK4/9) and Histone Deacetylase 1 (HDAC1) against Malignant Cancer. *J. Med. Chem* 2018, 61, 3166–3192. [PubMed: 29518312]
- (49). Chen Y; Yuan X; Zhang W; Tang M; Zheng L; Wang F; Yan W; Yang S; Wei Y; He J; Chen L Discovery of Novel Dual Histone Deacetylase and Mammalian Target of Rapamycin Target Inhibitors as a Promising Strategy for Cancer Therapy. *J. Med. Chem* 2019, 62, 1577–1592. [PubMed: 30629434]
- (50). Liang X; Zang J; Li X; Tang S; Huang M; Geng M; Chou CJ; Li C; Cao Y; Xu W; Liu H; Zhang Y Discovery of Novel Janus Kinase (JAK) and Histone Deacetylase (HDAC) Dual Inhibitors for the Treatment of Hematological Malignancies. *J. Med. Chem* 2019, 62, 3898–3923. [PubMed: 30901208]
- (51). Cakici M; Catir M; Karabuga S; Ulukanli S; Kilic H Synthesis and Asymmetric Catalytic Activity of (1*S*,1'*S*)-4,4'-Biquinazoline-Based Primary Amines. *Tetrahedron: Asymmetry* 2011, 22, 300–308.
- (52). Wei M; Zhang X; Wang X; Song Z; Ding J; Meng LH; Zhang A SAR Study of 5-Alkynyl Substituted Quinazolin-4(3H)-ones as Phosphoinositide 3-Kinase Delta (PI3K δ) Inhibitors. *Eur. J. Med. Chem* 2017, 125, 1156–1171. [PubMed: 27846451]
- (53). Adveef A Permeability—PAMPA In Absorption and Drug Development; John Wiley & Sons, Inc: New York, 2012; pp 319–498.
- (54). Patel L; Chandrasekhar J; Evarts J; Forseth K; Haran AC; Ip C; Kashishian A; Kim M; Koditek D; Koppenol S; Lad L; Lepist EI; McGrath ME; Perreault S; Puri KD; Villasenor AG; Somoza JR; Steiner BH; Therrien J; Treiberg J; Phillips G Discovery of Orally Efficacious Phosphoinositide 3-Kinase Delta Inhibitors with Improved Metabolic Stability. *J. Med. Chem* 2016, 59, 9228–9242. [PubMed: 27660855]
- (55). Patel L; Chandrasekhar J; Evarts J; Haran AC; Ip C; Kaplan JA; Kim M; Koditek D; Lad L; Lepist EI; McGrath ME; Novikov N; Perreault S; Puri KD; Somoza JR; Steiner BH; Stevens KL; Therrien J; Treiberg J; Villasenor AG; Yeung A; Phillips G 2,4,6-Triaminopyrimidine as a Novel Hinge Binder in a Series of PI3K δ Selective Inhibitors. *J. Med. Chem* 2016, 59, 3532–3548. [PubMed: 26980109]
- (56). Perreault S; Chandrasekhar J; Cui ZH; Evarts J; Hao J; Kaplan JA; Kashishian A; Keegan KS; Kenney T; Koditek D; Lad L; Lepist EI; McGrath ME; Patel L; Phillips B; Therrien J; Treiberg J; Yahiaoui A; Phillips G Discovery of a Phosphoinositide 3-Kinase (PI3K) Beta/Delta Inhibitor for the Treatment of Phosphatase and Tensin Homolog (PTEN) Deficient Tumors: Building PI3K β Potency in a PI3K δ -Selective Template by Targeting Nonconserved Asp856. *J. Med. Chem* 2017, 60, 1555–1567. [PubMed: 28106991]
- (57). Hai Y; Christianson DW Histone Deacetylase 6 Structure and Molecular Basis of Catalysis and Inhibition. *Nat. Chem. Biol* 2016, 12, 741–747. [PubMed: 27454933]
- (58). NCI-60 Human Tumor Cell Lines Screen; National Cancer Institute, 2015; https://dtp.cancer.gov/discovery_development/nci-60/ (accessed 2019-10-10).
- (59). Celltiter-Glo Luminescent Cell Viability Assay; Promega, 2015; <https://www.promega.com/-/media/files/resources/protocols/technical-bulletins/0/celltiter-glo-luminescent-cell-viability-assay-protocol.pdf?la=en> (accessed 2019-10-15).

- (60). Weisberg E; Ray A; Nelson E; Adamia S; Barrett R; Sattler M; Zhang C; Daley JF; Frank D; Fox E; Griffin JD Reversible Resistance Induced by FLT3 Inhibition: A Novel Resistance Mechanism in Mutant FLT3-Expressing Cells. *PLoS One* 2011, 6, e25351. [PubMed: 21980431]
- (61). Bosshart H; Heinzelmann M THP-1 Cells as a Model for Human Monocytes. *Ann. Transl Med* 2016, 4, 438. [PubMed: 27942529]
- (62). Ramachandran RP; Madhivanan S; Sundararajan R; Wan-Ying Lin C; Sankaranarayanan K An in Vitro Study of Electro-poration of Leukemia and Cervical Cancer Cells In Electroporation-Based Therapies for Cancer; Sundararajan R, Ed.; Woodhead Publishing, Cambridge UK, 2014; Chapter 7, pp 161–183.
- (63). Matsuo Y; MacLeod RA; Uphoff CC; Drexler HG; Nishizaki C; Katayama Y; Kimura G; Fujii N; Omoto E; Harada M; Orita K Two Acute Monocytic Leukemia (AML-M5a) Cell Lines (MOLM-13 and MOLM-14) with Interclonal Phenotypic Heterogeneity Showing MLL-AF9 Fusion Resulting from an Occult Chromosome Insertion, Ins(11;9)(Q23;P22p23). *Leukemia* 1997, 11, 1469–1477. [PubMed: 9305600]
- (64). Liu X; Wang A; Liang X; Chen C; Liu J; Zhao Z; Wu H; Deng Y; Wang L; Wang B; Wu J; Liu F; Fernandes SM; Adamia S; Stone RM; Galinsky IA; Brown JR; Griffin JD; Zhang S; Loh T; Zhang X; Wang W; Weisberg EL; Liu J; Liu Q Characterization of Selective and Potent PI3K δ Inhibitor (PI3KDIN-015) for B-Cell Malignancies. *Oncotarget* 2016, 7, 32641–32651. [PubMed: 27081697]
- (65). Novotny-Diermayr V; Sangthongpitag K; Hu CY; Wu X; Sausgruber N; Yeo P; Greicius G; Pettersson S; Liang AL; Loh YK; Bonday Z; Goh KC; Hentze H; Hart S; Wang H; Ethirajulu K; Wood JM SB939, a Novel Potent and Orally Active Histone Deacetylase Inhibitor with High Tumor Exposure and Efficacy in Mouse Models of Colorectal Cancer. *Mol. Cancer Ther* 2010, 9, 642–652. [PubMed: 20197387]
- (66). Li X; Su Y; Madhambayan G; Edwards H; Polin L; Kushner J; Dzinic SH; White K; Ma J; Knight T; Wang G; Wang Y; Yang J; Taub JW; Lin H; Ge Y Antileukemic Activity and Mechanism of Action of the Novel PI3K and Histone Deacetylase Dual Inhibitor CUDC-907 in Acute Myeloid Leukemia. *Haematologica* 2019, 104, 2225–2240. [PubMed: 30819918]
- (67). Yin L; Wu Z; Avigan D; Rosenblatt J; Stone R; Kharbanda S; Kufe D MUC1-C Oncoprotein Suppresses Reactive Oxygen Species-Induced Terminal Differentiation of Acute Myelogenous Leukemia Cells. *Blood* 2011, 117, 4863–4870. [PubMed: 21422470]
- (68). Martinez NJ; Asawa RR; Cyr MG; Zakharov A; Urban DJ; Roth JS; Wallgren E; Klumpp-Thomas C; Coussens NP; Rai G; Yang S-M; Hall MD; Marugan JJ; Simeonov A; Henderson MJ A Widely-Applicable High-Throughput Cellular Thermal Shift Assay (CETSA) Using Split Nano Luciferase. *Sci. Rep* 2018, 8, 9472. [PubMed: 29930256]
- (69). Molecular Operating Environment (MOE), 2013.08; Chemical Computing Group ULC, 2013; <https://www.chemcomp.com/Products.htm> (accessed 2019-03-02).
- (70). Halgren TA Merck Molecular Force Field. I. Basis, Form, Scope, Parameterization, and Performance of MMFF94. *J. Comput. Chem* 1996, 17, 490–519.
- (71). The UniProt Consortium. Uniprot: The Universal Protein Knowledgebase. *Nucleic Acids Res.* 2017, 45, D158–D169. [PubMed: 27899622]
- (72). Sun H; Nguyen K; Kerns E; Yan Z; Yu KR; Shah P; Jadhav A; Xu X Highly Predictive and Interpretable Models for PAMPA Permeability. *Bioorg. Med. Chem* 2017, 25, 1266–1276. [PubMed: 28082071]
- (73). Shah P; Kerns E; Nguyen D-T; Obach RS; Wang AQ; Zakharov A; McKew J; Simeonov A; Hop CECA; Xu X An Automated High-Throughput Metabolic Stability Assay Using an Integrated High-Resolution Accurate Mass Method and Automated Data Analysis Software. *Drug Metab. Dispos* 2016, 44, 1653. [PubMed: 27417180]

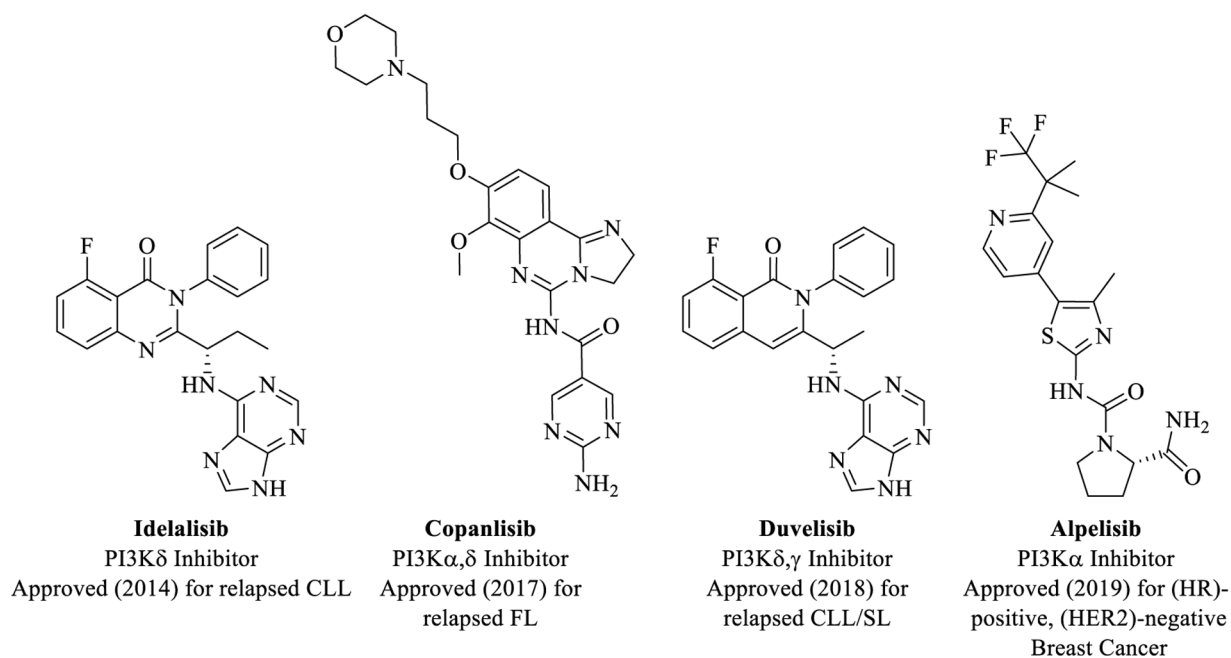
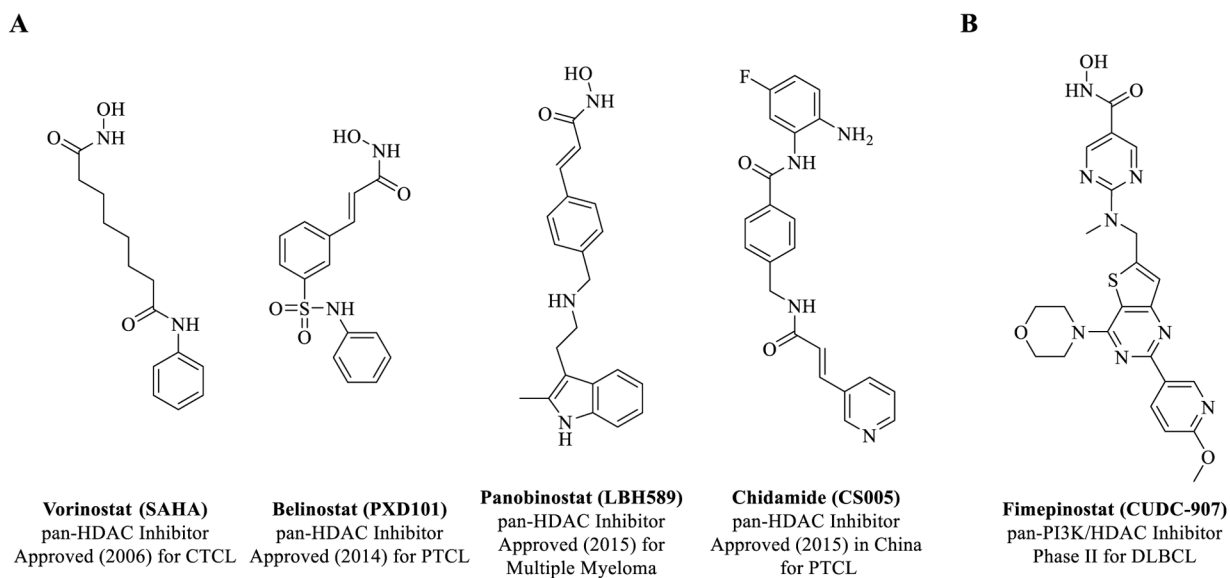


Figure 1.

FDA Approved PI3K inhibitor drugs for cancer (CLL = chronic lymphocytic leukemia; FL = follicular lymphoma; SLL = small lymphocytic lymphoma).

**Figure 2.**

(A) Selected approved HDAC inhibitor drugs for cancer. (B) Chemical structure of dual PI3K/HDAC inhibitor, Fimepinostat (CTCL = cutaneous T-cell lymphoma; PTCL = peripheral T-cell lymphoma; DLBCL = diffuse large B-cell lymphoma).

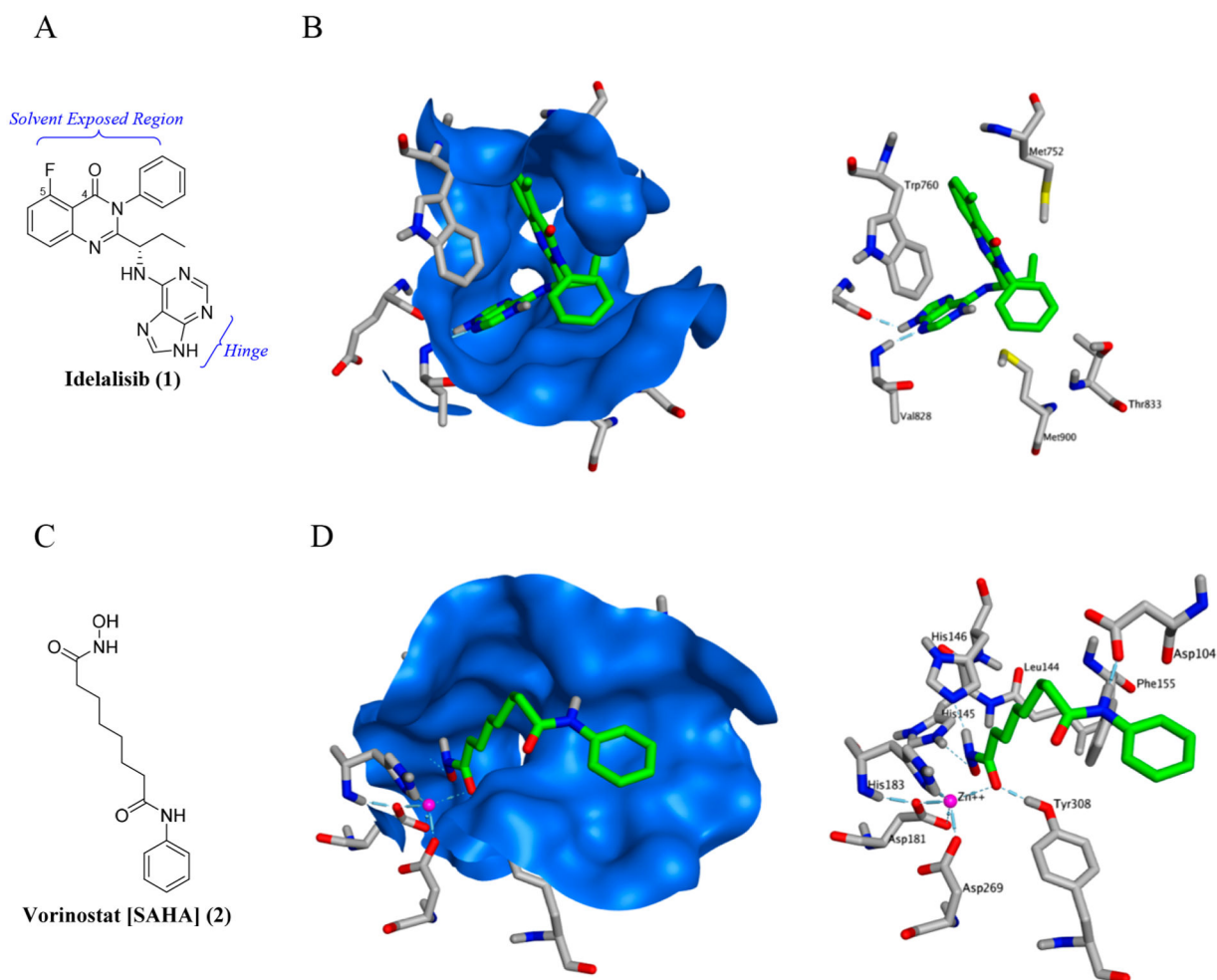


Figure 3. (A) Chemical structure of the PI3K δ inhibitor, Idelalisib (**1**). (B) Crystal structures of Idelalisib (**1**) [top view] bound to PI3K δ (PDB 4XE0) with protein surface (blue) and without protein surface, respectively. (C) Chemical structure of the HDAC inhibitor, Vorinostat (**2**). (D) Crystal structures of Vorinostat (**2**) bound to HDAC2 (PDB 4LXZ) with protein surface (blue) and without protein surface, respectively.

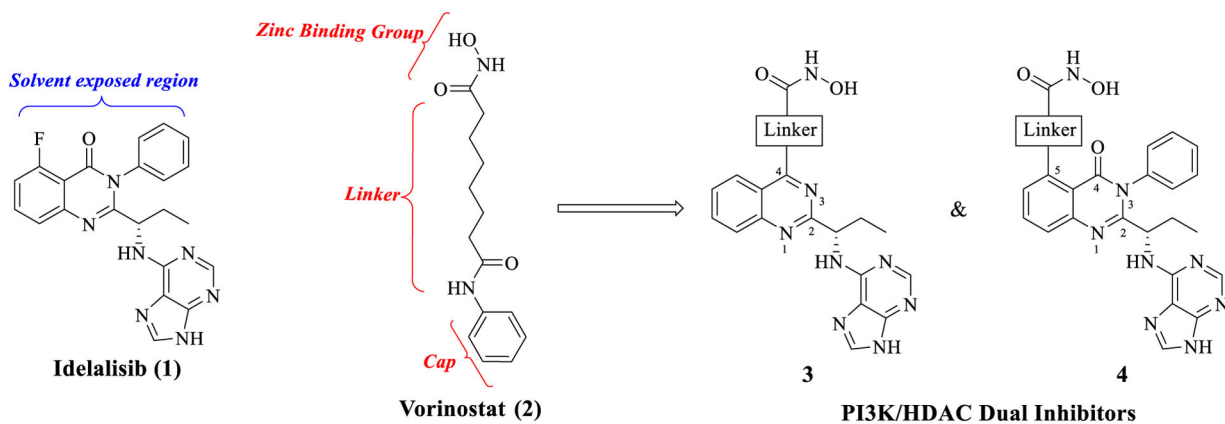


Figure 4.
Design strategy for dual PI3K/HDAC inhibitor types **3** and **4**.

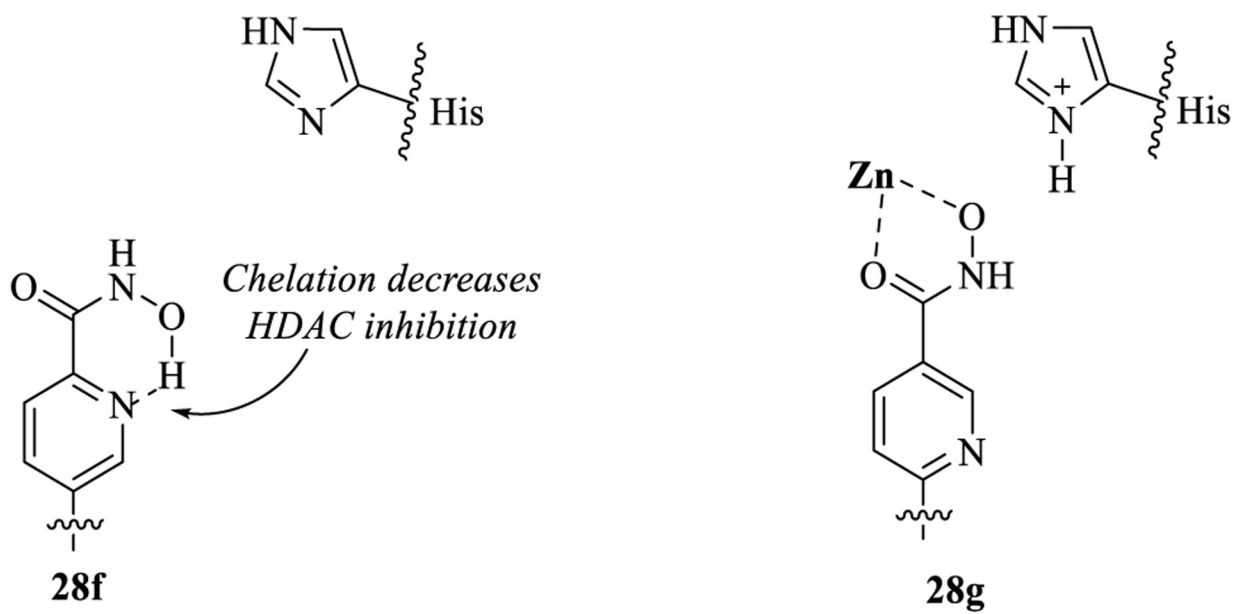


Figure 5.
Hydrogen bonding rationale for HDAC activity comparison in **28f** and **28g**.

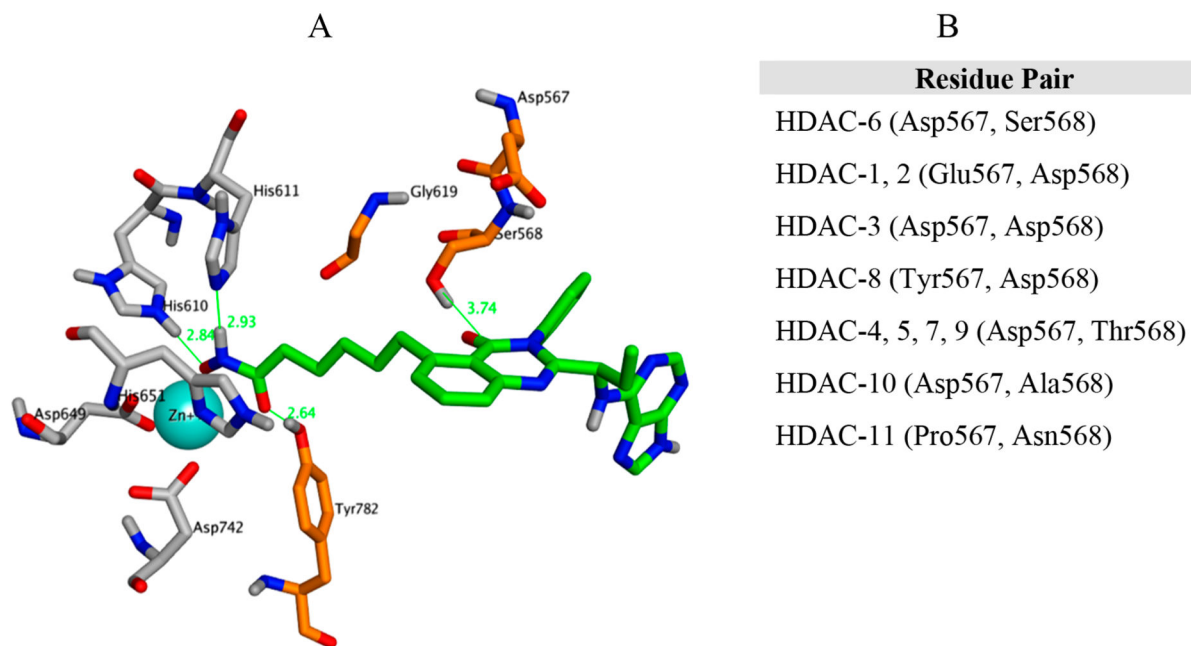


Figure 6. (A) Compound **19b** bound to HDAC6 (PDB 5EDU.pdb). (B) Variation in amino acid residues at positions 567 and 568 across different HDACs.

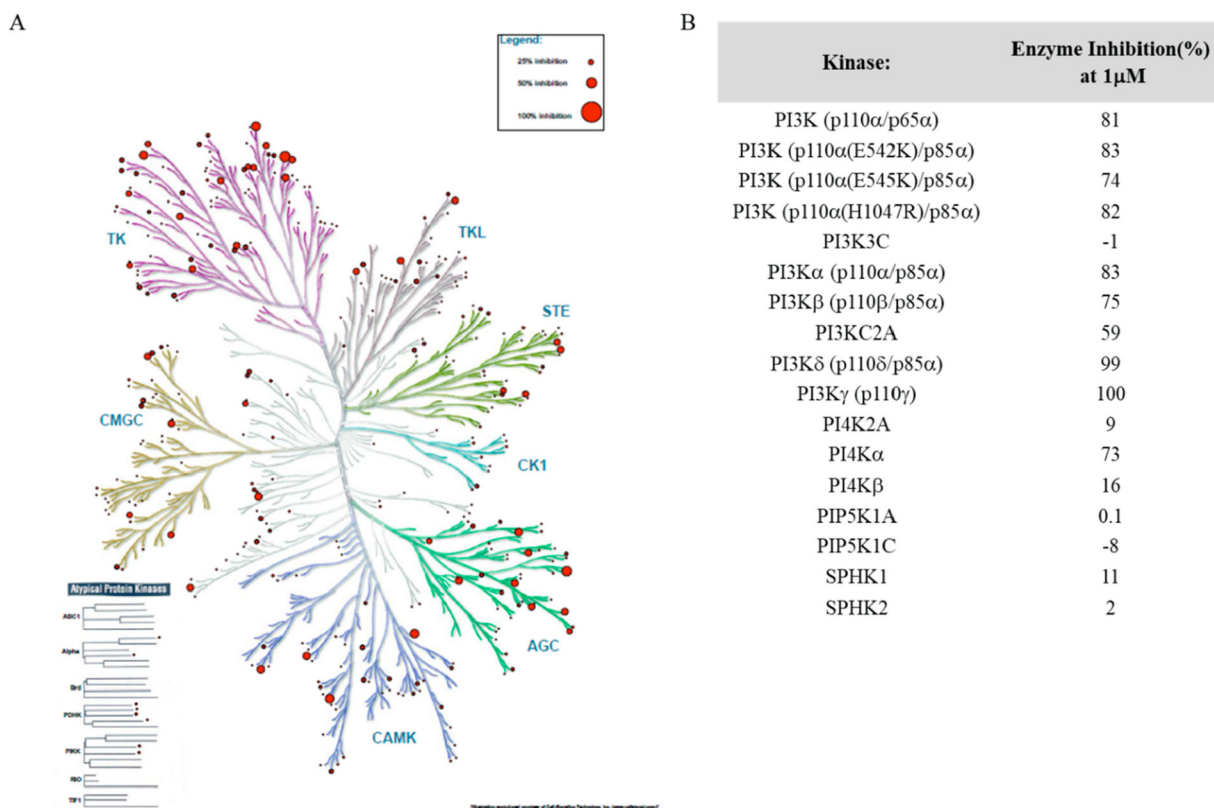
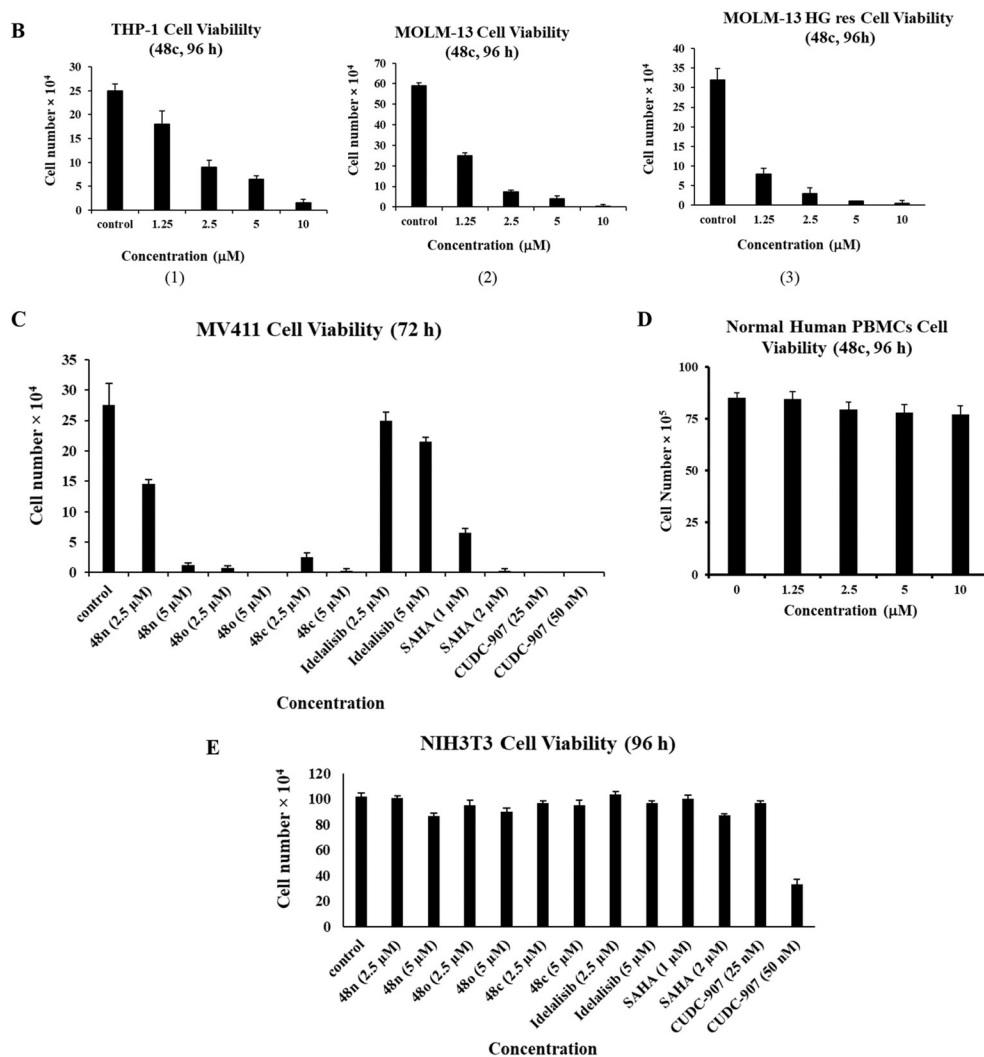


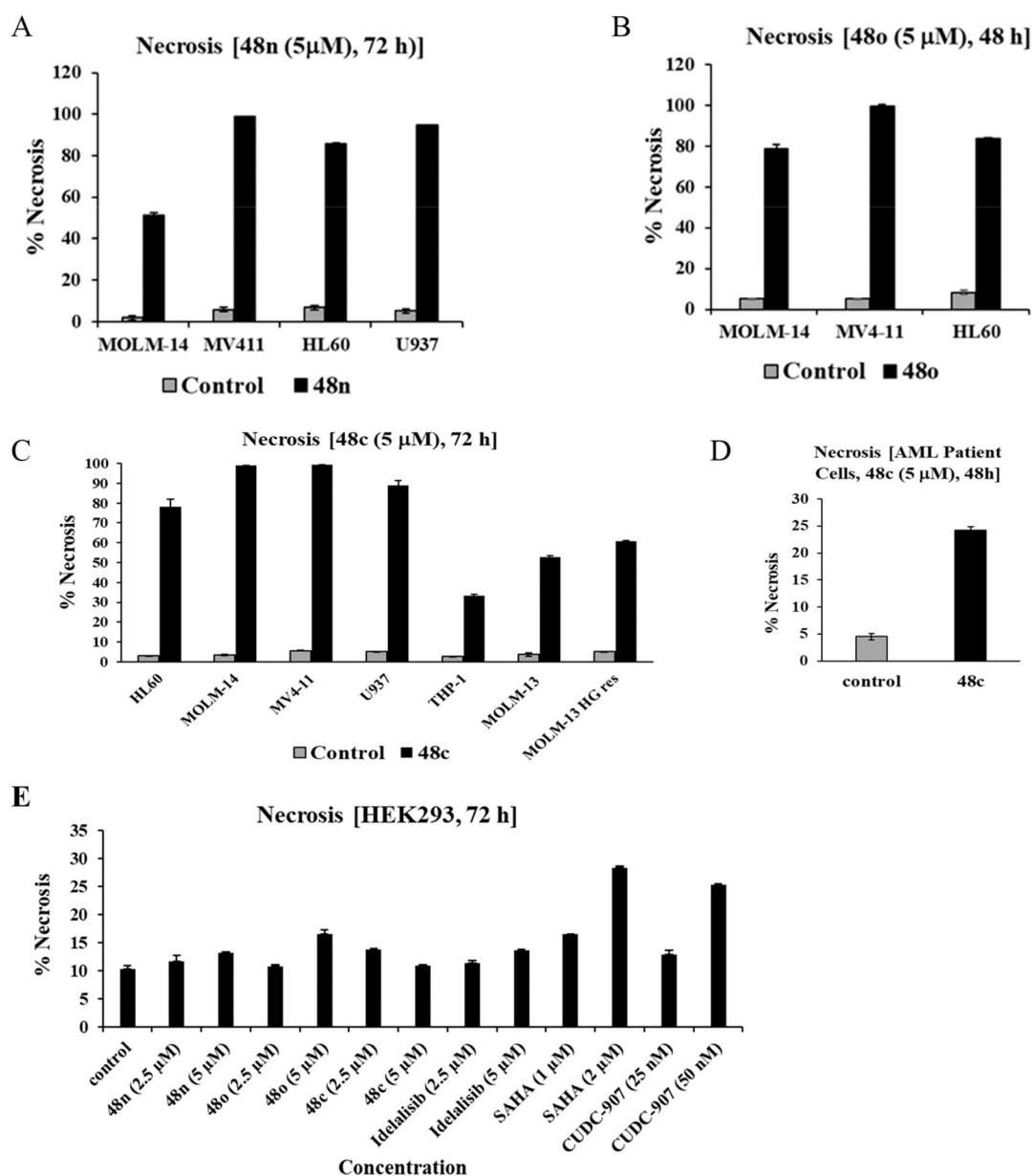
Figure 7.
 (A) Kinase selectivity profile of compound **48c** (1 μ M concentration) against 412 kinases.
 (B) Selectivity data (% Inhibition at 1 μ M) of compound **48c** against lipid kinases. Kinase profiling was done at Reaction Biology, Malvern, PA, USA.

A Anti-proliferative activity of **48c** against human blood cancer cell lines

Compound	IC ₅₀ (μM)						
	RPMI 8226	U266	HL60	MOLM-14	MV4-11	U937	K562
48c	2.1 ± 0.30	1.9 ± 0.32	2.4 ± 0.26	2.4 ± 0.01	2.5 ± 0.03	2.6 ± 0.29	4.6 ± 0.07

**Figure 8.**

(A) Cell viability assays were performed in duplicate with IC₅₀ values expressed as mean ± SD of two independent runs. (B) In vitro cell-kill activity of **48c**. (C) In vitro cell-kill activity of compounds **48n**, **48o**, **48c**, Idelalisib, SAHA, and CUDC-907 against MV411 cells. (D) PBMCs viability with **48c** treatment. (E) NIH3T3 cell viability upon treatment with compounds **48n**, **48o**, **48c**, Idelalisib, SAHA, and CUDC-907.

**Figure 9.**

(A) Necrosis rate (%) of **48n** at 5 μ M concentration. (B) Necrosis rate (%) of **48o** at 5 μ M concentration. (C) Necrosis rate (%) of **48c** at 5 μ M concentration. (D) Necrosis rate (%) of **48c** at 5 μ M concentration against primary AML blasts. (E) Necrosis rate (%) of compounds **48n**, **48o**, **48c**, Idelalisib, SAHA, and CUDC-907 against HEK293 cells. Necrosis assays were performed in duplicate and % necrosis values are expressed as mean \pm SD of two independent runs.

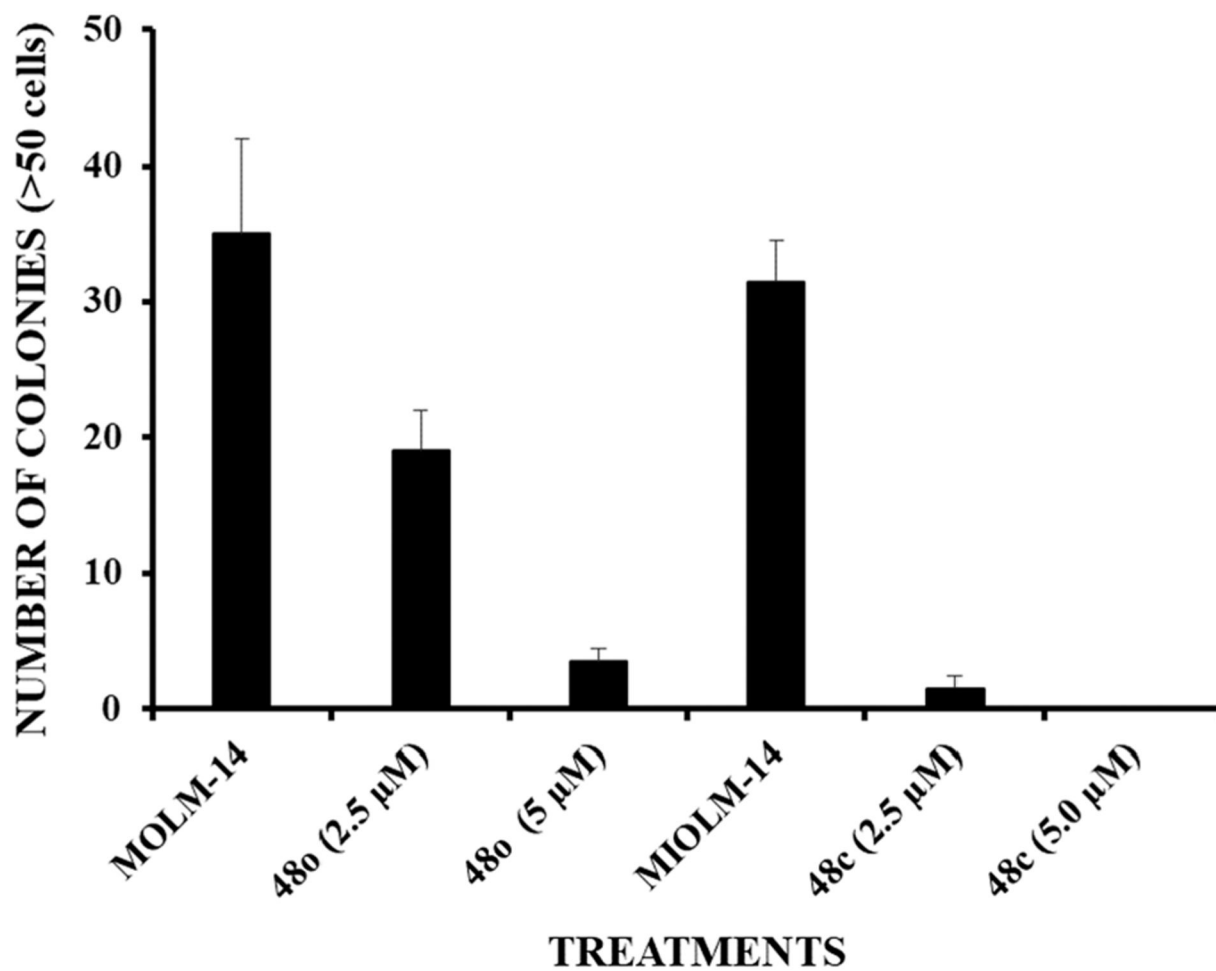


Figure 10.
Inhibition of MOLM-14 colony formation by **48c** and **48o**.

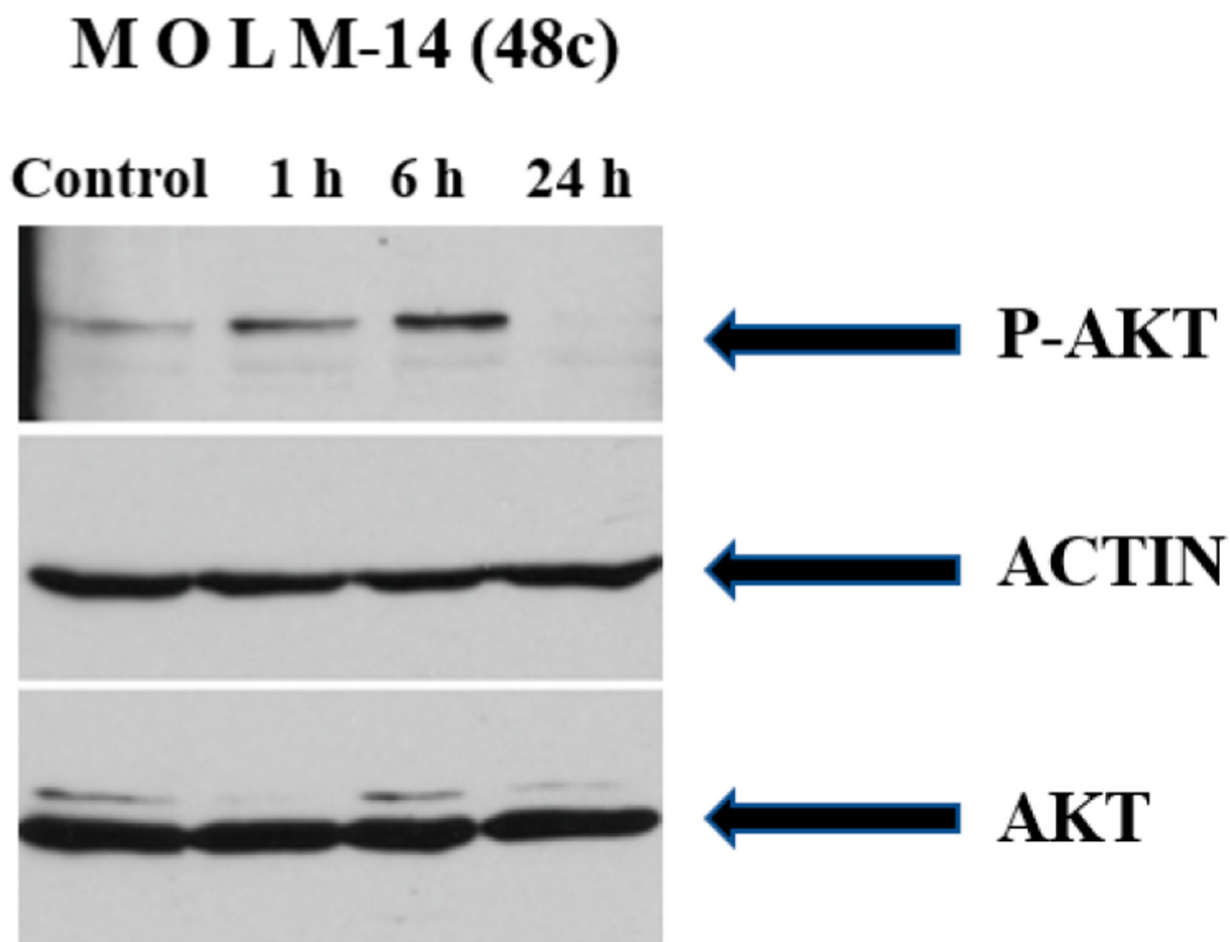
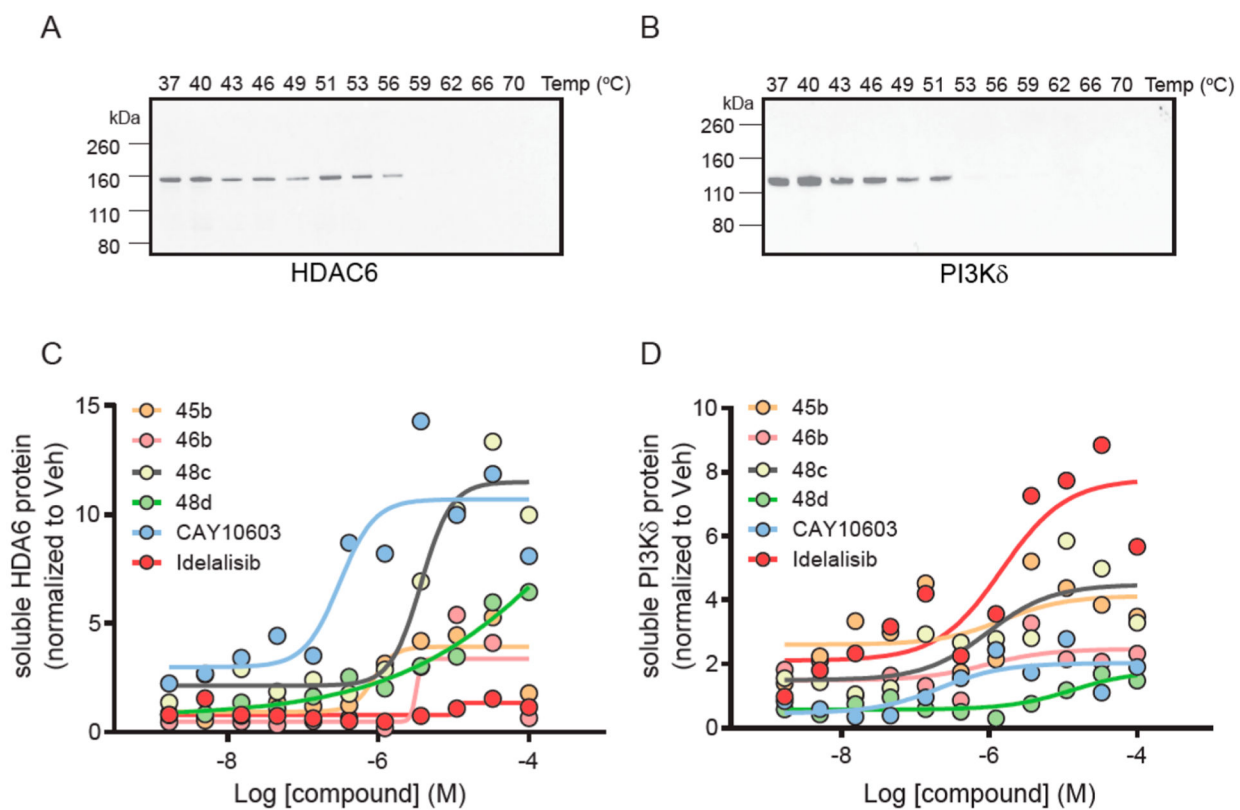


Figure 11.
Immunoblot analysis for PI3K inhibition in MOLM-14 cells.

**Figure 12.**

CETSA analysis. (A) T_{agg} measurement for HDAC6 in MV411 cells, (B) T_{agg} measurement for PI3K δ in MV411 cells, (C) melt profile for HDAC6, (D) melt profile for PI3K δ .

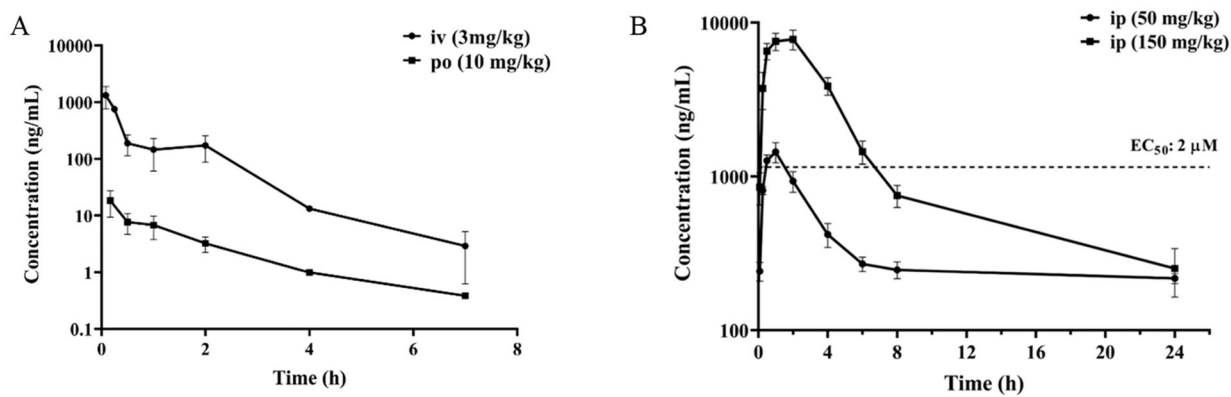
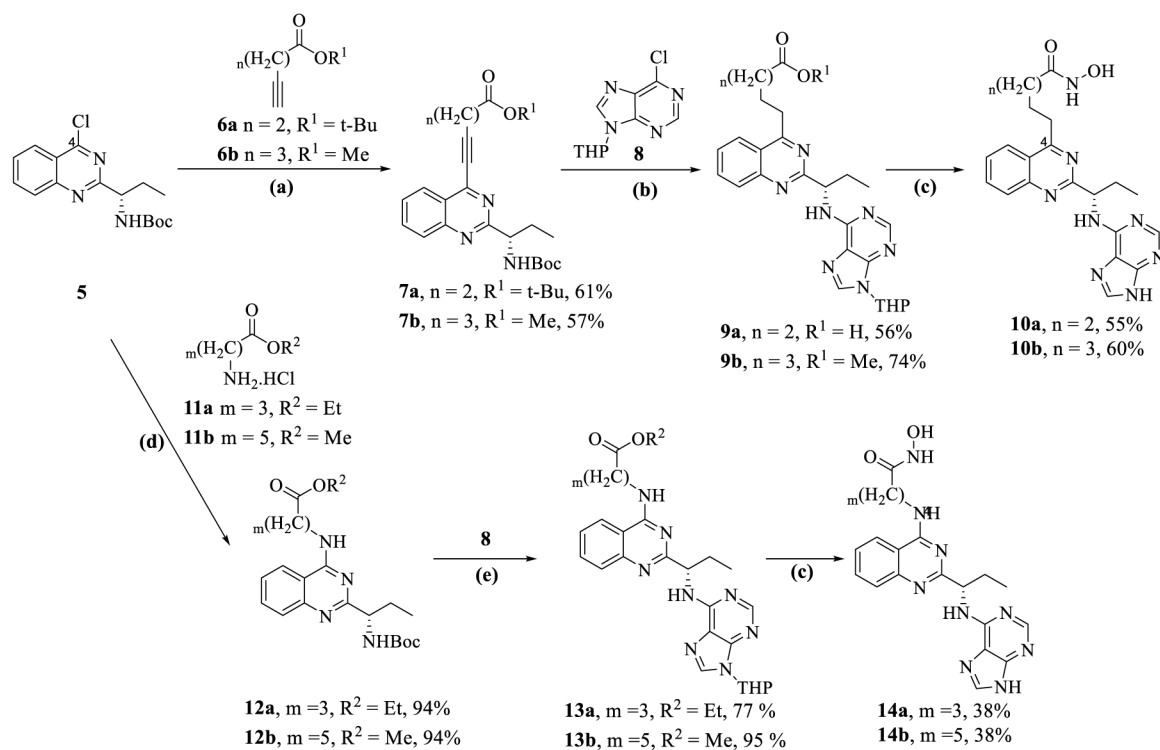
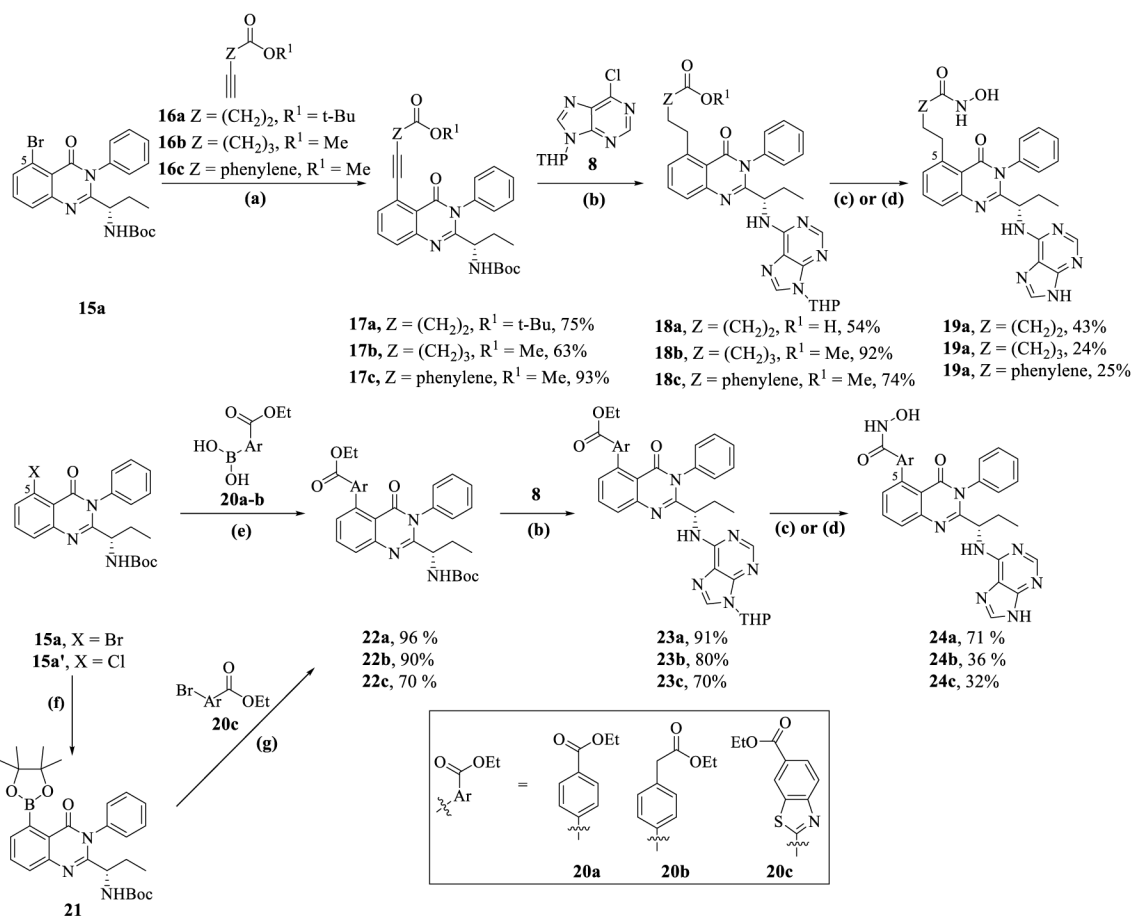


Figure 13. Plasma concentration vs time profiles for **48c** in female Balb/c mice via: (A) iv (3 mg/kg) and po (10 mg/kg) dosing, and (B) ip (50 mg/kg and 150 mg/kg) dosing.

**Scheme 1.**

Synthesis of C-4 Alkyl/Amino-alkyl Substituted Quinazolines (**10a,b** and **14a,b**)^a

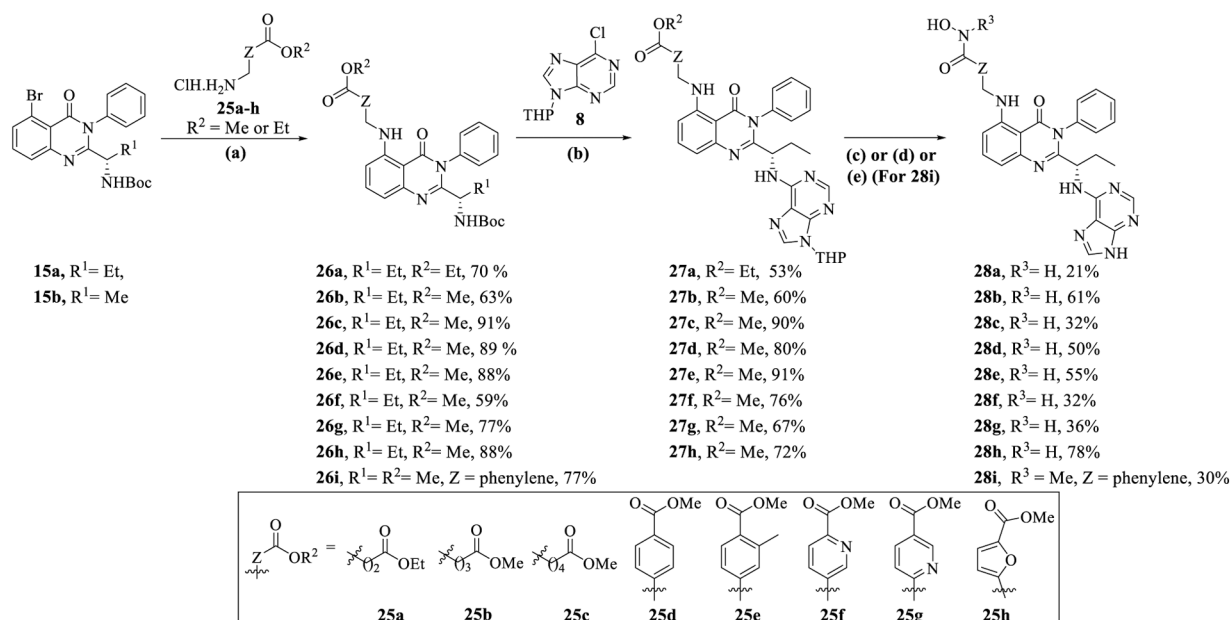
^aReagents and conditions: (a) **6a**, **6b** (1.2 equiv), $[\text{PdCl}(\text{allyl})]_2$ (0.05 equiv), $\text{P}_t\text{Bu}_3\text{HBF}_4$ (0.20 equiv), 1,4-dioxane, 16 h, rt; (b) (i) 10 wt % Pd/C, H_2 balloon, EtOAc, 20 h, rt, (ii) $\text{CF}_3\text{CO}_2\text{H}$ (20.0 equiv), DCM, 3 h, rt, (iii) **8** (2.0 equiv), triethylamine (4.0 equiv), EtOH, 1 h, MW, 100 1/2C; (c) (i) LiOH·H₂O (2.0 equiv), MeOH/H₂O, 10 h, rt, (ii) NH_2OTHP (3.1 equiv), *N*-methyl morpholine (3.0 equiv) 3-(((ethylimino)-methylene)amino)-*N,N*-dimethylpropan-1-amine hydrochloride [EDC·HCl] (1.4 equiv), 1*H*[1,2,3]triazolo[4,5-*b*]pyridin-1-ol [HOAT] (1.2 equiv), DMF, 16 h rt; (iii) $\text{CF}_3\text{CO}_2\text{H}$ (20.0 equiv), DCM, 20 h, rt (For **9a**, only c(ii) and c(iii) were used); (d) **11a,b** (2.0 equiv), triethylamine (4.0 equiv), EtOH, 1 h, 100 1/2C; (e) **8** (2.0 equiv), triethylamine (4.0 equiv), EtOH, 1 h, 100 1/2C.



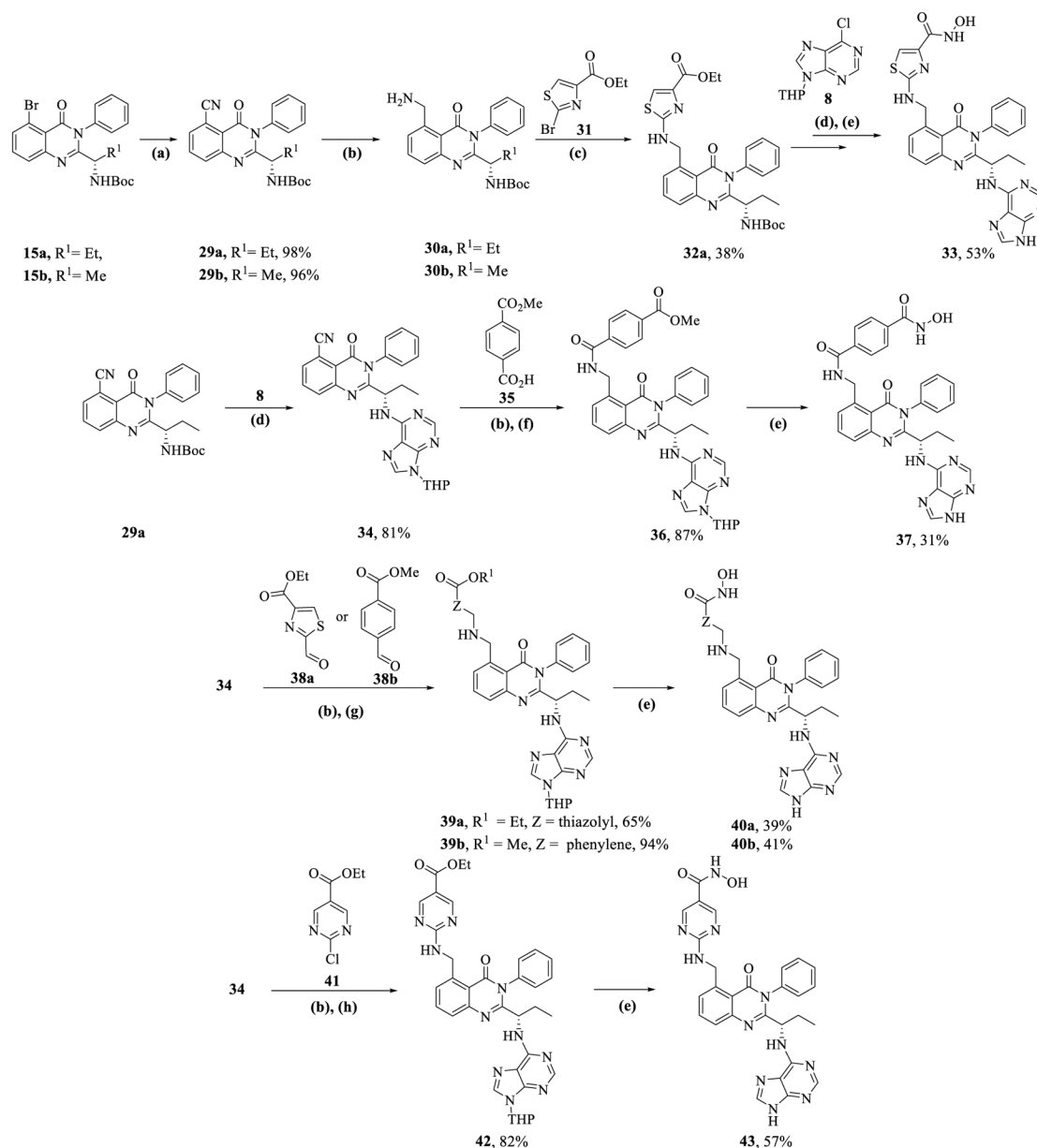
Scheme 2.

Synthesis of C-5 Alkyl/Aryl Substituted Quinazolinones (19a–c and 24a–c)^a

^aReagents and conditions: (a) **16a**, **16b**, **16c** (1.2 equiv), [PdCl(allyl)]₂ (0.05 equiv), P₄Bu₃HBF₄ (0.20 equiv), 1,4-dioxane, 16 h, rt; (b) (i) 10 wt % Pd/C, H₂ balloon, EtOAc, 20 h, rt, (ii) CF₃CO₂H (20.0 equiv), DCM, 3 h, rt, (iii) **8** (1.5–2.5 equiv), triethylamine (3.0–5.0 equiv), EtOH, 4 h, MW, 100 1/2C; (c) (i) LiOH·H₂O (2.0 equiv), MeOH/H₂O, 10 h, rt, (ii) NH₂OTHP (3.1 equiv), *N*-methyl morpholine (3.0 equiv) 3-(((ethylimino)methylene)amino)-*N,N*-dimethylpropan-1-amine hydrochloride [EDC·HCl] (1.4 equiv), 1*H*-[1,2,3]triazolo[4,5-*b*]pyridin-1-ol [HOAT] (1.2 equiv), DMF, 16 h, rt, (iii) CF₃CO₂H (20.0 equiv), DCM/MeOH, 20 h, rt, (*For 17a*, only *c(ii)* and *c(iii)* were used); (d) (i) aq 50 wt % NH₂OH (30.0 equiv), LiOH·H₂O (1.1 equiv), MeOH/H₂O, 20 h, 0 1/2C to rt, (ii) CF₃CO₂H (20.0 equiv), DCM/MeOH, 20 h, rt; (e) boronic acid/ester **20a,b** (1.2 equiv), [XPhos Pd(crotyl)Cl] (0.05 equiv), K₃PO₄ (3.0 equiv), 1,4-dioxane/water, 1–2 h MW, 100 1/2C; (f) [Bpin]₂ (1.2 equiv), [Pd(dppf)Cl₂] (0.05 equiv), KOAc (3.0 equiv) 1,4-dioxane, 16 h, 100 1/2C; (g) **20c** (0.85 equiv), [XPhos Pd(crotyl)Cl] (0.05 equiv), K₃PO₄ (3.0 equiv), 1,4-dioxane/water, 10 h, 100 1/2C; (h) (i) CF₃CO₂H (20.0 equiv), DCM, 3 h, rt, (ii) **8** (1.5–2.5 equiv), triethylamine (3.0–5.0 equiv), EtOH, 4 h, 100 1/2C.

**Scheme 3.**Synthesis of C-5 Amino-alkyl/Aryl Substituted Quinazolinones (28a–i)^a

^aReagents and conditions: (a) **25a–h** (1.3 equiv), [Xantphos Palladacycle Gen. 4] (0.03 equiv), Cs₂CO₃ (3.0 equiv), toluene or 1,4-dioxane, 16 h, rt; (b) (i) CF₃CO₂H (20.0 equiv), DCM, 3 h, rt, (ii) **8** (1.5–2.5 equiv), triethylamine (3.0–5.0 equiv), EtOH, 4 h, MW, 100 1/2C; (c) (i) LiOH·H₂O (2.0 equiv), MeOH/H₂O, 10 h, rt, (ii) NH₂OTHP (3.1 equiv), *N*-methylmorpholine (3.0 equiv) 3-((ethylimino)methylene)amino)-*N,N*-dimethylpropan-1-amine hydrochloride [EDC·HCl] (1.4 equiv), 1*H*-[1,2,3]triazolo[4,5-*b*]pyridin-1-ol [HOAT] (1.2 equiv), DMF, 16 h, rt, (iii) CF₃CO₂H (20.0 equiv), DCM/MeOH, 20 h, rt; (d) (i) aq 50 wt % NH₂OH (30.0 equiv), LiOH·H₂O (1.1 equiv), MeOH/H₂O, 20 h, 0 1/2C to rt, (ii) CF₃CO₂H (20.0 equiv), DCM/MeOH, 20 h, rt; (e) (i) LiOH·H₂O (1.1 equiv), MeOH/H₂O, 20 h, 0 1/2C to rt, (ii) *N*-methylhydroxylamine hydrochloride (1.5 equiv), HATU (1.5), DIPEA (2.5 equiv), DMF, rt, (iii) CF₃CO₂H (20.0 equiv), DCM/MeOH, 20 h, rt.

**Scheme 4.**Synthesis of C-5 Alkyl-amino Substituted Quinazolinones (**33**, **37**, **40**, and **43**)^a

^aReagents and conditions: (a) Pd(PPh₃)₄ (0.05 equiv), Zn(CN)₂ (1.2 equiv), DMF, 100 °C, 16 h; (b) Raney Ni, H₂, MeOH, 20 h; (c) **31** (2.0 equiv) DIPEA (4.0 equiv), DMF, 180 °C, MW, 30 min; (d) (i) CF₃CO₂H (20.0 equiv), DCM, 3 h, rt, (ii) **8** (1.5–2.5 equiv), triethylamine (3.0–5.0 equiv), EtOH, 4 h, MW, 100 °C; (e) (i) LiOH·H₂O (2.0 equiv), MeOH/H₂O, 10 h, rt, (ii) NH₂OTHP (3.1 equiv), *N*-methyl morpholine (3.0 equiv) 3-(((ethylimino)methylene)amino)-*N,N*-dimethylpropan-1-amine hydrochloride [EDC·HCl] (1.4 equiv), 1*H*-[1,2,3]triazolo[4,5-*b*]pyridin-1-ol [HOAT] (1.2 equiv), DMF, 16 h, rt, (iii) CF₃CO₂H (20.0 equiv), DCM/MeOH, 20 h, rt; (f) **35** (1.5 equiv), HATU (1.2 equiv), DIPEA

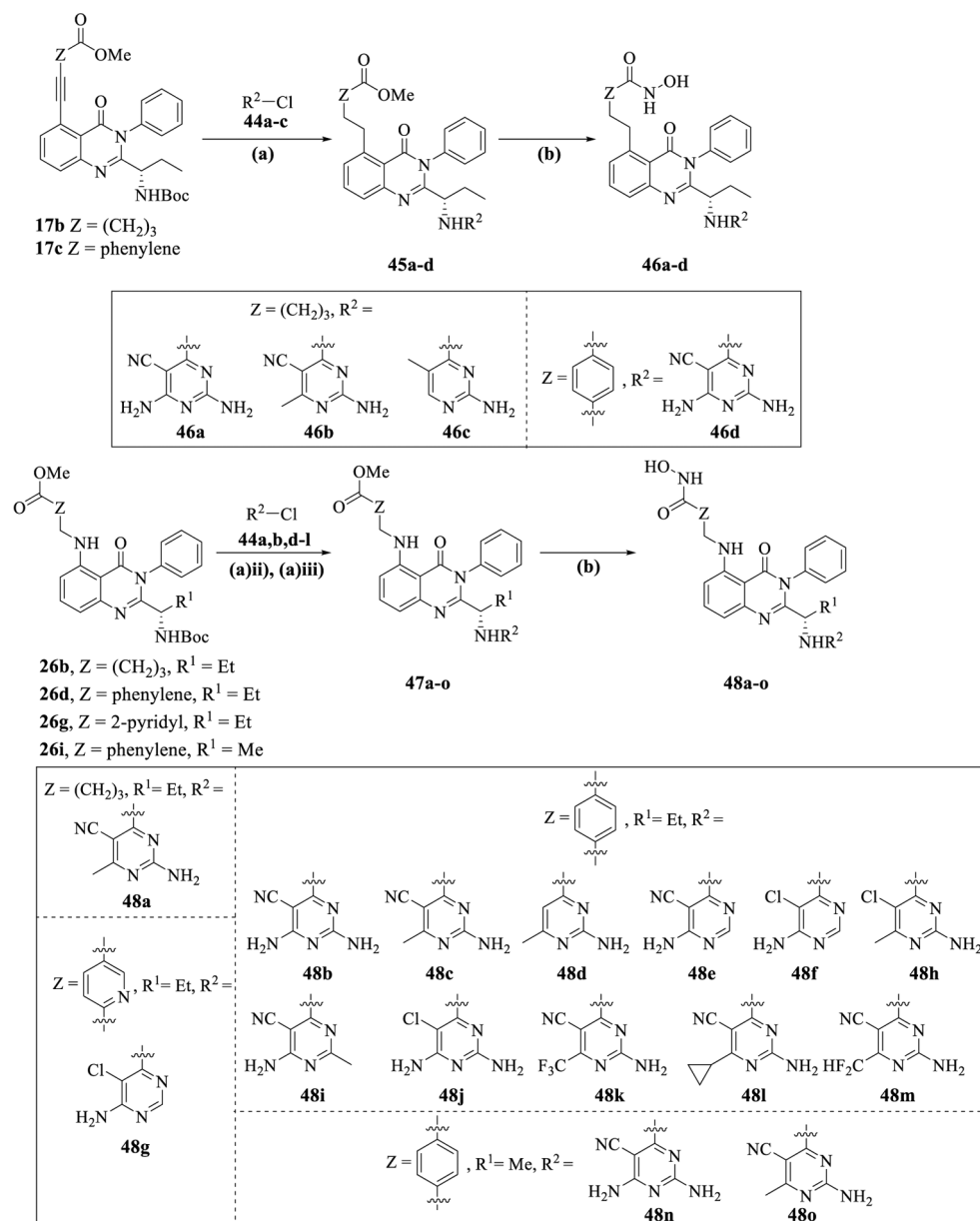
(3.0 equiv), DMF, 16 h, rt; (g) **38** (1 equiv), cat. AcOH, DCE, 2 h, then NaBH(OAc)₃ (3.0 equiv), 2 h; (h) **41** (2.0 equiv), triethylamine (4.0 equiv), EtOH, 100 °C, MW, 3 h.

Author Manuscript

Author Manuscript

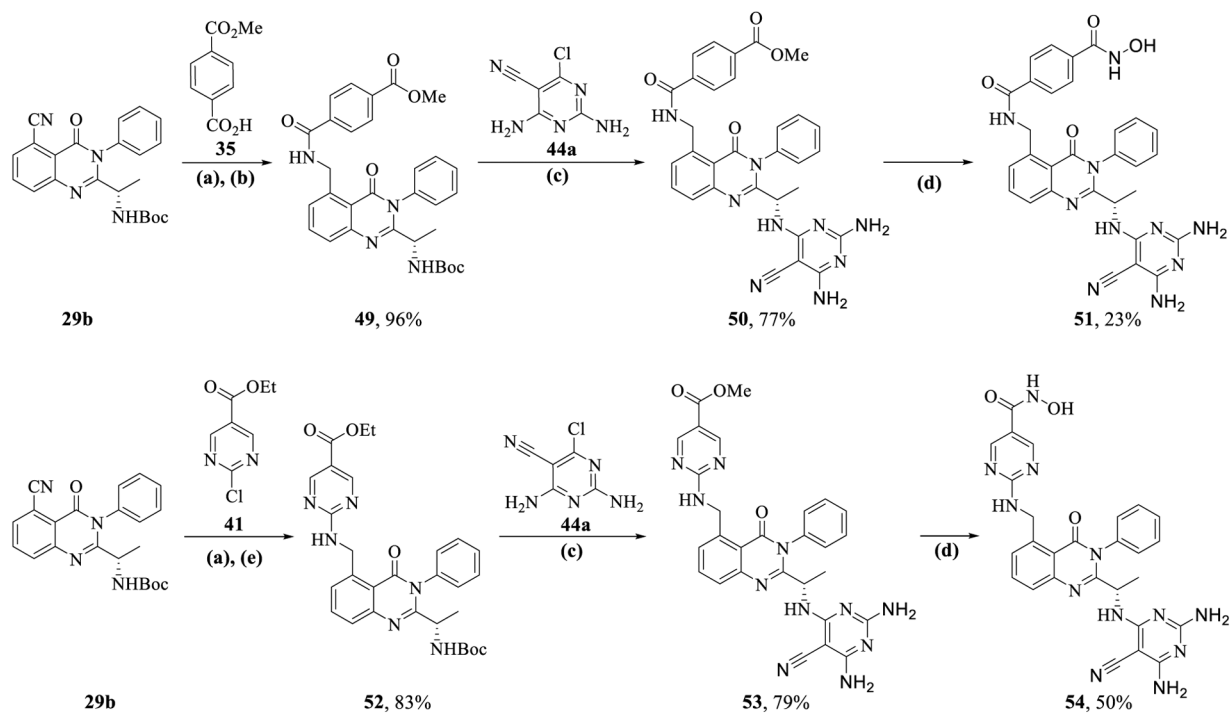
Author Manuscript

Author Manuscript



Scheme 5. Synthesis of C-5 Substituted Quinazolinones with Pyrimidine Hinge Binding Groups (46a–d and 48a–o)^a

^aReagents and conditions: (a) (i) 10 wt % Pd/C, H₂ balloon, EtOAc, 20 h, rt, (ii) CF₃CO₂H (20.0 equiv), DCM, 3 h, rt, (iii) **44** (1.5–2.0 equiv), DIPEA (3.0–4.0 equiv), *n*-butanol, 2–3 h, MW, 130 1/2C, 38–88% (3 steps); (b) aq 50 wt % NH₂OH (30.0 equiv), LiOH·H₂O (1.1 equiv), MeOH/H₂O, 20 h, 0 1/2C to rt; 36–82%.

**Scheme 6.****Synthesis of C-5 Alkyl-amino Substituted Quinazolinones (51 and 54)^a**

^aReagents and conditions: (a) Raney Ni, H₂, MeOH, 20 h; (b) **35** (1.5 equiv), HATU (1.2 equiv), DIPEA (3.0 equiv), DMF, 16 h; (c) (i) CF₃CO₂H (20.0 equiv), DCM, 3 h, rt, (ii) **44a** (1.5 equiv), DIPEA (3.0 equiv), *n*-butanol, 2–5 h, MW, 130–150 1/2C; (d) aq 50 wt % NH₂OH (30.0 equiv), LiOH·H₂O (1.1 equiv), MeOH/H₂O, 20 h, 0 1/2C to rt; (e) **41** (1.5 equiv), DIPEA (3.0 equiv), *n*-butanol, 2 h, MW, 130 1/2C.

Author Manuscript

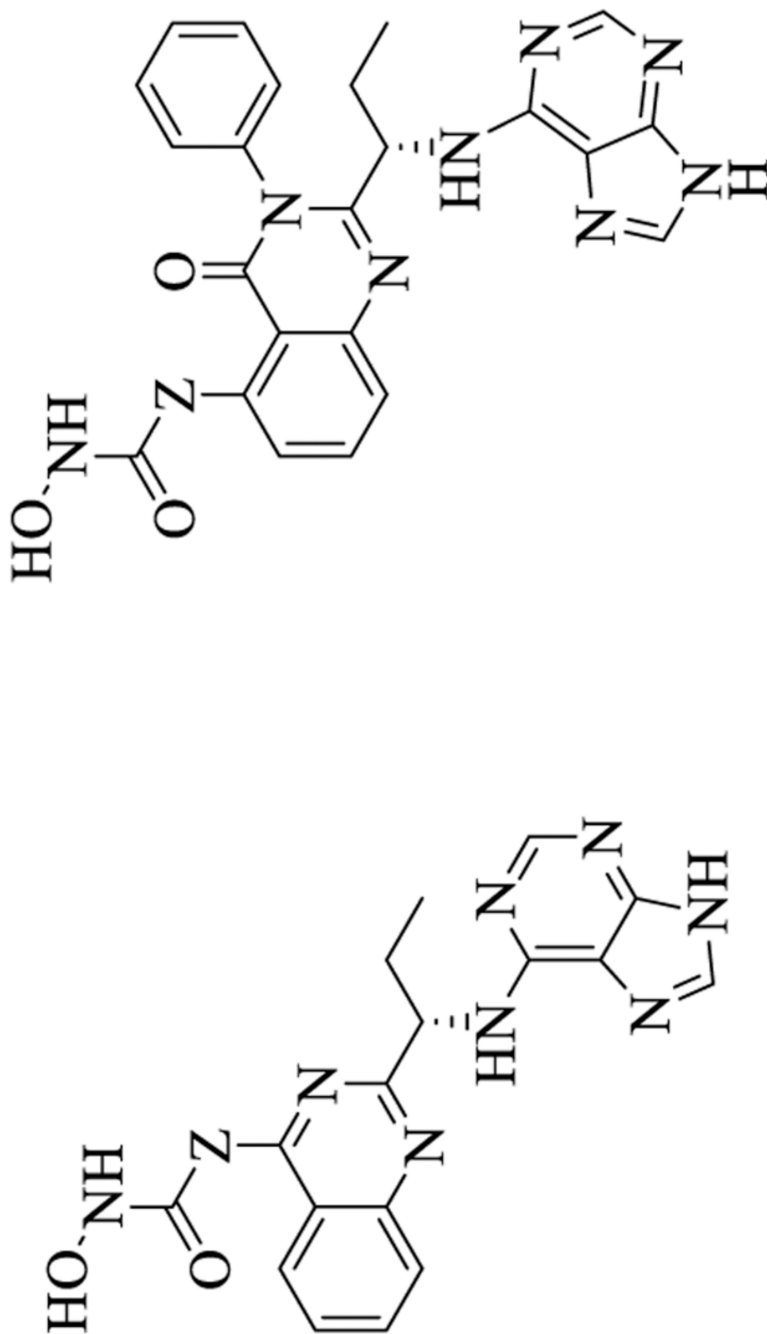
Author Manuscript

Author Manuscript

Author Manuscript

Table 1.

Enzyme Inhibitory Activities of 4-Substituted Quinazolines (10a,b, 14a) vs 5-Substituted Quinazolines (19a,b, 28a)^a



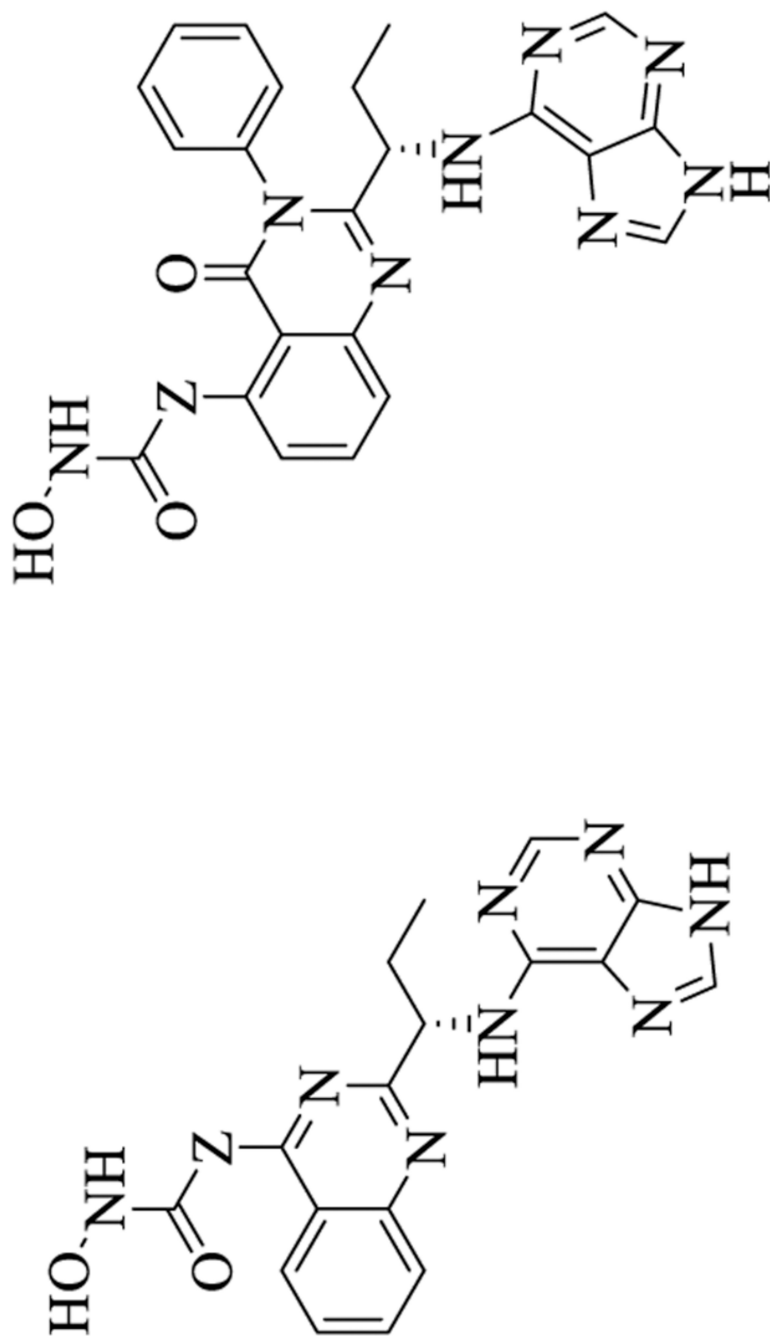
compd	PI3Kδ	HDACs									
		1	2	3	4	5	6	7	8	9	10
10a	49	5846	18190	7075		2169	1937		33730		23030

Author Manuscript

Author Manuscript

Author Manuscript

Author Manuscript

IC₅₀ (nM)

HDACs

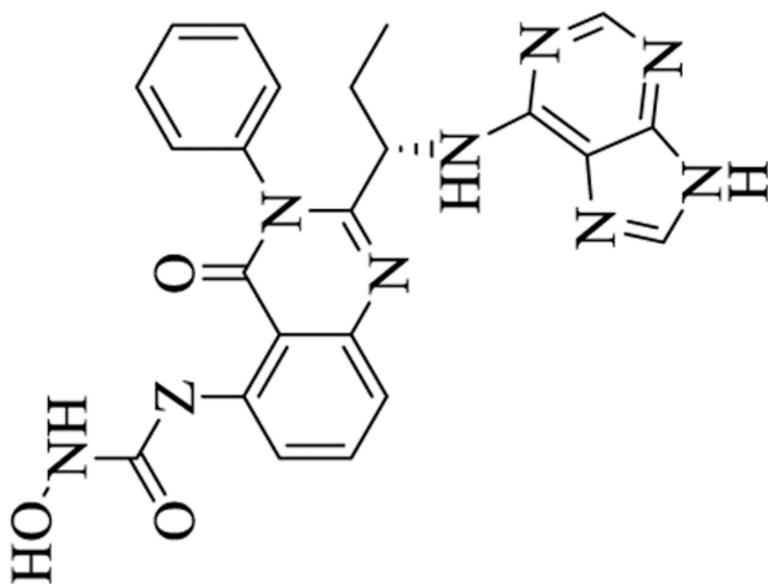
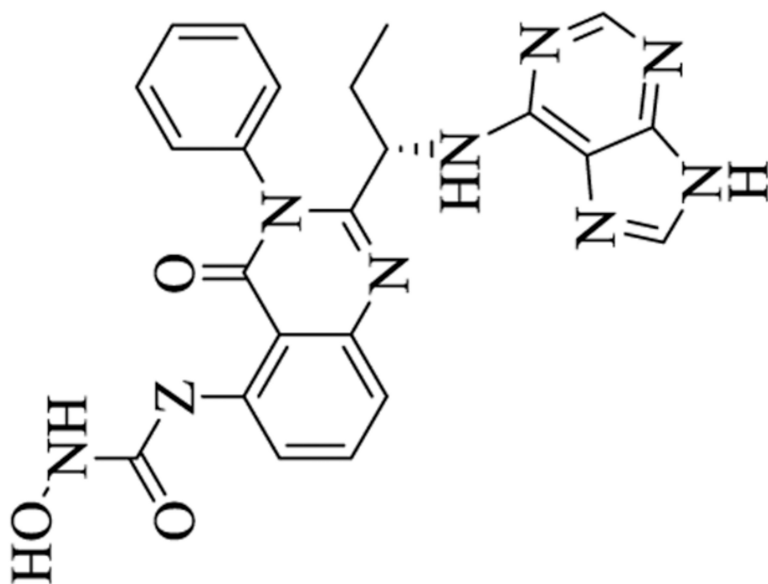
compd	1	2	3	4	5	6	7	8	9	10	11
P13K6											
19a	<5	429	427	70910	23610	36	90810	385	>10 ⁵	2073	2089

Author Manuscript

Author Manuscript

Author Manuscript

Author Manuscript

**10a** Z = (CH₂)₄**10b** Z = (CH₂)₅**14a** Z = NH(CH₂)₃**19a** Z = (CH₂)₄**19b** Z = (CH₂)₅**28a** Z = NH(CH₂)₃IC₅₀ (nM)

HDACs

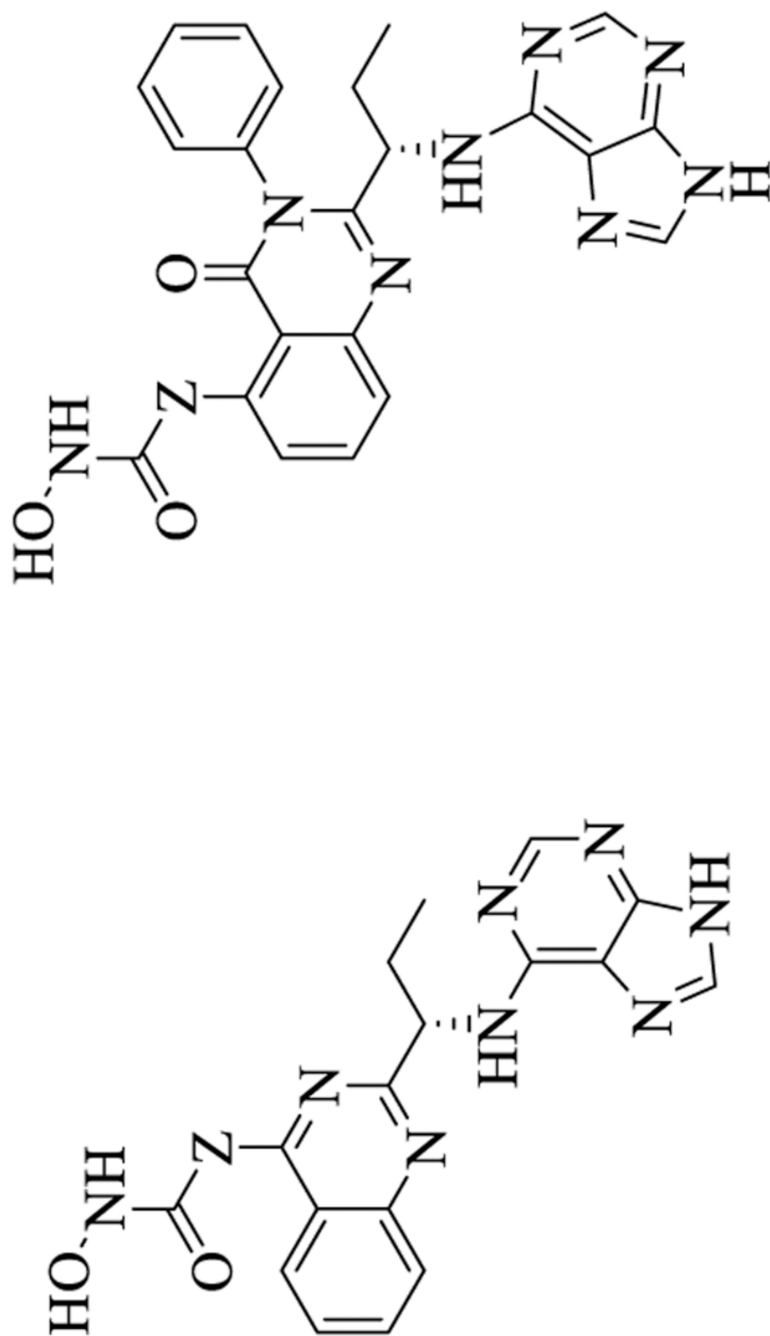
compd	P13K6	1	2	3	4	5	6	7	8	9	10	11
10b	68	5390	14100	10600	>10 ⁵	43700	39		353		16900	9819

Author Manuscript

Author Manuscript

Author Manuscript

Author Manuscript

**10a** Z = (CH₂)₄**10b** Z = (CH₂)₅**14a** Z = NH(CH₂)₃**19a** Z = (CH₂)₄**19b** Z = (CH₂)₅**28a** Z = NH(CH₂)₃IC₅₀ (nM)

HDACs

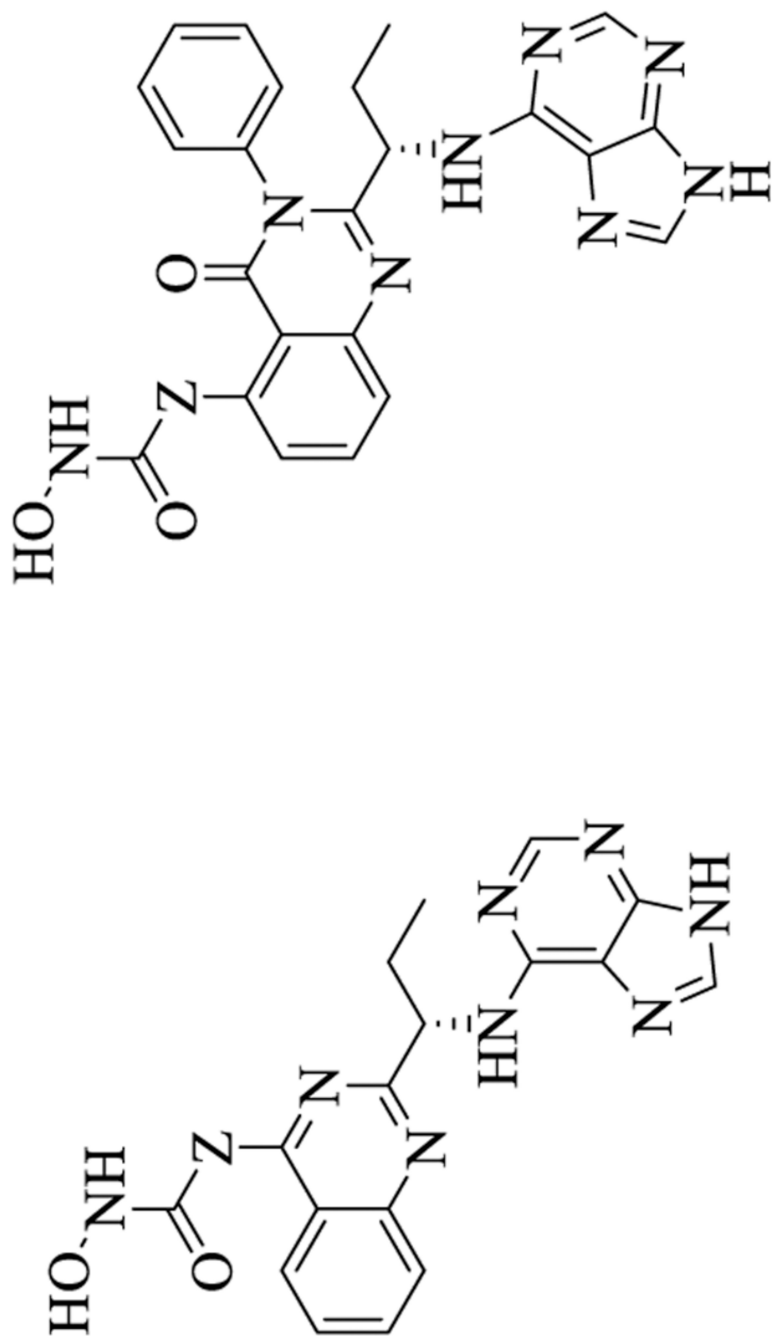
compd	1	2	3	4	5	6	7	8	9	10	11
19b	0.2	388		11290	8106	5	24400	253	34850	1502	2155

Author Manuscript

Author Manuscript

Author Manuscript

Author Manuscript

**10a** Z = (CH₂)₄**10b** Z = (CH₂)₅**14a** Z = NH(CH₂)₃**19a** Z = (CH₂)₄**19b** Z = (CH₂)₅**28a** Z = NH(CH₂)₃IC₅₀ (nM)

HDACs

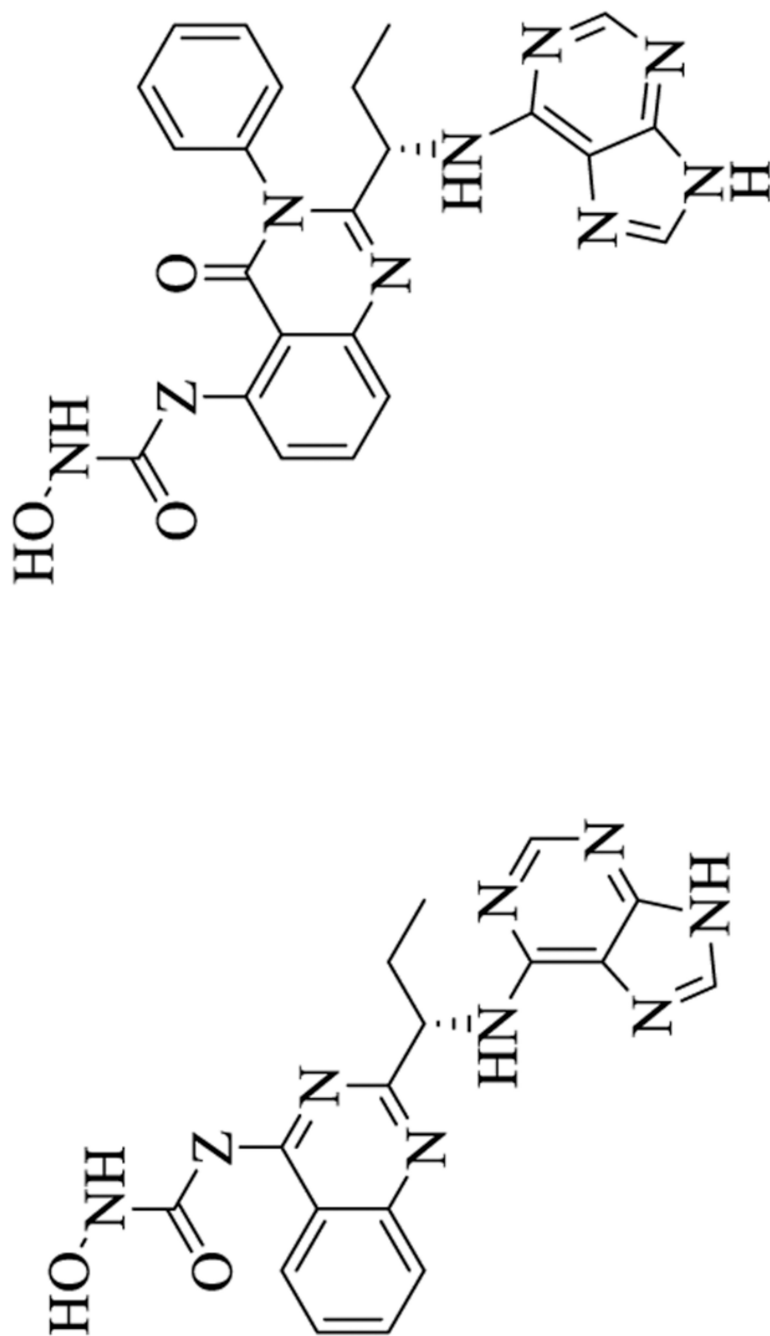
compd	1	2	3	4	5	6	7	8	9	10	11
14a	520	>10 ⁵	>10 ⁵	>10 ⁵	>10 ⁵	431		6194			74140

Author Manuscript

Author Manuscript

Author Manuscript

Author Manuscript

IC₅₀ (nM)

HDACs

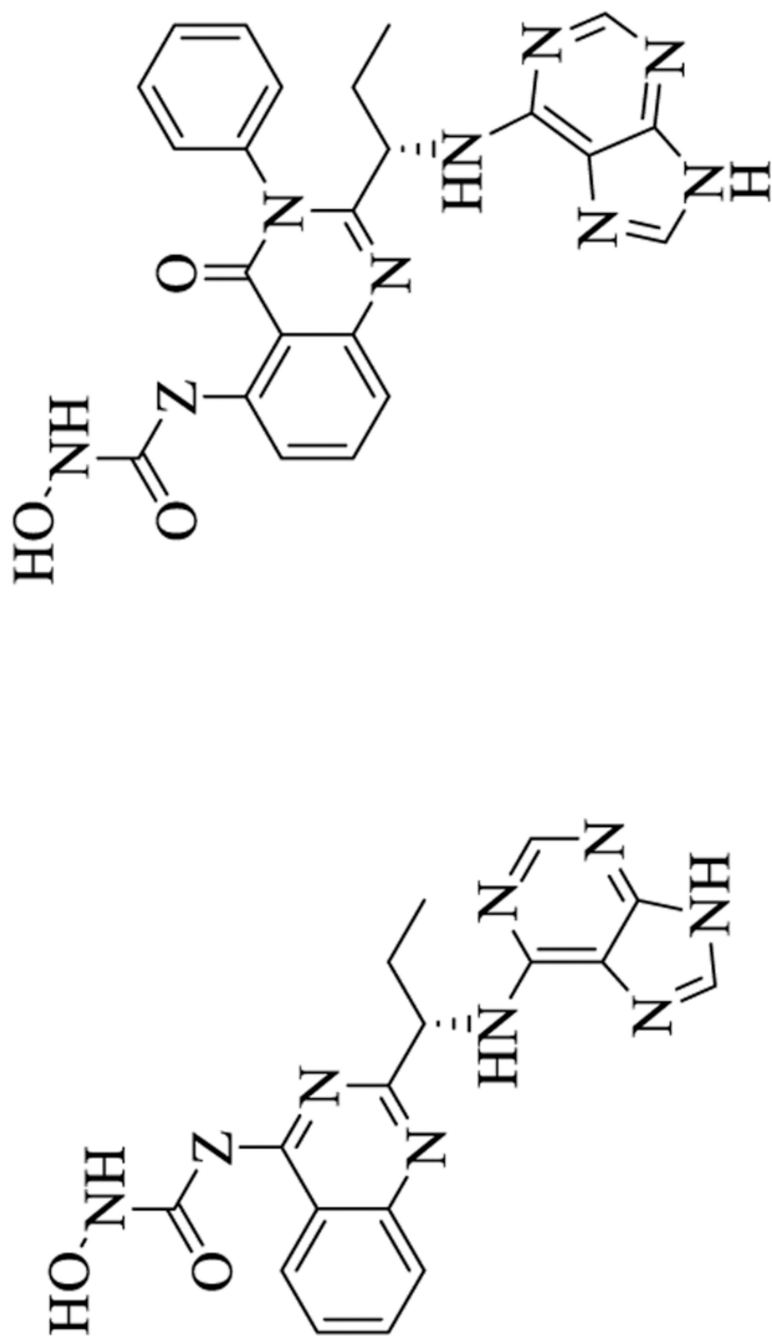
compd	1	2	3	4	5	6	7	8	9	10	11
P13K6											
28a	46	1575	3247	1031	9087	37		1758		NT	3362

Author Manuscript

Author Manuscript

Author Manuscript

Author Manuscript

**10a** Z = (CH₂)₄**10b** Z = (CH₂)₅**14a** Z = NH(CH₂)₃**19a** Z = (CH₂)₄**19b** Z = (CH₂)₅**28a** Z = NH(CH₂)₃IC₅₀ (nM)

HDACs

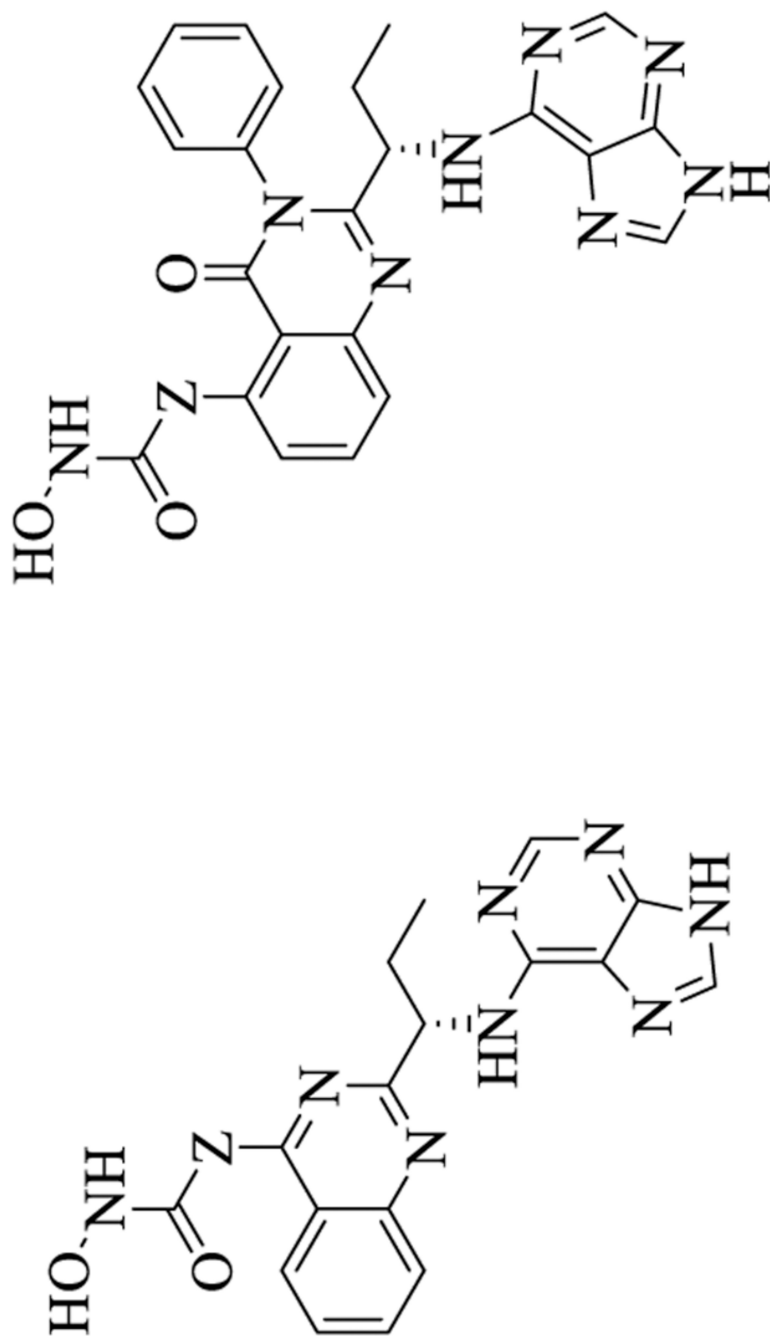
compd	HDACs											
	1	2	3	4	5	6	7	8	9	10	11	
PI3K6	1	NT	NT	NT	NT	NT	NT	NT	NT	NT	NT	NT
PI-103	3	NT	NT	NT	NT	NT	NT	NT	NT	NT	NT	NT

Author Manuscript

Author Manuscript

Author Manuscript

Author Manuscript

**10a** Z = (CH₂)₄**10b** Z = (CH₂)₅**14a** Z = NH(CH₂)₃**19a** Z = (CH₂)₄**19b** Z = (CH₂)₅**28a** Z = NH(CH₂)₃IC₅₀ (nM)

HDACs

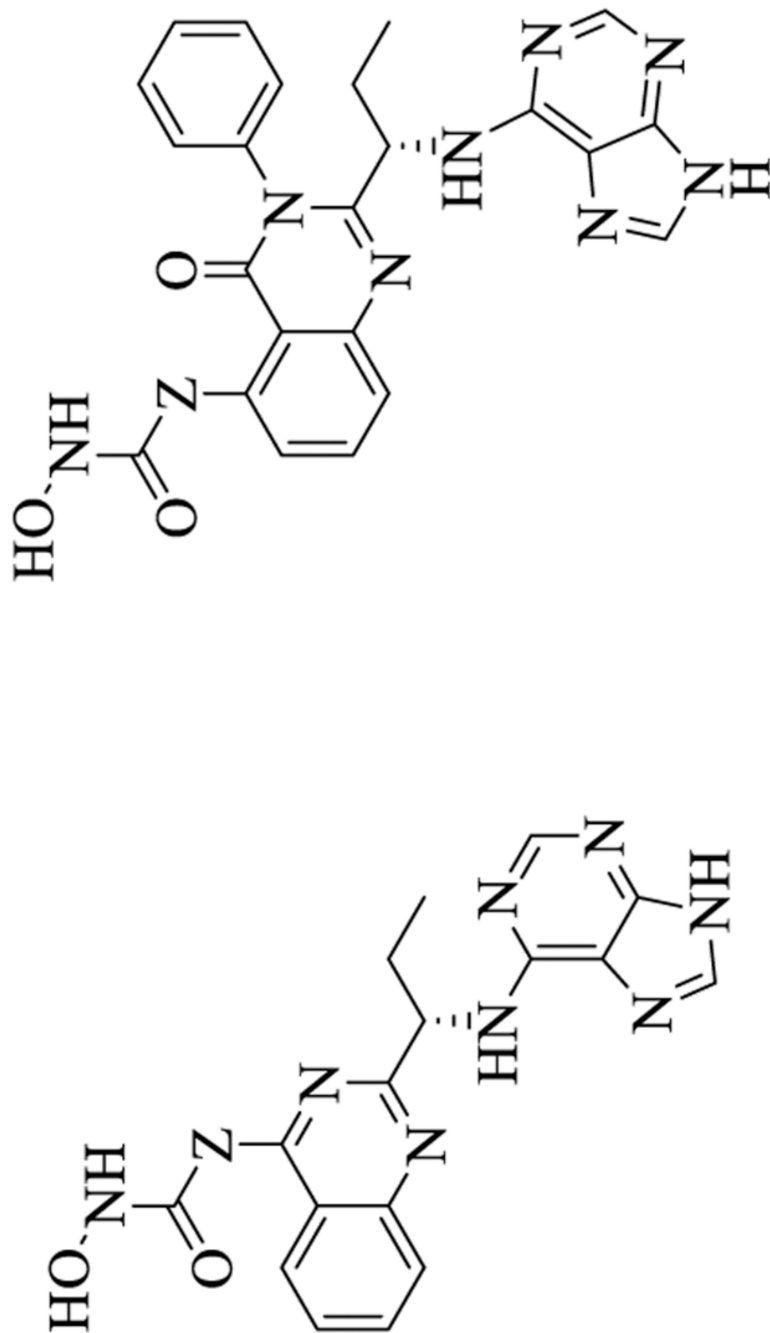
compd	1	2	3	4	5	6	7	8	9	10	11
P13K6	9	25	14	NT	NT	3	NT	371	NT	61	3470
TSA	NT			NT	NT		NT				

Author Manuscript

Author Manuscript

Author Manuscript

Author Manuscript

IC₅₀ (nM)

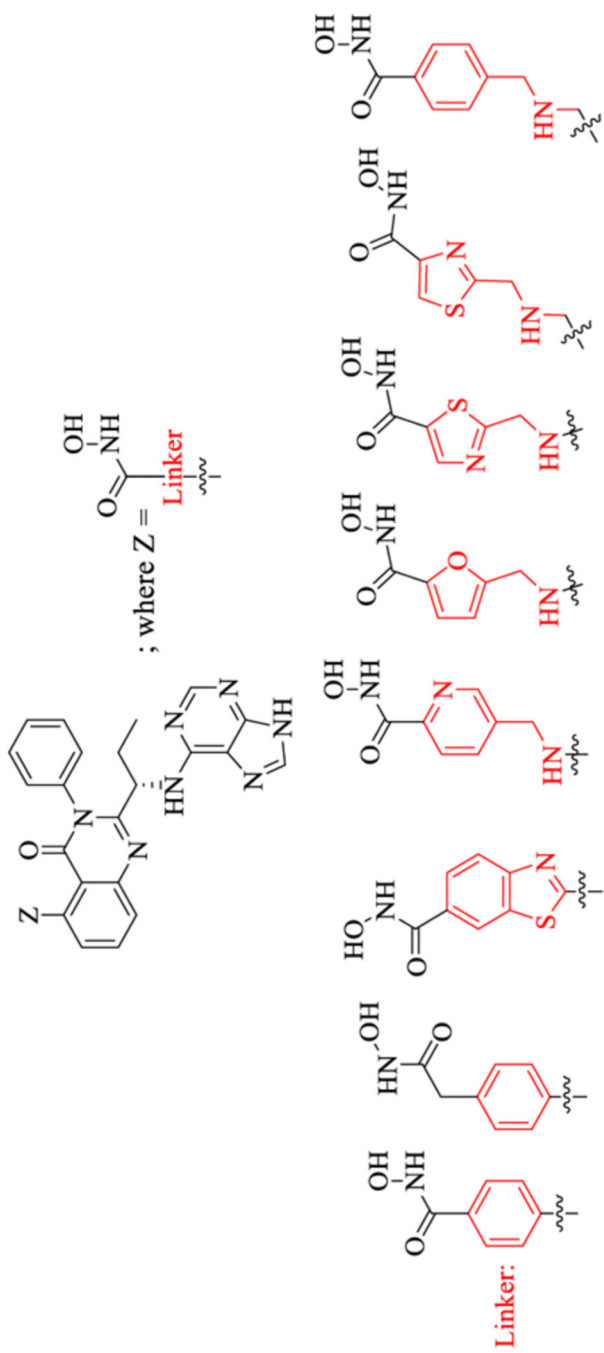
HDACs

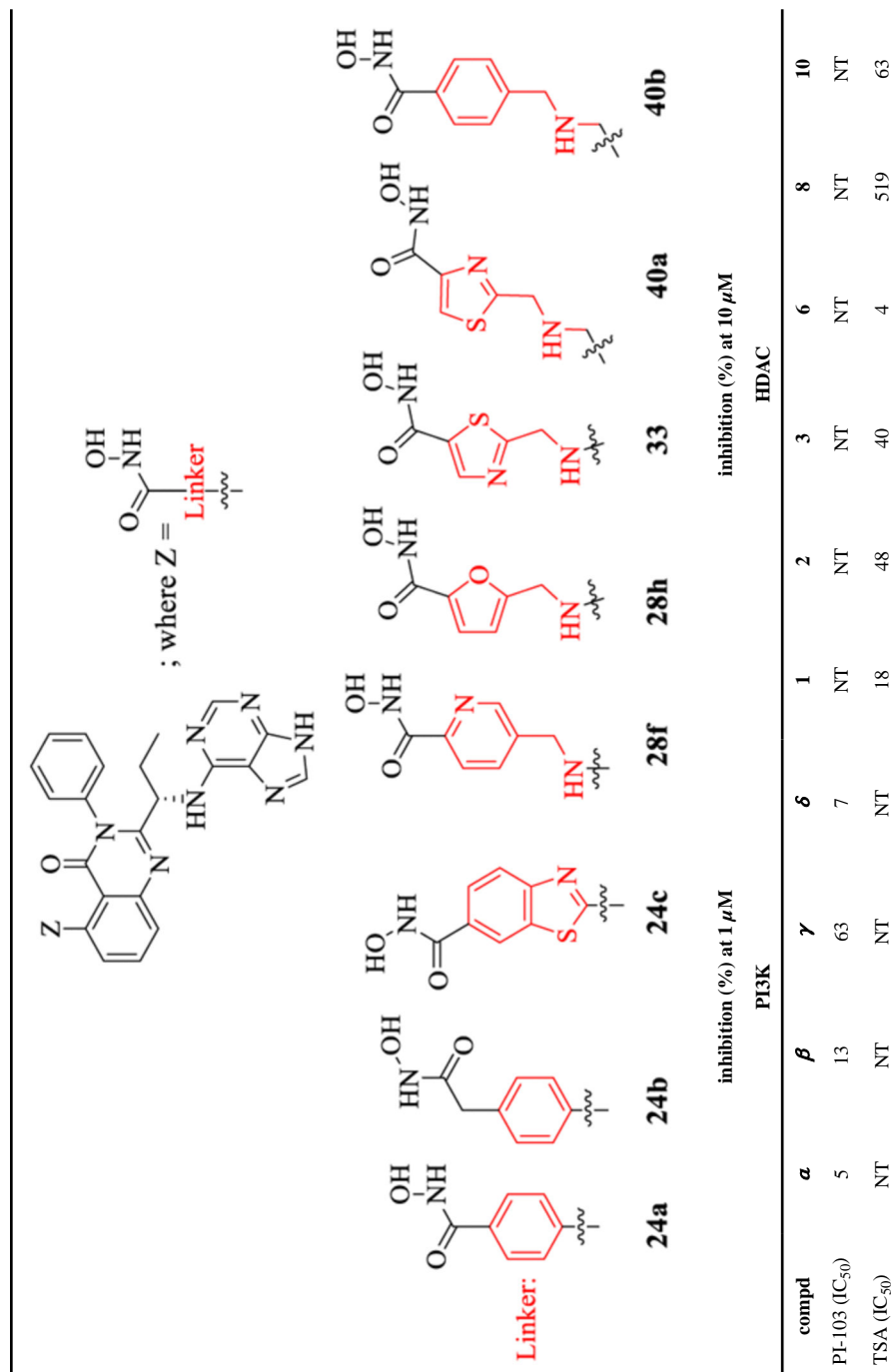
compd	1	2	3	4	5	6	7	8	9	10	11
P13K6	NT	NT	NT	281	333	NT	108	NT	49	NT	NT
TMP 269	NT	NT	NT	281	333	NT	108	NT	49	NT	NT

Compounds were tested in singlet 10-dose IC₅₀ mode with 3-fold serial dilution starting at 1 μ M for HDAC1–11 enzymes. Empty cells indicate no inhibition or compound activity that could not be fit to an IC₅₀ curve. NT = Compound not tested against enzyme. PI-103 was used as a control compound for PI3K δ , whereas trichostatin A (TSA) and TMP 269 were used as control compounds for HDAC enzymes.

Table 2. PI3K/HDAC Enzyme Inhibition (%) Activities of 5-Substituted Quinazolinones with Purine as the Hinge Binding group^a

compd	inhibition (%) at 1 μ M PI3K						inhibition (%) at 10 μ M HDAC			
	α	β	γ	δ	1	2	3	6	8	10
24a	84.5 \pm 0.3	44.0 \pm 0.6	81.6 \pm 0.2	94.7 \pm 0.02	63.3 \pm 3.2	52.3 \pm 0.4	48.2 \pm 0.9	93.3 \pm 0.3	99.1 \pm 0.1	54.0 \pm 0.3
24b	64.1 \pm 1.0	37.5 \pm 2.4	79.1 \pm 0.02	95.8 \pm 1.3	-0.9 \pm 2.8	11.5 \pm 0.1	-13.4 \pm 0.3	70.7 \pm 2.9	70.1 \pm 0.6	20.0 \pm 0.6
24c	84.7 \pm 0.2	38.6 \pm 1.4	88.0 \pm 0.6	92.6 \pm 0.6	50.0 \pm 2.3	40.5 \pm 1.7	20.9 \pm 7.2	95.6 \pm 0.4	98.2 \pm 0.3	33.1 \pm 0.1
28f	45.8 \pm 2.7	4.4 \pm 4.3	39.9 \pm 5.0	88.3 \pm 0.5	20.5 \pm 0.3	16.3 \pm 0.9	14.3 \pm 1.6	90.5 \pm 0.7	87.2 \pm 0.1	-7.0 \pm 1.6
28h	18.1 \pm 0.4	3.8 \pm 1.3	48.0 \pm 1.3	61.2 \pm 1.0	18.3 \pm 6.7	28.0 \pm 3.6	-6.3 \pm 3.2	72.3 \pm 0.03	68.4 \pm 3.3	17.0 \pm 2.8
33	45.6 \pm 1.0	6.8 \pm 0.7	59.9 \pm 0.4	95.2 \pm 0.1	5.2 \pm 3.9	4.1 \pm 1.1	2.0 \pm 3.5	89.1 \pm 0.1	58.4 \pm 0.8	-4.6 \pm 4.7
40a	1.8 \pm 0.7	5.3 \pm 0.3	-12.2 \pm 0.7	56.0 \pm 1.0	24.3 \pm 3.3	30.4 \pm 3.8	-4.3 \pm 1.1	79.9 \pm 0.7	54.5 \pm 0.3	26.4 \pm 0.7
40b	-6.8 \pm 0.2	-6.0 \pm 0.3	-9.1 \pm 3.4	20.5 \pm 0.7	65.6 \pm 2.0	57.2 \pm 5.7	19.1 \pm 1.4	99.2 \pm 0.7	93.5 \pm 0.3	57.2 \pm 1.2



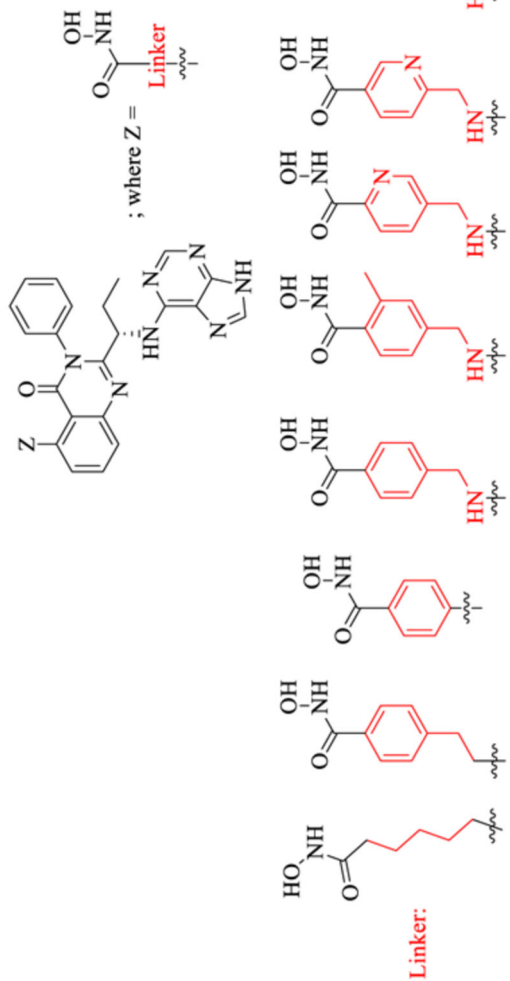


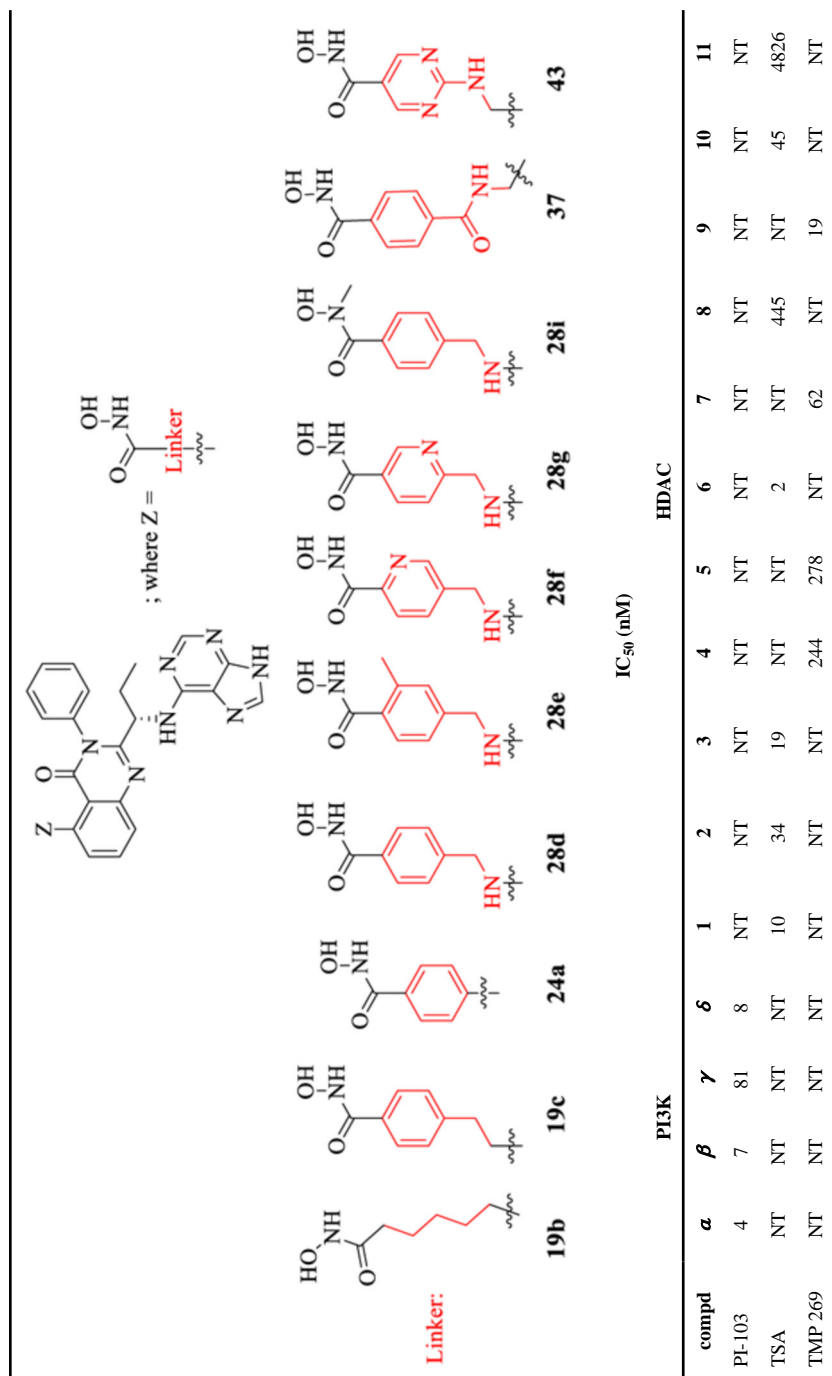
^aCompounds were tested in single dose duplicate at 1 μ M for PI3Ks and 10 μ M for HDAC enzymes. NT = Compound not tested against enzyme. PI-103 was used as a control compound for PI3K δ , whereas trichostatin A (TSA) was used as control compounds for HDAC enzymes.

Table 3.

PI3K/HDAC Enzyme Inhibitory Activities of 5-Substituted Quinazolinones with Purine Hinge Binding Group^a

compd	PI3K											HDAC										
	α	β	γ	δ	1	2	3	4	5	6	7	8	9	10	11	IC ₅₀ (nM)						
19b	122	286	43	0.2	1390	3030	2400		8060	13	856	1240		1840								
19c	NT	NT	NT	5	NT	NT	NT		>10 ⁵	889	3840	NT	NT	9000								
24a	NT	NT	NT	0.7	NT	NT	NT		NT	362	71	NT	NT	NT								
28d	254	254	103	47	3925	7173	6699	1751	2144	5	250	3335	14700	324								
28e	517		203	41	NT	NT	NT	NT	NT	2699	6922	NT	NT	NT								
28f	NT	NT	NT	43	NT	NT	NT	NT	NT	169	NT	NT	NT	NT								
28g	392		135	26	6067	10990	381	439	9	104	204	922	9996	2255								
28i	387		162	81																		
37	266		234	0.6	8434	25480		1428	3827	10	23120	138	19890	1778								
43	422		995	49	67870			6	60	6	320	5349										





^aCompounds were tested in singlet 10-dose IC₅₀ mode with 3-fold serial dilution starting at 1 μ M for PI3K α , β , γ , δ , and 10 μ M for HDAC1–11 enzymes. Empty cells indicate no inhibition or compound activity that could not be fit to an IC₅₀ curve. NT = Compound not tested against enzyme. PI-103 was used as a control compound for PI3Ks, whereas trichostatin A (TSA) and TMP 269 were used as control compounds for HDAC enzymes.

Table 4.PAMPA Permeability Data of Selected 5-Substituted Quinazolinones with Purine Hinge Binding Group^a

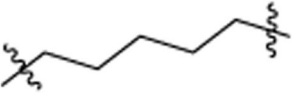
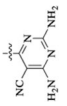
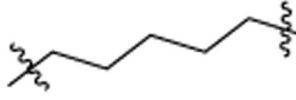
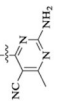
compd	PAMPA permeability ^{a,b}
19b	<1
24a	1.2 ± 0.2
24c	2.4 ± 0.1
28d	6.4 ± 0.8
28e	2.6 ± 0.1
33	1.3 ± 0.4
37	<1
40b	<1
43	<1

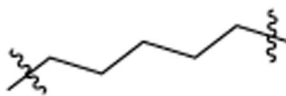
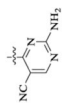
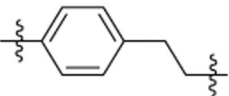
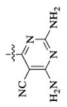
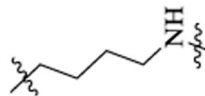
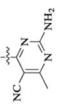
^a Average of two runs ± standard deviation (SD). PAMPA permeability values were determined at pH 7.4 (10^{-6} cm/s).

^b No SD values provided if all PAMPA permeability values are less than 1.

Table 5.

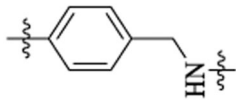
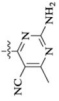
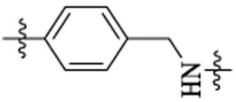
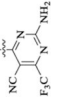
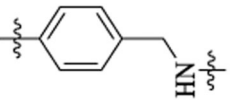
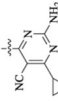
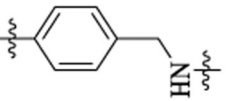
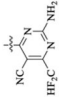
PI3K/HDAC Enzyme Inhibitory Activities of 5-Substituted Quinazolinones with Amino-pyrimidine Hinge Binders^a

Compound	L	R ¹	R ²	IC ₅₀ (nM)				HDAC6 isoform selectivity ^b	
				PI3K	HDAC6	α	β		γ
46a		Et		52	33	3	0.7	69	>13
49b		Et		9	12	2	0.2	28	>36

Compound	L	R ¹	R ²	IC ₅₀ (nM)				HDAC6 isoform selectivity ^b	
				α	β	γ	δ		
46c		Et		5210	1769	96	45	>22	
46d		Et		13	26	2	0.2	77	>7
48a		Et		186	279	8	5	1238	>2

Compound	L	R ¹	R ²	IC ₅₀ (nM)				HDAC6 isoform selectivity ^b	
				α	β	γ	δ		
48b		Et		50	842	45	32	4	>73
48c		Et		47		9	7.0	12	>39
48d		Et						4	>58
48e		Et		444		752	60	4	>113

Compound	L	R ¹	R ²	IC ₅₀ (nM)			HDAC6	HDAC6 isoform selectivity ^b
				α	β	γ		
48f		Et		133	4	>5		
48g		Et		189	3	>81		
48h		Et		663	22	>15		
48i		Et		491	14	>20		

Compound	L	R ¹	R ²	IC ₅₀ (nM)			HDAC6 isoform selectivity ^b	
				PI3K	γ	δ		
				α	β			
48j		Et				269	9	>24
48k		Et					52	>13
48l		Et					47	>9
48m		Et				222	27	>6

Compound	L	R ¹	R ²	IC ₅₀ (nM)				HDAC6 isoform selectivity ^b
				α	β	γ	δ	
48n		Me		42	159	4	4	>31
48o		Me		75	188	2	4	>15
51		Me		18	379	10	0.7	>6
54		Me		42	293	15	3	>25
PI-103	-	-	-	4	7	55	5	NT

Compound	L	R ¹	R ²	IC ₅₀ (nM)					HDAC6 isoform selectivity ^b
				PI3K		HDAC6			
				<i>α</i>	<i>β</i>	<i>γ</i>	<i>δ</i>	6	NT
TSA	-	-	-	NT	NT	NT	NT	6	-
TMP269	-	-	-	NT	NT	NT	NT	NT	-

Author Manuscript

Author Manuscript

Author Manuscript

Author Manuscript

Table 6.

PAMPA Permeability Data of Selected 5-Substituted Quinazolinones with Amino-pyrimidine Hinge Binding Groups

compd	PAMPA permeability ^{a,b}
46b	25.3 ± 0.8
46c	22.7 ± 7.6
48b	4.9 ± 0.1
48c	12.0 ± 0.7
48d	15.7 ± 5.6
48f	50.5 ± 12.6
48g	77.5 ± 11.7
48h	30.2 ± 3.2
48i	12.4 ± 1.2
48j	149.1 ± 2.1

^aCompounds were tested in singlet 10-dose IC₅₀ mode with 3-fold serial dilution starting at 1 μ M for PI3K α , β , γ , δ , and 10 μ M for HDAC1–11 enzymes. Empty cells indicate no inhibition or compound activity that could not be fit to an IC₅₀ curve. NT = Compound not tested against enzyme. PI-103 was used as a control compound for PI3Ks, whereas trichostatin A (TSA) and TMP 269 were used as control compounds for HDAC enzymes.

^bSelectivity of HDAC6 inhibition over other HDAC isoforms (1, 2, 3, 4, 5, 7, 8, 9, 10, and 11). Please see Table S1 in Supporting Information for full IC₅₀ data against HDAC1–11.

^aAverage of two runs ± standard deviation (SD). PAMPA permeability values were determined at pH 7.4 (10⁻⁶ cm/s).

^bNo SD values provided if all PAMPA permeability values are less than 1.

Table 7.

Antiproliferative Activities of Selected Dual Inhibitors against Various Human Cancer Cell Lines at NCI-60^a

cancer type	cell line	GI ₅₀ (μM)										
		28d	46b	48b	48c	48o	Idelalisib	Vorinostat (SAHA)				
leukemia	CCRF-CEM	3.1	0.4	1.6	0.7	0.05	22.3					0.7
	SR	2.5	1.2	1.4	0.7	0.6						0.4
non-small cell lung cancer	HOP-62	11.8	2.7	1.9	2.4	1.4	>100.0					1.6
	HOP-92	2.2	0.2	1.1	0.9	0.3	14.1					2.9
colon cancer	HCT-2998	3.0	2.2	1.7	2.1	1.8	38.5					1.9
	KM-12	2.3	4.0	1.9	1.7	0.4	1.2					0.8
CNS cancer	SNB-75	3.0	0.3	1.3	0.7	0.4	1.2					0.8
	U251	2.5	1.5	1.7	1.7	1.4	53.2					1.6
melanoma	LOX IMVI	1.8	1.4	1.8	1.6	1.5	33.5					1.2
	M14	5.5	1.8	2.3	1.8	1.5	37.8					1.3
ovarian cancer	IGROV1	2.3	0.5	1.9	1.5	0.9	4.8					1.1
	OVCAR3	3.4	1.2	2.2	1.2	1.3	17.7					1.4
renal cancer	A498	6.1	0.2	1.4	1.0	0.7	1.1					1.4
	CAKI-1	14.6	1.3	3.2	1.3	0.8	20.5					1.2
breast cancer	RXF 393	3.2	0.2	1.4	1.2	0.5	1.4					1.3
	MDA-MB-231/ATCC	2.8	1.8	2.3	1.8	1.5	42.3					2.5
	HS 578T	4.5	0.4	2.5	2.0	0.9	6.0					3.6
	T-47D	1.7	0.3	1.6	1.2	0.3	5.2					0.5

^aCompounds were tested at NCI-60 panel in singlet 5-dose IC₅₀ mode with 10-fold serial dilution starting at a concentration of 100 μM.

Table 8.

In Vitro Metabolic Stability (Liver Microsome and Cytosol) and Caco-2 Permeability of Selected Dual PI3K/HDAC Inhibitors^a

compd	microsomal stability ($t_{1/2}$, min) ^{b,d}			cytosolic stability ($t_{1/2}$, min) ^{c,d}			Caco-2 efflux ratio (BA/AB) ^e
	HLM	MLM	RLM	HLC	MLC	RLC	
19b	93.1 ± 4.9	9.0 ± 0.03	19.1 ± 0.1	40.6 ± 7.5	27.7 ± 1.5	19.1 ± 0.1	9.5/0.9
46b	91.5 ± 2.2	9.0 ± 0.4	49.8 ± 3.6	>120	>120	>120	ND
48b	45.7 ± 15.1	60.4 ± 1.4	95.4 ± 4.5	>120	52.1 ± 4.7	>120	7.5/1.4
48c	22.4 ± 2.2	51.7 ± 0.02	100.6 ± 14.6	116.5 ± 4.9	78.4 ± 13.5	>120	6.5/1.9
48n	95.1 ± 30.6	92.8 ± 17.3	>120	>120	>120	>120	ND
48o	32.2 ± 2.7	74.4 ± 5.3	98.6 ± 12.5	105.7 ± 20.2	>120	>120	ND

^a Average of two runs ± standard deviation (SD).

^b Multispecies liver microsomal stability in human (HLM), mouse (MLM) and rat (RLM).

^c Multispecies liver cytosolic stability in human (HLC), mouse (MLC) and rat (RLC).

^d No SD values provided if all replicate half-life values exceeded 120 min.

^e Caco-2 permeability [apical to basolateral (AB); basolateral to apical (BA)]; 10^{-6} cm/s. ND = not determined.

Table 9.

PK Profile of Compound 48c^a

	dosing route			
	iv	po	ip	ip
dose (mg/kg)	3	10	50	150
$t_{1/2}$ (h)	1.01	1.4	2.7 ^b	1.7 ^b
T_{max} (h)		0.167	1	2
C_{max} (ng/mL)		18.4	1443	7783
AUC_{0-t} (h·ng/mL)	869	20.1	8493	40100
AUC_{0-t}/D (h·mg/mL)	291	2.1	170	267
$V_{d_{ss}}$ (L/kg)	3.6			
CL_p (mL/min/kg)	57			
F (%)		0.7	NC ^c	NC ^c

^aFormulation: IV (3 mg/kg), EtOH/PEG-300/sterile water (10:60:30); PO (10 mg/kg), EtOH/PEG-300/sterile water (10:60:30); IP (50 mg/kg), DMSO/PEG-300/sterile water (10:40:50); IP (150 mg/kg), DMSO/PEG-300/20% HP- β -CD in water (1:4) (10:40:50), adjusted to pH 3.0 with 1 M HCl.

^bThe 24 h data point was excluded for terminal half-life ($t_{1/2}$) calculation.

^cNC = not calculated.